

**Please cite the Published Version**

Alam, Sayed (2019) Revising the Mechanism of Polyolefin, Degradation and Stabilisation: Insights from Chemiluminescence, Volatiles and Extractables. Doctoral thesis (PhD), Manchester Metropolitan University.

**Downloaded from:** <https://e-space.mmu.ac.uk/625280/>

**Usage rights:**  [Creative Commons: Attribution-Noncommercial-No Derivative Works 4.0](#)

**Enquiries:**

If you have questions about this document, contact [openresearch@mmu.ac.uk](mailto:openresearch@mmu.ac.uk). Please include the URL of the record in e-space. If you believe that your, or a third party's rights have been compromised through this document please see our Take Down policy (available from <https://www.mmu.ac.uk/library/using-the-library/policies-and-guidelines>)

**REVISING THE MECHANISM OF POLYOLEFIN  
DEGRADATION AND STABILISATION: INSIGHTS FROM  
CHEMILUMINESCENCE, VOLATILES AND EXTRACTABLES**

**Syed Raihan Alam**

A thesis submitted in partial fulfilment of the requirements of the Manchester Metropolitan  
University for the degree of Doctor of Philosophy

**Department of Natural Sciences  
Faculty of Science and Engineering  
Manchester Metropolitan University**

**2019**

**For Akinur and my family**

## **Declaration**

This is to certify that the material contained in this thesis has not been accepted in substance for any other degree and is not currently submitted in candidature for any other academic award.

**Syed Raihan Alam**

## **Acknowledgements**

Firstly, I would like to thank Dr Michele Edge (MMU) for giving me the opportunity to undertake a PhD at MMU. I would also like to thank my industry liaison/sponsor, Klaus Keck (Songwon Industrial Ltd) for his knowledge and support during my years as a PhD student. Without both, the completion of this PhD would not be possible.

I am also grateful for all the technical staff and various lecturers who were involved and have given their support to me during my years at the university.

Finally, I would like to thank my wife, Akinur and my mother, Sahara for constantly given me their unconditional love and support when I needed it the most. Again, without both, I would not have had the strength to complete my PhD.

## Abstract

In this study the thermal-oxidative degradation of the polyolefins: polypropylene (PP), high-density polyethylene (PE-HD), and linear low-density polyethylene (PE-LLD) have been evaluated after melt processing and multiple extrusion passes.

Recent literature on the initiation of autoxidation in polyolefins suggests that oxygen-containing radicals that are already present in polyolefin reactor powders ( $\text{ROO}\bullet$ ,  $\bullet\text{OH}$ ) can abstract hydrogen, trigger  $\beta$ -scission reactions and oxidative propagation. An overview of the literature also supports the premise that, at least in the first instance, abstraction of hydrogen occurs preferentially from allylic sites, since this process is thermodynamically more favoured. Chemiluminescence (CL) has been used to characterise the nature of species arising in the melt at  $180^\circ\text{C}$  in the range of 350-680 nm as expected, characteristic changes do occur in the CL spectra as a function of residence time in the melt and in air. Data points under the integral CL curve have been related to the formation of a transition-state cage cited by other workers<sup>1</sup>. Unlike the Russell mechanism, this follows the decomposition of primary, secondary and tertiary peroxides via a tetroxide that cleaves in an asymmetric manner. The CL results support this premise, suggesting that luminescence arises from cage recombination of peroxy radicals and explains why some antioxidants are more effective than others in their participation in Hydrogen Atom Transfer (HAT). The CL data also questions the roles of secondary antioxidants as peroxide decomposers, suggesting instead that they scavenge alkoxy radicals from cage decomposition.

Because primary and secondary peroxy from cage termination reactions give non-radical products (alcohols, ketones and aldehydes), whilst tertiary peroxy cannot undergo this asymmetric cage reaction (instead escaping the cage as alkoxy radicals) this has been used to explain the range of volatiles and extractables observed during polyolefin oxidation. The polyolefins investigated contain different amounts of chain branching and the data shows that although the types of volatiles are similar regardless of polyolefin type (hydrocarbons (branched, cyclic linear); aldehydes; carbon dioxide; ketone; carboxylic acids; esters; ethers and furans) the rate of thermal oxidation is faster for polyolefins with higher levels of branching.

The results emphasise the fact that the Basic Auto-oxidation Scheme (BAS) which has been the accepted standard cycle for thermo-oxidative degradation, is not as simple as depicted. Therefore, revisions to the BAS of polymer thermal oxidation have been proposed based on this information.

## Acronyms/Abbreviations

**ΔG:** Gibbs free energy

**Å:** Angstroms

**AO:** Antioxidants

**ATR:** Attenuated total reflection

**BAS:** Basic Autoxidation Scheme

**BDE:** Bond-Dissociation Energy

**BHA:** Butylated hydroxyanisole

**BHT:** Butylated hydroxytoluene

**CaSt:** Calcium stearate

**CBA:** Chain-breaking acceptor

**CBD:** Chain-breaking donor

**CL:** Chemiluminiscence

**DABCO:** Diazobicyclooctane

**DSTDP:** Distearyl thiodipropionate

**FTIR:** Fourier-transform infrared spectroscopy

**GA-80:** 3, 9-Bis [2-[3-(3-tert-butyl-4-hydroxy-5-methylphenyl) propionyloxy]-1, 1-dimethylethyl] - 2, 4, 8, 10-tetraoxaspiro, undecane

**GC-MS:** Gas chromatography-mass spectroscopy

**GG:** Gauche-Gauche

**HAT:** Hydrogen Atom Transfer

**iPP:** Isotactic Polypropylene

**M:** Metallocene

**MFI:** Melt flow Index

**MSSV:** Micro-Scale Sealed Vessel

**MW:** Molecular weight

**•OH:** Hydroxyl radicals

**PDMS:** Polydimethylsiloxane



**PE:** Polyethylene

**PE-HD:** High-density polyethylene

**PE-LD:** Low-density polyethylene

**PE-LLD:** Linear low-density polyethylene

**PFTA:** Perfluorotetradecanoic acid

**PP:** Polypropylene

**R•:** Alkyl radicals

**RO•:** Alkoxy radicals

**ROO•:** Peroxy radicals

**ROOH:** Hydroperoxide

**SPME:** Solid-phase Microextraction

**TEMPO:** (2,2,6,6-tetramethylpiperidin-1-yl)oxidanyl

**UV:** Ultraviolet

**Vitamin E:**  $\alpha$ -tocopherol

**V-L-E:** Volatiles, Leachates and Extractables

**VOCs:** Volatile organic compounds

**YI:** Yellowness index

**ZN:** Ziegler-Natta

## Contents

Declaration.....	3
Acknowledgements.....	4
Abstract.....	5
Acronyms/Abbreviations .....	7
Contents .....	9
Figures .....	11
Equations .....	13
Schemes .....	14
Tables.....	15
1 Introduction.....	1
1.1 Background and context.....	1
1.2 Polyolefins .....	2
1.3 Polymer Oxidation .....	3
1.3.1 Initiation.....	5
1.3.1.1 The role of oxygen in the initiation step .....	6
1.3.1.2 The influence of peroxy species as residual impurities from polymerisation.....	6
1.3.1.3 The role of chain imperfections .....	7
1.3.1.4 The role of chain-ends.....	9
1.3.1.5 $\beta$ -scission .....	10
1.3.2 Propagation .....	11
1.3.2.1 Hydrogen atom transfer during chain propagation .....	11
1.3.2.2 Influence of chain conformation on propagation .....	11
1.3.2.3 Crystallinity, Tacticity and Chain Conformations .....	13
1.3.3 Chain Branching .....	14
1.3.3.1 Peroxides.....	14
1.3.4 Termination.....	16
1.3.4.1 Peroxyls.....	16
1.3.4.2 Bimolecular termination of secondary versus tertiary peroxy.....	17
1.4 Loss of Polymer Oxidation Products: Volatiles, Leachates and Extractables .....	20
1.4.1 Volatiles from the polymer .....	20
1.5 Antioxidants.....	24
1.5.1 Inhibition of oxidation by scavenging alkyl radicals ( $R\bullet$ ) [CBA Antioxidants].....	26

1.5.2	Inhibition of oxidation by scavenging peroxy radicals (RO <sub>2</sub> •).....	28
1.5.2.1	Phenolic Antioxidants .....	28
1.5.2.2	Natural Phenolic antioxidants .....	31
1.5.2.3	Aminic Antioxidants .....	39
1.5.2.4	Organosulfur Antioxidants.....	39
1.5.2.5	Organophosphite Antioxidants .....	41
1.5.3	Inhibition of oxidation by decomposing polymer hydroperoxides (ROOH) .....	42
1.5.3.1	Organosulfur Antioxidants.....	42
1.5.3.2	Organophosphite Antioxidants .....	43
1.5.4	Issues with Antioxidants .....	44
1.5.4.1	Colour formation from Antioxidant Transformation Products .....	44
1.5.4.2	Loss of Antioxidants and Antioxidant Transformation Products: Volatiles and Extractables.....	45
1.6	Aims and objectives.....	46
2	Experimental.....	48
2.1	Materials .....	48
2.1.1	Polymer Resins .....	48
2.1.2	Antioxidants.....	49
2.1.2.1	Rationale for selection of the AO formulation.....	49
2.1.3	Formulations .....	50
2.2	Sample analysis.....	53
2.2.1	Chemiluminescence methodology .....	53
2.2.2	GC-MS methodology.....	55
2.2.2.1	Sample Preparation for Detection of Volatiles .....	55
2.2.2.2	Hexane – PP.....	59
2.2.2.3	Hexane – HDPE (Natural AO).....	59
2.2.2.4	Ethanol – PP.....	60
2.2.2.5	Ethanol – HDPE (Natural AO) .....	60
3	Results and Discussion .....	61
3.1	Chemiluminescence .....	61
3.2	Volatiles .....	83
3.2.1	Volatiles from Polypropylene .....	83
3.2.1.1	Volatiles from Polyethylene PE-LLD.....	112
3.2.1.2	Volatiles from Polyethylene PE-HD.....	114
4	Conclusions.....	120

5	Further work.....	123
5.1	Computational Analysis.....	123
5.1.1	Kinetic Modelling of thermo-oxidative degradation in PP/PE .....	123
5.1.2	Ab initio molecular orbital theory calculations.....	124
5.2	Further experimental work.....	124
5.2.1	GC-MS - Quantitative Analysis .....	124
5.2.2	CL Studies – Natural AO .....	124
5.2.3	Metallocene Polymers.....	125
5.2.4	Various Stabilisers .....	126
5.2.5	Other work .....	127
	References.....	128
6	Appendix.....	132
6.1	Antioxidant description.....	132

## Figures

Figure 1.1:	3-D model of PE.....	3
Figure 1.2:	3-D model of PP .....	3
Figure 1.3:	Frequency of branch points on PE-HD and PE-LLD chains.....	9
Figure 1.4:	Unsaturated chain ends as sites for radical initiation (reproduced from <sup>19</sup> ).....	10
Figure 1.5:	Transition state for abstraction of hydrogen by peroxy.....	12
Figure 1.6:	Helical structure of PP.....	12
Figure 1.7:	Crystalline and amorphous regions in semi-crystalline polymers <sup>21</sup> .....	13
Figure 1.8:	Free-valence migration routes for radical capture <sup>22</sup> .....	14
Figure 1.9:	Bimolecular decomposition of hydroperoxides.....	15
Figure 1.10:	Volatiles arising from PP in oxygen detected by FTIR and mass spectrometry <sup>48</sup> .....	22
Figure 1.11:	(Cycle I = Propagation; Cycle II = Chain Branching) <sup>21</sup> .....	24
Figure 1.12:	Derived from <sup>21</sup> .....	26
Figure 1.13:	The structure of BHT.....	29
Figure 1.14:	Structure of $\alpha$ -tocopherol. ....	33
Figure 1.15:	BHA compound.....	35
Figure 1.16:	Structure of Quercetin .....	36
Figure 1.17:	Rutin structure .....	37
Figure 1.18:	Gallic acid structure.....	38
Figure 1.19:	<i>syn</i> versus <i>anti</i> HAT transition-state structures <sup>54</sup> .....	40
Figure 1.20:	Formation of potential Arvins from phenolic AO .....	45
Figure 1.21:	Formation of potential Arvins from phosphite AO .....	46
Figure 2.1:	Typical CL spectrophotometer and accompanying integral spectra obtained (above) and spectrum obtained at given time of ageing from the integral curve.....	54
Figure 2.2:	An example of a CL spectrum, where A is an unstabilised polymer and B is a stabilised polymer <sup>53</sup> .....	54
Figure 2.3:	Dynamic SPME adsorption unit to enable identification of volatiles by GC-MS <sup>80</sup> .....	55
Figure 2.4:	6-port Mini-vap Evaporator.....	57
Figure 2.5:	Example of a sample under the same method as section 2.2.2.5 .....	60
Figure 3.1:	Chemiluminescence intensity (arbitrary) for polypropylene in melt at 180°C stabilised with formulations A, B, D and F.....	61

Figure 3.2: Overall CL intensities for formulations A, B, D and F .....	62
Figure 3.3: Chemiluminescence intensity (arbitrary) for polypropylene in melt at 180°C stabilised with formulations A, C, E and G .....	64
Figure 3.4: Overall CL intensities for formulations A, C, E and G .....	64
Figure 3.5: Chemiluminescence intensity (arbitrary) for polypropylene in melt at 180°C stabilised with formulations H, I, J and K .....	65
Figure 3.6: Overall CL intensities for formulations H, I, J and K .....	66
Figure 3.7: Chemiluminescence intensity (arbitrary) for polypropylene in melt at 180°C stabilised with formulations L, M and O .....	67
Figure 3.8: Overall CL intensities for formulations L, M and O .....	67
Figure 3.9: Maximum CL intensity (arbitrary) from PP (extrusion pass 5) containing stabiliser formulations A to O .....	68
Figure 3.10: CL spectra in the wavelength range 380-620 nm under each data point in the CL versus time OIT plot for formulation PP-A. Data obtained in air at 180°C .....	69
Figure 3.11: CL spectra in the wavelength range 380-620 nm under each data point in the CL versus time OIT plot for formulation PP-B. Data obtained in air at 180°C .....	70
Figure 3.12: CL spectra in the wavelength range 380-620 nm under each data point in the CL versus time OIT plot for formulation PP-D. Data obtained in air at 180°C .....	71
Figure 3.13: CL spectra in the wavelength range 380-620 nm under each data point in the CL versus time OIT plot for formulation PP-F. Data obtained in air at 180°C .....	71
Figure 3.14: CL spectra in the wavelength range 380-620 nm under each data point in the CL versus time OIT plot for formulation PP-C. Data obtained in air at 180°C .....	73
Figure 3.15: CL spectra in the wavelength range 380-620 nm under each data point in the CL versus time OIT plot for formulation PP-E. Data obtained in air at 180°C .....	73
Figure 3.16: CL spectra in the wavelength range 380-620 nm under each data point in the CL versus time OIT plot for formulation PP-G. Data obtained in air at 180°C .....	74
Figure 3.17: CL spectra in the wavelength range 380-620 nm under each data point in the CL versus time OIT plot for formulation PP-H. Data obtained in air at 180°C .....	75
Figure 3.18: CL spectra in the wavelength range 380-620 nm under each data point in the CL versus time OIT plot for formulation PP-I. Data obtained in air at 180°C .....	76
Figure 3.19: CL spectra in the wavelength range 380-620 nm under each data point in the CL versus time OIT plot for formulation PP-J. Data obtained in air at 180°C .....	76
Figure 3.20: CL spectra in the wavelength range 380-620 nm under each data point in the CL versus time OIT plot for formulation PP-K. Data obtained in air at 180°C .....	77
Figure 3.21: CL spectra in the wavelength range 380-620 nm under each data point in the CL versus time OIT plot for formulation PP-L. Data obtained in air at 180°C .....	78
Figure 3.22: CL spectra in the wavelength range 380-620 nm under each data point in the CL versus time OIT plot for formulation PP-M. Data obtained in air at 180°C .....	78
Figure 3.23: CL spectra in the wavelength range 380-620 nm under each data point in the CL versus time OIT plot for formulation PP-O. Data obtained in air at 180°C .....	79
Figure 3.24: Maximum CL intensity (arbitrary) from PE-HD (extrusion pass 5) containing phenol, phosphite, thioester and amine antioxidant formulations .....	82
Figure 3.25: Rate of growth in CL intensity (arbitrary) from PE-HD (extrusion pass 5) containing phenol, phosphite, thioester and amine antioxidant formulations .....	82
Figure 3.26: Alkanes as relative % total of volatiles from stabilised PP (extrusion pass 5) formulations A to O during air oxidation at 150°C for 2-20 hours by SPME GC-MS .....	85
Figure 3.27: Alkenes as relative % total of volatiles from stabilised PP (extrusion pass 5) formulations A to O during air oxidation at 150°C for 2-20 hours by SPME GC-MS .....	85
Figure 3.28: Volatiles as relative % total for polypropylene, stabilised with formulations A, B, D and F, in air at 150°C for 2 hours by dynamic SPME-GC-MS .....	91

Figure 3.29: Oxidised species as Log of relative % total volatiles for polypropylene stabilised with formulations A, B, D and F, in air at 150°C for 2 hours and by dynamic SPME-GC-MS .....	91
Figure 3.30: Volatiles as relative % total volatiles for polypropylene stabilised with formulations A, C, E and G, aged in air at 150°C for 2 hours and analysed by dynamic SPME-GC-MS .....	100
Figure 3.31: Oxidised species as Log of relative % total volatiles for polypropylene stabilised with formulations A, C, E and G, in air at 150°C for 2 hours by dynamic SPME-GC-MS .....	101
Figure 3.32: Volatiles as relative % total volatiles for polypropylene stabilised with formulations H, I, J and K, in air at 150°C for 2 hours by dynamic SPME-GC-MS .....	102
Figure 3.33: Oxidised species as Log of relative % total volatiles for polypropylene stabilised with formulations H, I, J and K, in air at 150°C for 2 hours by dynamic SPME-GC-MS .....	102
Figure 3.34: Volatiles as relative % total volatiles for polypropylene stabilised with formulations H, I, J and K, in air at 150°C for 2 hours by dynamic SPME-GC-M .....	103
Figure 3.35: Oxidised species as Log of relative % total volatiles for polypropylene stabilised with formulations H, I, J and K, in air at 150°C for 2 hours by dynamic SPME-GC-MS .....	104
Figure 3.36: Alkanes as relative % total of volatiles and extractables in hexane and ethanol from stabilised PP (extrusion pass 5) formulations A to O during air oxidation at 150°C for 2-20 hours by SPME GC-MS .....	104
Figure 3.37: Alkanes as relative % total of volatiles and extractables in hexane and ethanol from stabilised PP (extrusion pass 5) formulations A to O during air oxidation at 150°C for 2-20 hours by SPME GC-MS .....	105
Figure 3.38: Volatiles arising from thermal oxidation of PP, PE-LD and PE-HD in air at 150°C (adapted from data <sup>43</sup> ) .....	109
Figure 3.39: Oxidized fragments as relative % total of extractables in hexane from stabilised PE-HD for extrusion Pass 5 .....	113
Figure 3.40: Alkanes as relative % of total extractables in hexane and ethanol from PE-HD stabilised with natural antioxidants (extrusion pass 5) .....	115
Figure 3.41: Alkenes as relative % of total extractables in hexane and ethanol from PE-HD stabilised with natural antioxidants (extrusion pass 5) .....	115
Figure 3.42: Oxidized fragments as relative % of total extractables in hexane and ethanol from PE-HD stabilised with natural antioxidants (extrusion pass 5) .....	116
Figure 3.43: Antioxidant fragments as relative % total of extractables in hexane from unstabilised PE-HD as a function of extrusion pass .....	116
Figure 5.1: Structure of metallocene catalyst and examples of specific catalyst .....	126
Figure 5.2: DABCO structure .....	127

## Equations

$RH + O_2 \rightarrow R\bullet + HOO\bullet$ (Equation 1.1) .....	6
$RO_2\bullet + GG \rightarrow [RO_2\bullet \cdots GG]^\ddagger \rightarrow ROOH + GG\bullet$ (Equation 1.2) .....	12
$R\bullet + O_2 \rightarrow RO_2\bullet$ (Equation 1.3) .....	27
$ROO\bullet + ArOH \rightarrow ROOH + ArO\bullet$ (Equation 1.4) .....	28
$ROO\bullet + ArO\bullet \rightarrow \text{non-radical products}$ (Equation 1.5) .....	28
$ROO\bullet + ArOH \rightarrow ROO^- + ArOH^{+\bullet}$ (Equation 1.6) .....	29
$ArOH^{+\bullet} \rightarrow ArO\bullet + H^+ + ROO^- \rightarrow ROOH$ (Equation 1.7) .....	29
$P(OAr)_3 + ROO\bullet \rightarrow O=P(OAr)_3 + RO\bullet$ (Equation 1.8) .....	41
$P(OAr)_3 + RO\bullet \rightarrow RO-P(OAr)_2 + ArO\bullet$ (Equation 1.9) .....	41
$P(OAr)_3 + RO\bullet \rightarrow O=P(OAr)_3 + R\bullet$ (Equation 1.10) .....	41

## Schemes

Scheme 1.1: Reactions leading to short-chain branches (A: ethyl and B: butyl) in PE-LLD .....	2
Scheme 1.2: Basic Autoxidation Scheme (BAS) derived from the work of Bolland and Gee <sup>8</sup> .....	5
Scheme 1.3: $\beta$ -scission processes in PP and PE .....	10
Scheme 1.4: Redox decomposition of hydroperoxides by metal ions .....	16
Scheme 1.5: Russell mechanism for chain termination by secondary peroxy <sup>37</sup> .....	17
Scheme 1.6: Decomposition of primary peroxy radical via a tetroxide transition state into aldehyde, primary alcohol and oxygen.....	18
Scheme 1.7: Decomposition of secondary peroxy radical via a tetroxide transition state into ketone, secondary alcohol and oxygen .....	18
Scheme 1.8: Reaction of nitroxyl radicals from hindered piperidine with polymer alkyl radicals.....	27
Scheme 1.9: Reaction of quinone from hindered phenols with polymer alkyl radicals.....	27
Scheme 1.10: Reaction of aryl benzofuranone with polymer alkyl radicals.....	28
Scheme 1.11: Reaction mechanism between hindered phenol and peroxy radical.....	29
Scheme 1.12: Reaction mechanism between Peroxy radical and $\alpha$ -tocopherol. Peroxy radical abstracting Hydrogen from $\alpha$ -tocopherol. 'R' group represents the Polymer.....	33
Scheme 1.13: Reaction showing $\alpha$ -tocopheroxy radical being formed with stable Hydroperoxy molecule as a result of the reaction in Scheme 1.12. ....	34
Scheme 1.14: Reaction mechanism between aromatic amine and peroxy radical.....	39
Scheme 1.15: Cope-type elimination n followed by HAT <sup>54</sup> .....	40
Scheme 1.16: Nucleophilic substitution followed by HAT <sup>54</sup> .....	40
Scheme 1.17: Bimolecular homolytic substitution <sup>54</sup> .....	41
Scheme 1.18: Phosphite reactions with peroxy and alkoxy radicals.....	41
Scheme 1.19: Mechanism of thioethers as hydroperoxide decomposers.....	42
Scheme 1.20: Thermolysis of thioethers to form sulphenic acid .....	43
Scheme 1.21: Reaction of sulphur dioxide decomposing hydroperoxides .....	43
Scheme 1.22: Decomposition reaction of a typical phosphite with hydroperoxide.....	43
Scheme 1.23: Mechanisms of phosphite reactions, which improves colour.....	44
Scheme 3.1: Proposed recombination mechanism for peroxy (reproduced from reference <sup>1</sup> ).....	81
Scheme 3.2: Initial degradation pathways for generation of primary and secondary alkyl radicals in PP during polymer processing.....	84
Scheme 3.3 Breakdown products resulting from the oxidation of secondary alkyl radicals in PP during polymer processing .....	86
Scheme 3.4: Breakdown products resulting from the oxidation of primary alkyl radicals in PP during polymer processing .....	87
Scheme 3.5: Further oxidation of Aldehydes to generate carbon monoxide, carbon dioxide and carboxylic acids from PP during polymer processing.....	88
Scheme 3.6: Further oxidation of Aldehydes to generate carbon monoxide, carbon dioxide and carboxylic acids from PP during polymer processing.....	88
Scheme 3.7: Further oxidation of Aldehydes to generate carbon monoxide, carbon dioxide and carboxylic acids from PP during polymer processing.....	89
Scheme 3.8: Further oxidation of Aldehydes to generate carbon monoxide, carbon dioxide and carboxylic acids from PP during polymer processing.....	90
Scheme 3.9: Mechanistic pathway for production of monomer and rearrangement of primary and secondary radicals to tertiary radicals.....	93
Scheme 3.10: Mechanistic pathway for the further rearrangement of primary and secondary radicals to tertiary radicals and for the further rearrangement of primary radicals to allow for the generation of alkanes and alkenes.....	94
Scheme 3.11: Mechanistic pathway for the further rearrangement of secondary radicals to allow for the generation of alkanes and alkenes.....	95

Scheme 3.12: Volatiles arising from thermal oxidation of iPP in air at 220°C and 280°C (adapted from data <sup>44</sup> ) .....	108
Scheme 3.13: Initial degradation pathways for generation of primary alkyl radicals in PE during polymer processing .....	110
Scheme 3.14: Initial degradation pathways for generation of primary alkyl radicals in PE during polymer processing .....	110
Scheme 3.15: Initial degradation pathways for generation of primary alkyl radicals in PE during polymer processing .....	111
Scheme 3.16: Initial degradation pathways for generation of primary alkyl radicals in PE during polymer processing .....	111

## Tables

Table 1.1: Equations representing the autoxidation of polyolefins.....	4
Table 1.2: Unsaturated chain ‘imperfections’ in PP and PE .....	7
Table 1.3: Free energy change ( $\Delta G$ ) for hydrogen abstraction at specific sites in PP and PE <sup>18</sup> .....	8
Table 1.4: Specific volatile products of PP thermo-oxidation of PP at 220-280°C .....	21
Table 1.5: Chain length for volatiles observed from polyolefins <sup>47</sup> .....	22
Table 1.6: Alkyl radicals and volatile compounds from fragmentation of primary and secondary alkoxy <sup>49</sup> .....	23
Table 1.7: Interaction of reactive species from polymer oxidation with stabilisers <sup>11</sup> .....	25
Table 1.8: Antioxidant HAT rate constants ( $k_{inh}$ ) and bond dissociation energies (BDEs).....	31
Table 1.9: Physical properties of selected natural phenols .....	32
Table 1.10: Organosulphur HAT rate constants ( $k_{inh}$ ) and bond dissociation energies (BDEs) <sup>54</sup> .....	39
Table 2.1: IUPAC names and corresponding structure codes for antioxidants .....	50
Table 2.2: PP formulations PP-A, PP-B, PP-D and PP-F .....	51
Table 2.3: PP formulations PP-A, PP-C, PP-E and PP-G .....	51
Table 2.4: PP formulations PP-H, PP-I, PP-J and PP-K .....	51
Table 2.5: PP formulations PP-L, PP-M and PP-O.....	52
Table 2.6: PE-LLD formulations LLD-A, LLD-B, LLD-C and LLD-D .....	52
Table 2.7: PE-HD formulations HD-A to HD-F .....	52
Table 2.8: PE-HD formulations HD-G to HD-K .....	52
Table 3.1: Assignments for volatile alkanes from stabilised PP formulations in air at 150°C for pathways I to IV to VII to X (outlined in Schemes 3.8 to 3.10) .....	95
Table 3.2: Assignments of volatile alkanes from stabilised PP formulations in air at 150°C for pathways I to IV to VII to X (outlined in Schemes 3.8 to 3.11) .....	96
Table 3.3: Assignments for volatile alkanes from stabilised PP formulations in air at 150°C for pathways II to V to IX to XI (outlined in Schemes 3.8 to 3.11) .....	96
Table 3.4: Assignments for volatile alkanes from stabilised PP formulations in air at 150°C for pathways II to V to IX to XI (outlined in Schemes 3.8 to 3.11) .....	96
Table 3.5: Assignments for volatile alkanes from stabilised PP formulations in air at 150°C for pathways II to V to IX to XI (outlined in Schemes 3.8 to 3.11) .....	97
Table 3.6: Assignments of volatile alkenes from stabilised PP formulations in air at 150°C.....	97
Table 3.7: Assignments for volatile alkenes from stabilised PP formulations in air at 150°C for pathways II to V to IX to XI (outlined in Schemes 3.8 to 3.11) .....	98
Table 3.8: Assignments of volatile alkenes from stabilised PP formulations in air at 150°C.....	98
Table 3.9: Table of half lifes of typical peroxides .....	99
Table 3.10: Low molecular weight species (alkanes and alkenes) observed in GC-MS spectra following extractions to hexane (■) or ethanol (■) or both (■) from PP (stabilised with formulations C to M) after extrusion Pass 5 .....	106



Table 3.11: Low molecular weight species (alcohols, aldehydes, ketones*) extracted to hexane (■) or ethanol (■) or both (■) from PP (stabilised with formulations C to M) after extrusion Pass 5	107
Table 3.12: Low molecular weight species (alkanes and alkenes) extracted to hexane from stabilised PE-LLD (Ti) after extrusion Pass 5	113
Table 3.13: Low molecular weight species (alcohols, aldehydes, ketones) extracted to hexane from stabilised PE-LLD (Ti) after extrusion Pass 5	114
Table 3.14: Low molecular weight species (ethers, epoxides, lactones, esters, carboxylic acids) extracted to hexane from stabilised PE-LLD (Ti) after extrusion Pass 5	114
Table 3.15: Low molecular weight species (alkanes and alkenes) extracted to hexane (■) or ethanol (■) or both (■) from PE-HD after extrusion Pass 5	117
Table 3.16: Low molecular weight species (alcohols, aldehydes*, ketones) extracted to hexane from PE-HD (Stabilised with formulations A to F and G to K) after extrusion Pass 5	119
Table 3.17: Low molecular weight species (ethers, epoxides, lactones, esters, carboxylic acids) extracted to hexane from PE-HD (Stabilised with formulations A to F and G to K) after extrusion Pass 5	119
Table 4.1: Revised BAS for the thermal oxidation of polyolefins	122

# **1 Introduction**

## **1.1 Background and context**

The polymer industry constantly faces challenges of increased globalisation of markets to improve profitability, along with societal demands for improved environmental performance. These challenges are most obvious during polymer processing in the melt at high temperatures and under high shear. In their raw, non-stabilised forms, polymers rapidly undergo autoxidation causing chain-scission, loss of volatiles and incorporation of oxidised functional groups into the polymer chain. Collectively these processes cause a deterioration in the physical and chemical properties of the polymer. Without the inclusion of antioxidants (AO), stability and longevity of the polymer cannot be achieved<sup>2</sup>. To keep abreast of changing requirements means continuing re-evaluation of the existing knowledge in the field.

It is ironic that AO are depleted by diffusion and evaporative loss, especially during processing operations, thereby reducing their performance in the polymer matrix. Consequently, modifications to individual AO structures have been undertaken to address this<sup>3</sup>. This is further exacerbated because AOs tend to fragment to smaller organic structures, which in their overall mechanistic action contribute to stabilisation. These fragments may also volatilise or leach out of the polymer matrix, adding to the problems of stabiliser depletion and/or environmental issues. Understanding the processes that lead to fragmentation and how AOs control (or are unable to control) this aspect of degradation is one subject of this study.

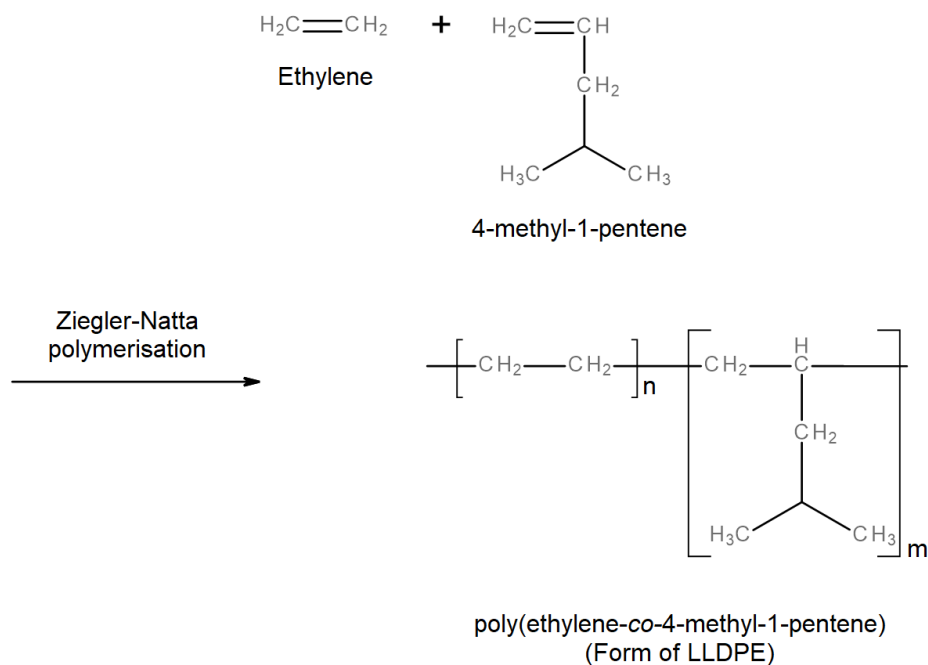
The largest volume usage of polymers in commodity applications are polyolefins: polypropylene (PP), high density polyethylene (PE-HD), and linear low-density polyethylene (PE-LLD). These polymers differ in their degree of branching along the main polymer chain and this gives rise to different rates of oxidation of the polymers<sup>4</sup>. Whether this has significance for the pathway of degradation will be explored in order to answer some of the puzzling questions that remain regarding the basic mechanism of autoxidation of polymers, that have been raised in the literature for several decades.

## 1.2 Polyolefins

Four different processes exist for the production of polyolefins based on the catalysts used: catalyst free and those based on Ziegler-Natta, Phillips and Metallocene catalysts.

PP and PE-HD use Ziegler-Natta catalysts at low temperatures ( $< 100^{\circ}\text{C}$ ) and pressures (0.1 to 5 MPa), leading to relatively broad molecular weight distributions. The catalytic process is heterogeneous using  $\text{TiCl}_3$  on a  $\text{MgCl}_2$  support enabling better process control. In modern processes, control of stereospecificity and the need for post-reactor removal of catalyst is mitigated by use of Lewis acids and bases.

PE-LLD is produced using Ziegler-Natta catalysts via a catalytic ethylene polymerisation reaction at low temperatures and pressures (temperature  $80\text{--}105^{\circ}\text{C}$ , pressure  $0.7\text{--}2\text{ MPa}$ )<sup>5</sup>. In particular, LLDPEs prepared via Ziegler-Natta catalysis have more uneven co-monomer distributions, whereas, a reverse trend is observed for those synthesized by metallocene catalysts.



**Scheme 1.1:** Reactions leading to short-chain branches in PE-LLD

As mentioned, although PE-LLD can be produced by metallocene catalysts, the influence of this catalyst on degradation has been researched by other workers<sup>6</sup> and will not be considered in this study.

PE-HD can also be produced using Phillips catalysts in a process exhibiting high stereospecificity. Here the support is usually CrO<sub>3</sub> on finely divided silica-alumina.

The three-dimensional structures of a basic PE and PP are given in **Figure 1.1** and **Figure 1.2**. Both PE-HD and PP are classified as semi-crystalline which is further discussed in **Section 1.3.2.3**.

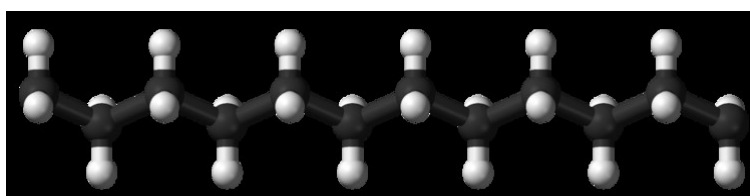


**Figure 1.1:** 3-D model of PE

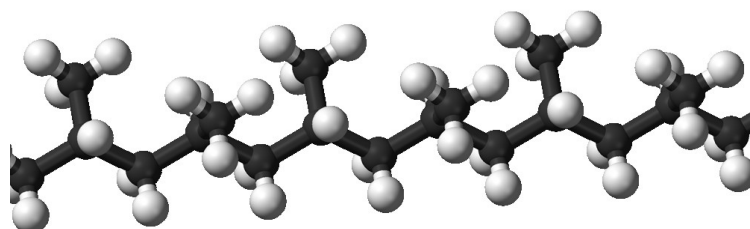


**Figure 1.2:** 3-D model of PP

All polyolefins are susceptible to oxidative degradation during processing and service-life. To date the mechanisms by which they undergo oxidation have been explained by a long-established polymer oxidation cycle outlined in **scheme 1.2** with further details on the polymers crystallinity in **section 1.3.2.3**.

### **1.3 Polymer Oxidation**

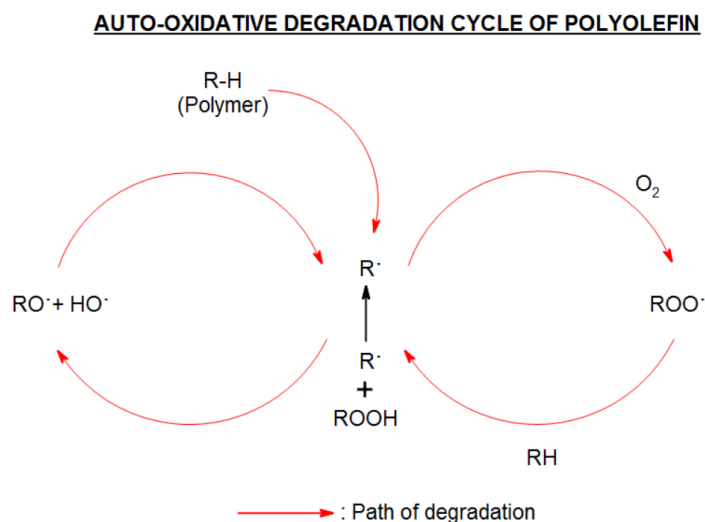
The radical chain autoxidation mechanism for polyolefin degradation can be represented by the reactions given in **Table 1.1**. During radical chain oxidation alkyl ( $R\bullet$ ), peroxy ( $ROO\bullet$ ), alkoxy ( $RO\bullet$ ), hydroxy ( $\bullet OH$ ) species are produced along with peroxides ( $ROOH$ ,  $ROOR$ ). The key steps involved in these reactions will be discussed in more detail in the following sections of this introduction.

**Table 1.1:** Equations representing the autoxidation of polyolefins

<b>Initiation</b>	$RH \rightarrow 2R\bullet$ $RH + O_2 \rightarrow R\bullet + HOO\bullet$ $R-R \rightarrow R\bullet + \bullet R'$ $\beta$ -scission (thermo-mechanical degradation) $R'\bullet \rightarrow \beta$ -scission $\rightarrow R''\bullet + \text{low molecular weight species}$
<b>Propagation</b>	$R\bullet + O_2 \rightarrow ROO\bullet$ $ROO\bullet + R'H \rightarrow ROOH + R'\bullet$
<b>Chain-Branching</b>	$ROOH \rightarrow RO\bullet + \bullet OH$ $2ROOH \rightarrow ROO\bullet + RO\bullet + H_2O$ $RO\bullet + RH \rightarrow ROH + R\bullet$ $HO\bullet + RH \rightarrow R\bullet + H_2O$
<b>Termination</b>	$ROO\bullet + ROO\bullet \rightarrow \text{inert products}$ $ROO\bullet + R\bullet \rightarrow ROOR$ $2R\bullet \rightarrow R-R$

The individual equations are more frequently presented by the oxidation scheme that is prevalent throughout the literature. This is the Basic Autoxidation Scheme (BAS) following from the work of Bolland and Gee<sup>7</sup>. These workers derived the basic cycle of autoxidation

from their work on lipids and rubbers and it is this scheme that has been assumed to apply to all polymers (**Scheme 1.2**).



**Scheme 1.2:** Basic Autoxidation Scheme (BAS) derived from the work of Bolland and Gee<sup>7</sup>

However, the BAS as it is currently written does not easily lend itself to formulation of kinetic models that can predict the lifetime of polymers. Firstly, the initiation step is generally ‘glossed over’ as being triggered by impurities and defect structures, with few, if any, details given. Secondly, the propagation step is not favoured thermodynamically because the bond dissociation energy of the R–H bond is significantly higher, than that of the ROO–H bond found in study by Coote *et al*<sup>8</sup>. Thirdly, though a key reaction in the termination step involves bimolecular recombination of polymer peroxy radicals and the generation of chemiluminescence (CL) this mechanism is not fully resolved. This warrants a closer inspection of the thermo-oxidative degradation cycle (BAS) in the first instance by critical evaluation of observations made in the literature.

Here the distinctly different rates of oxidation in polyolefins (PP and PE) will serve as the pretext for a review of the literature.

### **1.3.1 Initiation**

Both mechanistic and kinetic data remain controversial for this least investigated step of chain-initiation. Detailed study of the mechanism is not easy because rates of chain-initiation are ordinarily too low to be easily measured. However, certain factors that may be important in this step of oxidation will be examined in this section as follows.

#### **1.3.1.1 The role of oxygen in the initiation step**

Although the bimolecular reaction of oxygen with the polymer is written in the BAS as simple H-abstraction from the polymer (**Equation 1.1**), this warrants further clarification.



This is partly due to branched chain processes being the only processes that are weakly dependent upon the chain initiation rate<sup>9</sup>.

Furthermore, the BAS is not corrected for oxygen diffusion and solubility and this has been the subject of numerous studies<sup>10-12</sup>.

#### **1.3.1.2 The influence of peroxy species as residual impurities from polymerisation**

Tobita and co-workers<sup>13</sup> have examined initiation of oxidative degradation in PP reactor powder produced using a Ziegler-Natta catalyst. Adopting chemiluminescence under nitrogen as a technique to determine oxidation, they discovered that the just-synthesized PP spontaneously formed peroxy species when exposed to air even at ambient temperatures. Addition of TEMPO (a radical-trapping agent) to polymerization reactor powder substantially enhanced the stability of the polymer. However, there was no observed enhancement if the TEMPO was added after the polymer had been exposed to air. This suggests that initial radicals are already present from polymerization reactions. If this is the case, then hydrogen abstraction from polymer chains by peroxy radicals leading to propagation is a possibility from the onset of oxidation.

### 1.3.1.3 The role of chain imperfections

Several studies reinforce a correlation between concentration of 'defect' units in polymers and the ease of oxidation<sup>14-16</sup>.

Chain 'imperfections' produced in PE and PP, which depend on the polymerisation chemistry are vinyl, vinylene and vinylidene double bonds. (**Tables 1.2 and Table 1.3**).

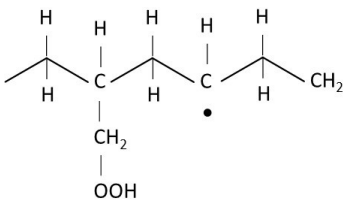
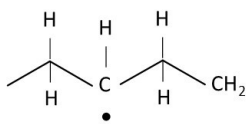
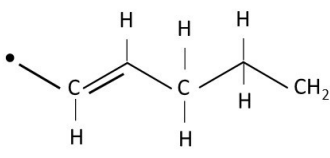
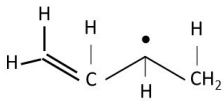
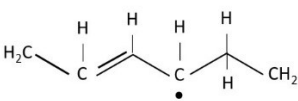
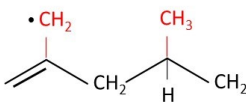
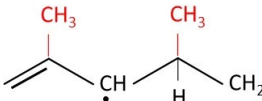
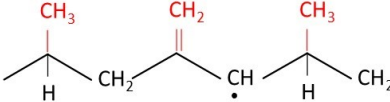
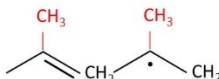
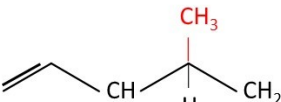
**Table 1.2:** Unsaturated chain 'imperfections' in PP and PE

	Vinyl			Vinylidene	
PP	$\begin{array}{c} \text{CH}_3 \quad \text{CH}_3 \\   \quad   \\ -\text{CH}-\text{CH}_2-\text{C}-\text{CH}_2- \\   \\ \text{CH} \\    \\ \text{CH}_2 \end{array}$	$\begin{array}{c} \text{CH}_3 \quad \text{CH}_3 \\   \quad   \\ -\text{CH}-\text{CH}_2-\text{CH}-\text{CH}- \\   \quad   \\ \text{CH} \quad \text{CH} \\    \quad    \\ \text{CH}_2 \quad \text{CH}_2 \end{array}$	$\begin{array}{c} \text{CH}_3 \quad \text{CH}_3 \\   \quad   \\ \text{CH}_2=\text{CH}-\text{CH}-\text{CH}_2-\text{CH}-\text{CH}_2- \end{array}$	$\begin{array}{c} \text{CH}_3 \\   \\ -\text{CH}-\text{CH}_2-\text{C}-\text{CH}_2- \\    \\ \text{CH}_2 \end{array}$ $\begin{array}{c} \text{CH}_3 \quad \text{CH}_3 \\   \quad   \\ -\text{CH}-\text{CH}_2-\text{CH}-\text{C}- \\    \quad   \\ \text{CH}_2 \end{array}$	-
PE	$\begin{array}{c} \text{H} \quad (\text{CH}_2)_n\text{CH}_3 \\   \quad   \\ -\text{CH}-\text{CH}_2-\text{C}-\text{CH}_2- \\   \\ \text{CH} \\    \\ \text{CH}_2 \end{array}$	$\begin{array}{c} \text{H} \quad \text{H} \\   \quad   \\ -\text{CH}-\text{CH}_2-\text{C}-\text{CH}_2- \\   \\ \text{CH} \\    \\ \text{CH}_2 \end{array}$	$\begin{array}{c} \text{H} \quad \text{H} \\   \quad   \\ \text{CH}_2=\text{CH}-\text{CH}-\text{CH}_2-\text{CH}-\text{CH}_2- \end{array}$	$\begin{array}{c} \text{H} \\   \\ -\text{CH}-\text{CH}_2-\text{C}-\text{CH}_2- \\    \\ \text{CH}_2 \end{array}$	$\begin{array}{c} \text{H} \\   \\ -\text{C}-\text{CH}_2-\text{CH}_2-\text{CH}=\text{CH}-\text{CH}_2- \end{array}$
	Mainly in HDPE			Mainly in LDPE	Mainly in LLDPE

From molecular modelling<sup>17</sup> it has been suggested that hydrogen abstraction is not favoured from saturated sites and that free energy is favourable only at unsaturated locations. From **Table 1.3** PE free energies ( $\Delta G$ ) for abstraction of hydrogens from the polymer chain are only negative for allyl end groups ( $\Delta G = -6.8 \text{ kJ mol}^{-1}$ ) and vinylidene internal sites ( $\Delta G = -6.3 \text{ kJ mol}^{-1}$ ). The same is evident for PP with allyl end groups and vinylidene sites showing  $\Delta G$  values of  $-7.5 \text{ kJ mol}^{-1}$  and  $-9.5 \text{ kJ mol}^{-1}$  respectively.



**Table 1.3:** Free energy change ( $\Delta G$ ) for hydrogen abstraction at specific sites in PP and PE<sup>17</sup>

Polypropylene	Polyethylene
 <p><math>\Delta G = 43.5 \text{ kJ mol}^{-1}</math></p>  <p><math>\Delta G = 36.8 \text{ kJ mol}^{-1}</math></p>  <p><math>\Delta G = -2.0 \text{ kJ mol}^{-1}</math></p>  <p><math>\Delta G = -7.5 \text{ kJ mol}^{-1}</math></p>  <p><math>\Delta G = -9.5 \text{ kJ mol}^{-1}</math></p>	<p><b>Vinylidene end groups:</b></p>  <p><math>\Delta G = 4.4 \text{ kJ mol}^{-1}</math></p>  <p><math>\Delta G = 0.2 \text{ kJ mol}^{-1}</math></p> <p><b>Vinylidene internal group:</b></p>  <p><math>\Delta G = -6.3 \text{ kJ mol}^{-1}</math></p> <p><b>Isobutenyl end groups:</b></p>  <p><math>\Delta G = 1.1 \text{ kJ mol}^{-1}</math></p> <p><b>Allyl end group:</b></p>  <p><math>\Delta G = -6.8 \text{ kJ mol}^{-1}</math></p>

Short and long-chain branches that are a consequence of deliberate inclusion by use of specific polymerisation catalysts may also play a part. It has also been claimed that branch points influence initiation since branched PEs oxidise more readily than their linear analogues in PE. However, it has been observed that the composition of oxidation products is largely independent of branch sites irrespective of their length. This raises the question as to what role, if any, branch points play in the oxidation of polyolefins. In PP there are (methyl) chain branches every monomer unit, while for PE chain branches are the result of the polymerisation process with the frequency along the main chain differing for PE-HD and PE-LLD (**Figure 1.3**). The effect of branching on the polymer properties depends on the number and length of the branches. Short branches interfere with the formation of crystals, that is, they reduce the amount of crystallinity whereas long branches undergo side chain crystallization because they are able to form lamellar crystals of their own. In the case of polyethylene, significant side chain crystallization can be expected around 40 carbon atoms. Long side chains also have a noticeable effect on the flow properties of the polymer, particularly when the length of the branches exceeds the average critical entanglement length. In that case, even a small amount of branching will greatly affect the processing properties.

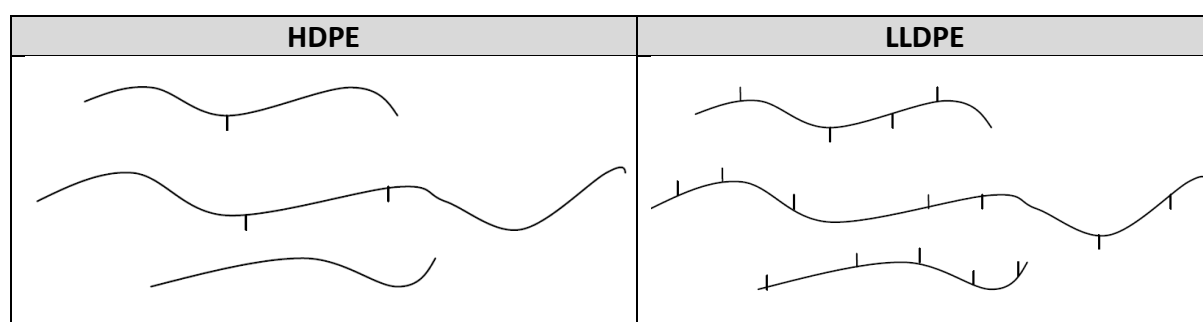


**Figure 1.3:** Frequency of branch points on PE-HD and PE-LLD chains

#### 1.3.1.4 The role of chain-ends

Nakatani *et al* suggested that unsaturated chain-ends act as radical initiator sites for the degradation of iPP (isotactic PP)(**Figure 1.4**)<sup>18</sup>.

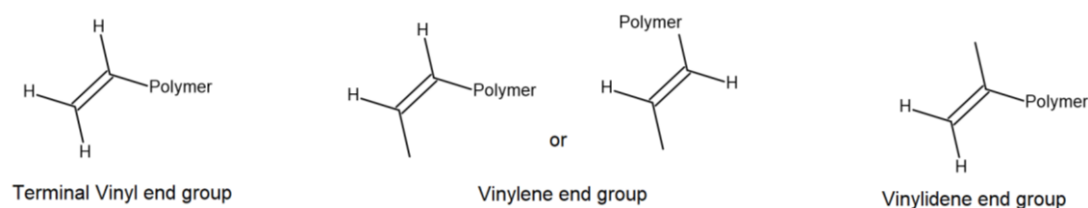
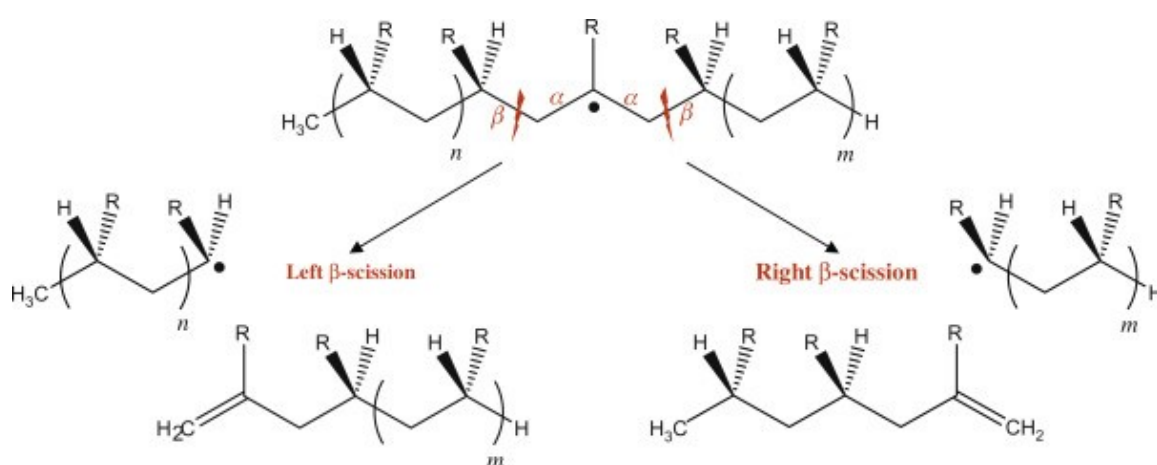


**Figure 1.4:** Unsaturated chain ends as sites for radical initiation (reproduced from<sup>18</sup>)

Using Metallocene (M) and Ziegler-Natta (ZN) catalysts to prepare iPP, with and without unsaturated chain-ends,  $^1\text{H}$ - and  $^{13}\text{C}$ -NMR were used to determine the chain-end content as a function of the ratio of ZNiPP:MiPP. Changes in molecular weight (size-exclusion chromatography) and mass loss (thermogravimetric analysis) were then measured to demonstrate that the higher the unsaturated chain-end content the faster oxidative degradation occurred.

### 1.3.1.5 $\beta$ -scission

$\beta$ -scission processes are considered to dominate the chemistry of polyolefin degradation. In the absence of oxygen,  $\beta$ -scission processes in PP and PE lead to the production of further alkyl radicals and unsaturated chain ends (**Scheme 1.3**). In the early stages of degradation,  $\beta$ -scission is the dominant reaction compared to hydrogen atom transfer. In the presence of oxygen, the formation of peroxy will compete effectively with these processes since the rate constant for this reaction is a large value<sup>19</sup>.



**Scheme 1.3:**  $\beta$ -scission processes in PP and PE

### 1.3.2 Propagation

#### 1.3.2.1 Hydrogen atom transfer during chain propagation

For successful autoxidation, hydrogen atom transfer (HAT) to peroxy radicals is considered to take place. However, this is questionable because, as stated previously (**Section 1.3.1.3**) this is not thermodynamically favourable for saturated polymers such as polypropylene and polyethylene. In fact, the original work by Bolland and Gee<sup>7</sup> used unsaturated polymers where abstraction of allylic hydrogen leads to resonance stabilised radicals in a reaction that is likely, both kinetically and thermodynamically.

It can be envisaged that impurity concentrations of double bonds or double bonds at chain ends or defect structures could facilitate hydrogen abstraction during propagation, but this would only be thermodynamically favourable if the products formed are removed irreversibly at relatively high rate. The data derived from the study given in **Table 1.3** by Smith *et al.* confirms this<sup>17</sup>.

#### 1.3.2.2 Influence of chain conformation on propagation

Propagation of the initial radicals is different in PP and PE. In PP chain-transfer by hydrogen atom abstraction takes place by an *intra*-molecular process, but for PE the predominant mode is by an *inter*-molecular process. The primary reason for this is the conformation of the chain structure. For hydrogen abstraction, the distance between the O---H and •C---H in the transition-state is about 1.4 Å and 1.2 Å (angstroms) respectively (**Figure 1.5**). Reaction is unlikely if the distance between O---H is greater 1.8 Å<sup>19</sup>.

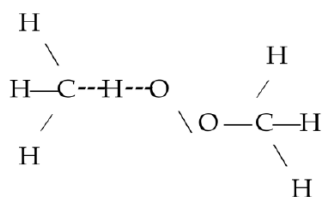


**Figure 1.5:** Transition state for abstraction of hydrogen by peroxy

Formation of the transition state is therefore dependent on conformation of chains. In PE for an intramolecular process to take place sequences of GG (gauche-gauche) dyads (**Equation 1.2**). This is where the rotation of the chain can affect the steric hindrance of the polymer itself<sup>19</sup>.



Although the fraction of such sequences is low in PE there is little steric hindrance to rotation of propagating chain. In PP the presence of methyl branches along the chain leads to a helical structure that has the conformation TGTGTG (**Figure 1.6**)

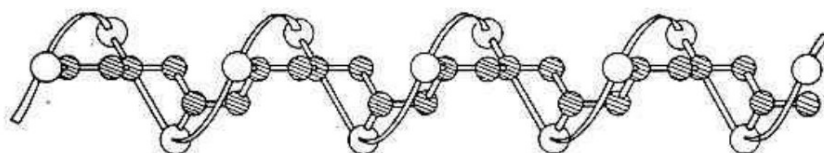
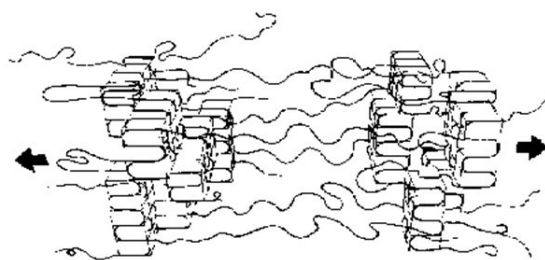


**Figure 1.6:** Helical structure of PP

The position of the methyl groups determines not only the configuration, but also the preferred conformation of the PP chain. Isotactic PP has the lowest intramolecular interactions in an alternating trans(T)-gauche(G) conformation, which gives the polymer a helical structure (a repeating 3/1 helix).

### 1.3.2.3 Crystallinity, Tacticity and Chain Conformations

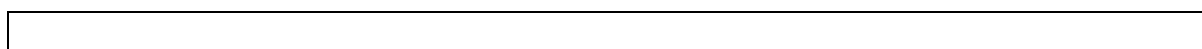
Polyolefins are normally semi-crystalline because the polymer is unable to crystallise perfectly due to kinetic and steric restrictions. Here the interphase between amorphous and crystalline parts of the polymer matrix plays an important role. Crystallite dimension are in the range 5-20 nm and the interphase region is *approx.* 0.5-3.5 nm (**Figure 1.7**)



**Figure 1.7:** Crystalline and amorphous regions in semi-crystalline polymers<sup>20</sup>

Chain segments residing in amorphous regions with connections to crystallites have restricted mobility. Following processing, oxidised chain-ends and terminal macro-alkyl radicals may be located within the amorphous or in the 'inter-phase' region. Accessibility-to and solubility-in the interphase region by antioxidants may be a factor in effective stabilisation performance.

During oxidation, free radicals may be captured by crystalline regions, where the concentration of oxygen is effectively zero. If the crystallites are very small then they cannot hold-on to the radicals for extended timescales, but larger crystallites are able to capture a greater portion of radicals. The fact that there is a lag in the time to oxygen absorption for iPP from the oxidation induction time (OIT) data<sup>21</sup>, suggests the role of chain termination at these sites in the early stages of polymer oxidation. **Figure 1.8** indicates with arrows potential free-valence migration pathways for radical capture by crystalline regions of polymer by linear recombination.



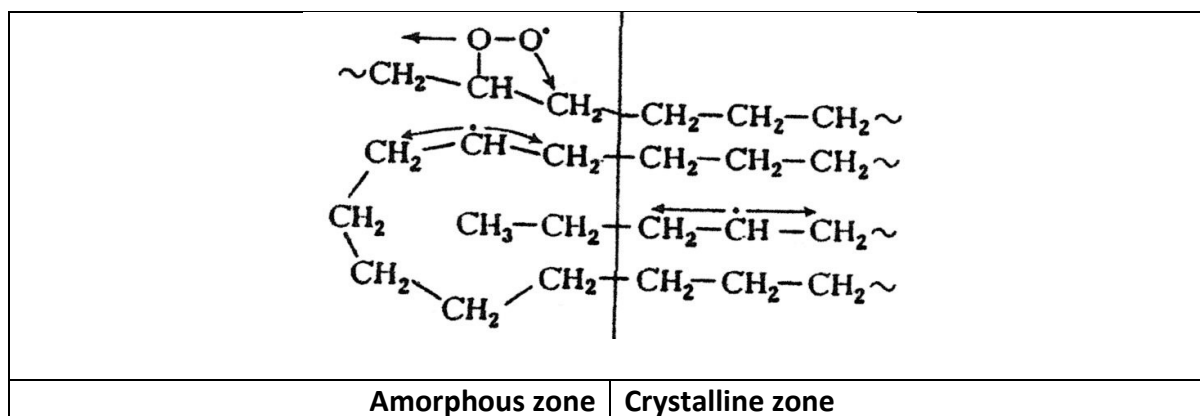


Figure 1.8: Free-valence migration routes for radical capture<sup>21</sup>

The role of tacticity and chain conformations will be considered in the propagation steps, since they have the greatest influence on hydrogen atom transfer.

### 1.3.3 Chain Branching

#### 1.3.3.1 Peroxides

Although it is the case that there is a first-order relationship between oxygen concentration and polymer hydroperoxides<sup>22</sup>, the nature of polymer hydroperoxides is rather ambiguous.

Only a fraction of the oxygen absorbed ( $1 \text{ mmol kg}^{-1}$ ) during oxidation is found in the form of hydroperoxide in polyolefins<sup>23</sup> compared with low molecular weight hydrocarbons<sup>24</sup>.

These reactions with oxygen, result in short blocks of polymer hydroperoxide groups in  $\beta$ -positions to each other: the concentrations of which will be determined by oxidation conditions.

About 50% of oxygen containing species may be extracted from oxidised polymer suggesting chain-scissions take place at small distances from such blocks leading to volatiles from oxidised and unoxidised chain segments. This in turn implies that oxidised groups are only formed in the polymer at later stages of degradation. Furthermore, it is likely that fragmentation of such blocks will lead to the formation of volatile hydroperoxides, which has implications for 'spreading' of oxidation.

It has also been suggested that the low amounts of polymer hydroperoxides may be due to short blocks facilitating  $\text{RO}_2\bullet$  decaying by chain termination<sup>25</sup>. If this were the case, it should be noted that this could not explain the large quantities of low molecular weight species in the early steps of oxidation.

The kinetics of decomposition of polymer hydroperoxides as-a-means-to identify different types of hydroperoxide structures (isolated, block, associated) has also been the subject of debate. Only in the very early stages of degradation does hydroperoxide decomposition approximate to a first-order process, thereafter decomposition follows a more complex rate law. For PP, containing isolated ROOH the rate of decomposition is high. However, this would also be true for blocks of ROOH that are H-bonded to each other, as this will lower their stability because bimolecular decomposition is facilitated (**Figure 1.9**). In contrast, ROOH adjacent to OH or CO groups would have increased stability by hydrogen bonding. The literature does discuss in detail the presence of ‘fast’ and ‘slow’ decomposing ROOH<sup>26, 27</sup> and isolated and associated ROOH<sup>28-31</sup>.

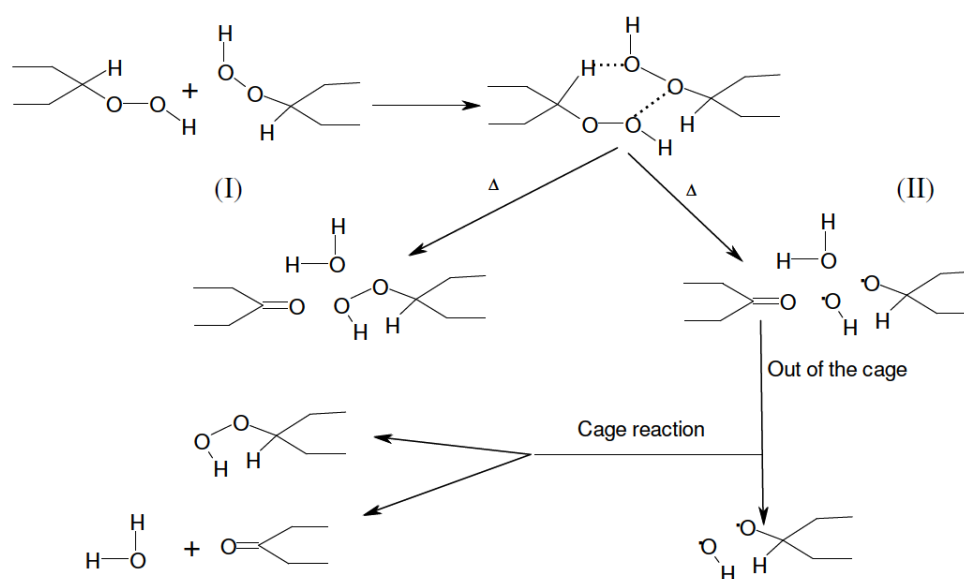


**Figure 1.9:** Bimolecular decomposition of hydroperoxides

In the presence of catalytic amounts of certain (transition) metal ions, hydroperoxides decompose readily at room temperature by a redox mechanism into radical products. The most active catalysts are those metals that are reduced or oxidised by one-electron transfer



e.g. Fe, Co, Mn, Cu, V, Ti. **(Scheme 1.4)** Metal deactivators are used to sequester metal ions preventing these reactions taking place. Metal deactivators function by chelating with transition metal ions to render them inactive as oxidation catalysts. The use of metal deactivators is most critical in applications where plastics are in direct contact with metal surfaces, such as wire and cable insulation and moulded parts having metal inserts. They are also useful to deactivate the transition metals present as impurities in some mineral fillers and inorganic pigments.

<b>Step 1:</b>	$\text{POOH} + \text{M}^{n+} \rightarrow \text{POO}\bullet + \text{M}^{(n-1)+} + \text{H}^+$
<b>Step 2:</b>	$\text{POOH} + \text{M}^{(n-1)+} \rightarrow \text{PO}\bullet + \text{M}^{n+} + \text{OH}^-$
<b>Overall:</b>	$2\text{POOH} \rightarrow \text{POO}\bullet + \text{PO}\bullet + \text{H}_2\text{O}$

**Scheme 1.4:** Redox decomposition of hydroperoxides by metal ions

Gugumus suggests that catalyst residues also have an important influence on the course of melt oxidation and further claims that this is most notable for the decomposition of hydroperoxides by chromium based (Phillips-type) catalysts. This author further states that, though not as obvious, this is similar in Ziegler-Natta (titanium-based) catalysts, which influence types of functional group formation<sup>32</sup>.

### 1.3.4 Termination

#### 1.3.4.1 Peroxyls

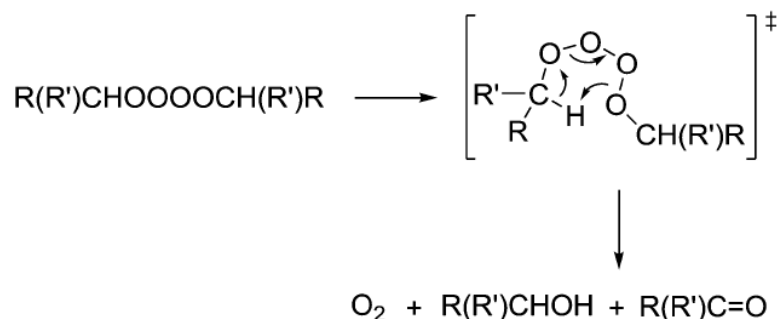
If peroxy termination is the preferred over hydrogen atom transfer then the character of functional groups primary, secondary, tertiary becomes a determining factor in autoxidation. In such a scenario, primary and secondary peroxy radicals would terminate to form non-radical products and not contribute to further chain-branching. On the other hand, tertiary peroxy radicals would terminate to form alkoxy radicals and in-turn hydroxy radicals that are able to undergo chain-transfer.

If peroxy termination is competitive with (or dominant over) peroxy transfer, then branch sites will be of prime importance in the degradation reactions of polyolefins. Indeed, several studies have demonstrated that autoxidation occurs at a faster rate in branched polymers<sup>33, 34</sup>.

#### 1.3.4.2 Bimolecular termination of secondary versus tertiary peroxy radicals

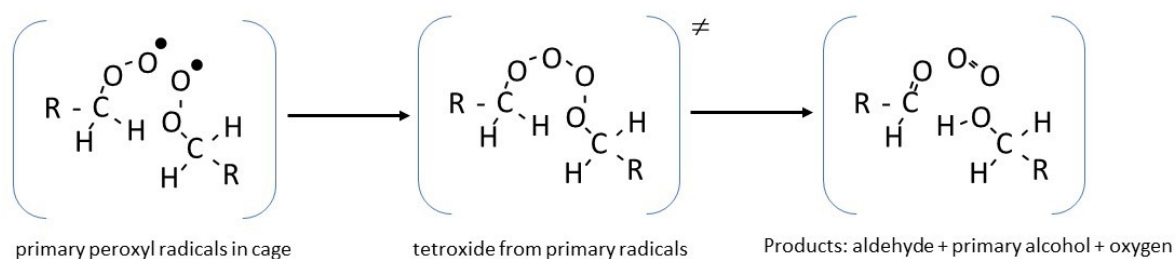
Bimolecular recombination of polymer peroxy radicals is worthy of attention because it would be expected that the rates of their reaction to be higher than observed, given that the reactions are diffusion-cage controlled. It is also of interest that the rate of recombination of tertiary peroxy radicals are several orders of magnitude (1000 x) slower than for secondary peroxy radicals<sup>35</sup>.

To date, products derived from bimolecular recombination of primary and secondary peroxy radicals has been accepted to take place according to the general mechanism proposed by Russell<sup>36</sup> (**Scheme 1.5**). Here is an intra-molecular rearrangement of the tetroxide to give inert products.

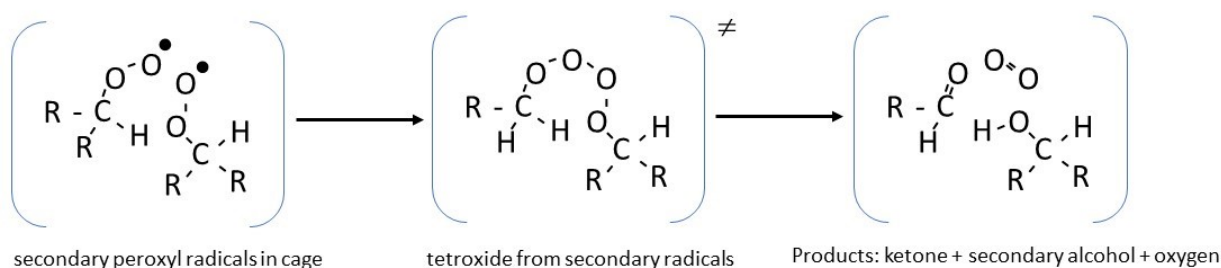


**Scheme 1.5:** Russell mechanism for chain termination by secondary peroxy radicals<sup>36</sup>

For primary peroxy radicals in the cage, this would lead to the formation of aldehydes, primary alcohols and oxygen and correspondingly ketones, secondary alcohols and oxygen would be formed from secondary peroxy radicals (Scheme 1.6 and Scheme 1.7).

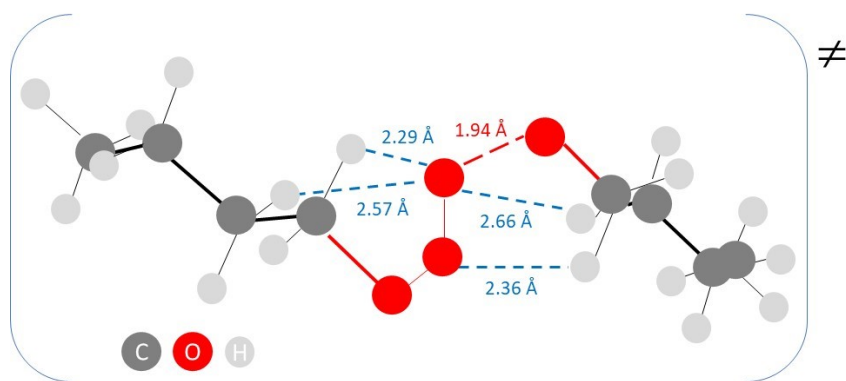


**Scheme 1.6:** Decomposition of primary peroxy radical via a tetroxide transition state into aldehyde, primary alcohol and oxygen

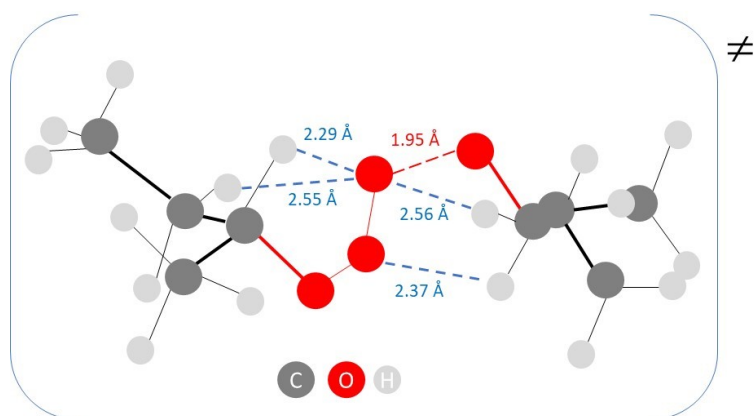


**Scheme 1.7:** Decomposition of secondary peroxy radical via a tetroxide transition state into ketone, secondary alcohol and oxygen

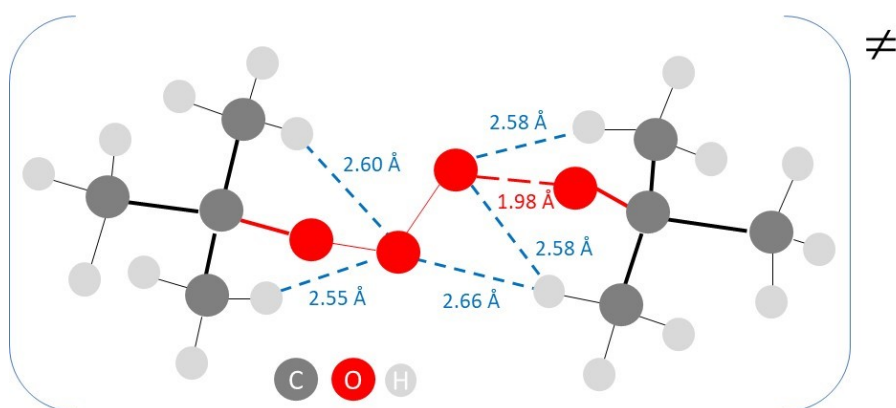
Because this mechanism is not available for tertiary peroxy radicals it has been used to explain the much faster rate of recombination of secondary peroxy radicals. However, recent information from high-level *ab initio* calculations suggests that for primary and secondary peroxy radical termination, a cage transition-state is formed, where evolving oxygen is stabilised by hydrogens at alpha-carbon positions. Cage cleavage takes place asymmetrically to give the inert products observed experimentally. Because such a cage decomposition to inert products is precluded for tertiary peroxy radicals, escape to yield alkoxy radicals is expected instead (**Structure 1.1**, **Structure 1.2** and **Structure 1.3**). On this basis, tertiary alkoxy radicals are more likely to escape the cage and undergo  $\beta$ -scission reaction generating further alkyl radicals. This means that chain propagation arises mainly from tertiary sites, consistent with the existing literature. It could be postulated that the nature of this transition-state dictates both the rate of decomposition of peroxy radicals to products, and the potential for interaction with antioxidants.



**Structure 1.1** Molecular model of transition state between primary peroxy radicals depicting asymmetric cleavage of oxygen (adapted from <sup>1</sup>)



**Structure 1.2:** Molecular model of transition state between secondary peroxy radicals depicting asymmetric cleavage of oxygen (adapted from <sup>1</sup>)

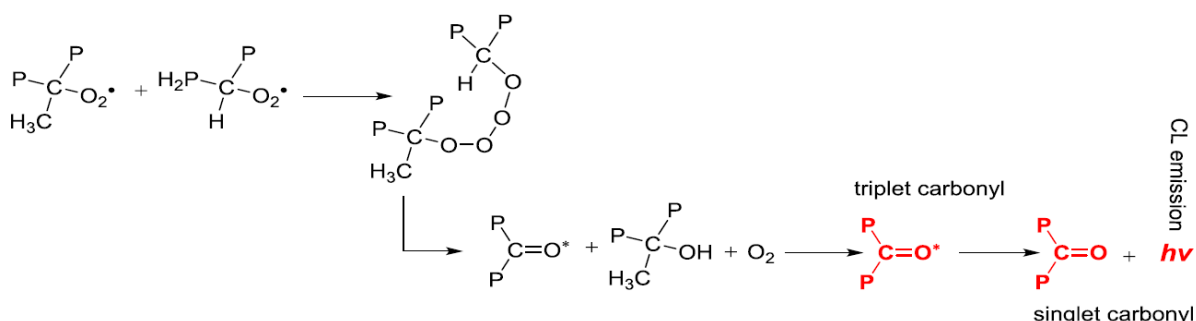


**Structure 1.3:** Molecular model of transition state between tertiary peroxy radicals (adapted from <sup>1</sup>)

#### 1.3.4.3 Monitoring hydroperoxide formation and peroxy decomposition

Many techniques have been employed to quantify the formation of peroxides<sup>37, 38</sup>, with quantification by iodometric methods being superseded by Fourier-transform infrared spectroscopy (FTIR) and Chemiluminescence (CL). As precursors for chain-branching, the types of peroxide formed (e.g. isolated, associated, primary, secondary, tertiary) are the subject of debate.

CL is increasingly being used as a tool to follow degradation. The CL itself is generally cited as arising, due to bimolecular termination reactions of peroxy radicals, via a tetroxide intermediate, according to the Russell mechanism.



**Structure 1.4:** Russell mechanism proposed to account for chemiluminescence in polyolefins

## 1.4 Loss of Polymer Oxidation Products: Volatiles, Leachates and Extractables

### 1.4.1 Volatiles from the polymer

Given the apparent complexities of polymer oxidation reactions it may be that the formation of volatiles, leachates and extractables can shed further light on the 'preferred' routes to degradation.

For polyolefins it is generally accepted that the VOCs generated during degradation differ only in their relative amounts as a function of the concentration of oxygen in the environment. The quantity of volatiles generated in an air environment is approximately 5-6 times less than that in an oxygen rich atmosphere and the onset time to generation of quantifiable amounts is delayed (approximately double).

The earliest studies on volatiles<sup>39, 40</sup> were able to detect only a limited range of volatiles. This comprised mainly water, carbon monoxide and dioxide. The latter studies in this selection were able to identify acetaldehyde as a major volatile followed by acetone, aldehydes and ketones.

As far back as the 1960s Bevilacqua and co-workers<sup>41</sup> suggested that an intramolecular reaction was the reason for the formation of acetic and formic acids as well as acetone (in addition to acetaldehyde and formaldehyde). This was the reason that low molecular weight analogues of PP and PE gave high oxidation yields when tertiary carbons were separated by a single carbon atom ( $\beta$ -attack) *c.f.* the low oxidation yields when tertiary carbon atoms were adjacent or separated by more than two carbon atoms in a row.

In the same decade (1969) Reich and Stivala<sup>42</sup> quantified the relative amounts of volatiles arising from thermal oxidation of polyolefins at 150°C showing that water was present in significant amounts followed by carbon monoxide and carbon dioxide, followed by aldehydes (formaldehyde and acetaldehyde) and carboxylic acids.

There has been an increased interest in the toxicological aspects of the degradation products of polymers in the last 40 years. Frostling, Hoff, Jabosson *et al* have used GC-MS to identify 47 volatile oxidation products. **Table 1.4** lists some of the volatile products of thermal degradation they identified in the temperature range 200 and 280°C<sup>43-45</sup>.

**Table 1.4:** Specific volatile products of PP thermo-oxidation of PP at 220-280°C

Hydrocarbons	Ethane; Propane; Butane; Ethene; Propene; Isobutene; Pentadiene; 2-Methyl-pentene; 5-Methyl-1-heptene; 2,4-Dimethyl-1-pentene
Aldehydes	<b>Formaldehyde; Acetaldehyde;</b> Acrolein; <b>Methacrolein;</b> Propanal; Butanal; 2-Methylpropanal; 3-Methylpentanal; 3-Methylhexanal, Octanal; Nonanal; Decanal; 2-Vinylcrotonaldehyde
Ketones	<b>Acetone;</b> Ethenone; 2-Butanone; 2-Buten-2-one; 1-Hydroxy-2-propenone; 1-Cyclopropylethanone; 3-Methyl-3-buten-2-one; 3-Penten-2-one; 2-Pentanone; 2,3-Buanedione; 1-Cyclopropyl-2-propanone; 2,4-Pentanedione; 4-Methyl-2-pentanone; 4-Methyl-2-heptanone
Acids	Formic acid; <b>Acetic Acid;</b> Propionic acid
Alcohols	Methanol; Ethanol; 2-Methyl-2-propen-1-ol
Ethers	2-Methylfuran; 2,5-Dimethylfuran

More recently, Andersson and Wesslén<sup>46</sup> examined the thermal oxidation of polyethylenes (PE-HD; PE-LD; PE-LLD) during film extrusion at 280°C with an 80 mm air gap between the die orifice and quench cooling. They demonstrated that the molecular structure of the PEs has a significant effect on the prevalent volatile degradation products (**Table 1.5**). It was noted that the linear PE-HD generated unsaturated alcohols and linear alkanes (e.g. decane, dodecane), while short-chain branched PE-LLD tended to produce branched alkanes. In contrast, the more highly branched PE-LD aldehydes (e.g. pentanal, hexanal, heptanal, octanal) tended to predominate.

**Table 1.5:** Chain length for volatiles observed from polyolefins<sup>46</sup>

PE-HD	C5>C6>C7>C4>>C2
PE-LD	C5>C4>C6>C7>>C2
PE-LLD	C5>C6>C4>C7>>C2

Heude and Co-workers have used an FTIR method to identify the key volatiles emanating from the oxidation of PP in both air and oxygen atmospheres. The types of volatiles observed remain the same though their relative amounts vary<sup>47</sup>.

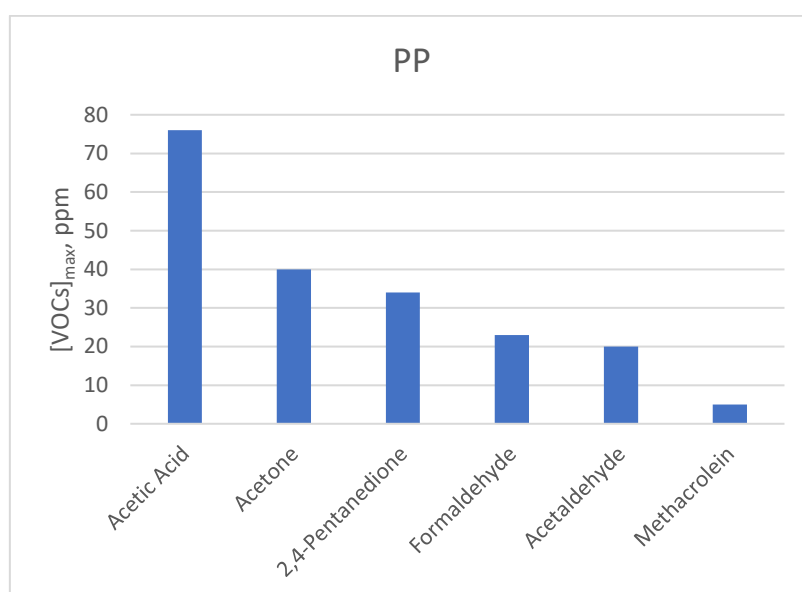


**Figure 1.10:** Volatiles arising from PP in oxygen detected by FTIR and mass spectrometry<sup>47</sup>

Their studies are supported by the earlier work of Chien and Kiang<sup>48</sup>, who attributed fragmentation of primary and secondary alkoxy radicals to main-chain scission, with or without HAT, to account for the range of volatile aldehydes and ketones observed experimentally for PP (Table 1.6).

**Table 1.6:** Alkyl radicals and volatile compounds from fragmentation of primary and secondary alkoxy radicals<sup>48</sup>

$-(\text{CH}_3)\text{CH}-\text{CH}_2-(\text{CH}_3)\text{CH}-\text{CH}_2-(\text{CH}_3)\text{CH}-\text{CH}_2-(\text{CH}_3)\text{CHO}\bullet$ (Secondary alkoxy)		$-\text{CH}_2-(\text{CH}_3)\text{CH}-\text{CH}_2-(\text{CH}_3)\text{CH}-\text{CH}_2-(\text{CH}_3)\text{CH}-\text{CH}_2-\text{HCHO}\bullet$ (Primary alkoxy)	
from	Volatile products	from	Volatile products
<b>C2-C1</b>	1° + acetaldehyde	<b>C2-C1</b>	2° + formaldehyde
<b>C3-C2</b>	2° + propanal + acetone	<b>C3-C2</b>	1° + propanal
<b>C4-C3</b>	1° + 3-methyl butanal + 2-pentanone	<b>C4-C3</b>	2° + 2-methylpropanal
<b>C5-C4</b>	2° + 3-methyl pentanal + 4-methyl-2-pentanone	<b>C5-C4</b>	1° + 2-methylpentanal
<b>C6-C5</b>	1° + 3,5 dimethyl hexanal + 4-methyl-2-heptanone	<b>C6-C5</b>	2° + 2,4-dimethylpentanal
<b>C7-C6</b>	2° + 3,5 dimethyl heptanal + 4,6-dimethyl-2-heptanone	<b>C7-C6</b>	1° + 2,4-dimethylhexanal

In a more sophisticated series of studies Bernstein *et al*<sup>49-51</sup> have attempted to characterise the origins in the polymer chain from which volatiles are produced by selective <sup>13</sup>C labelling of  $\gamma$ -irradiated PP in oxygen and for PP that has undergone thermal oxidation. Several mechanisms have been proposed to account for the volatiles observed. In conjunction with the generation of CO and CO<sub>2</sub> are important indicators of early degradation. Thornberg *et al.* used isotopic labelling of isotactic PP to determine the mechanism for their production<sup>51</sup>. According to their proposed mechanisms it is concluded that *ca.* 60% of CO<sub>2</sub> and >80% of CO originate from the methylene carbon. Although it is accepted that the tertiary carbon is responsible for most of the oxidation products that result from degradation of PP, it contributes only 33% of CO<sub>2</sub> and  $\leq$  5% of CO.

A more recent study by Arshad<sup>52</sup> examined the methodologies to evaluate volatiles from PP. Here a Micro-Scale Sealed Vessel (MSSV) approach was adopted and demonstrated enhanced sensitivity over standard methodologies adopted by industry standard VDA 278 which is the thermal desorption analysis of organic emissions for the characterization of non-metallic materials for automobiles. Collectively this work and that of other researchers illustrates that many of the differences in the volatiles observed during degradation of polyolefins may be attributed to methodological differences.



Because this study will evaluate the types and relative amounts from specified volatiles in specified polyolefin formulations, some of the key works of interest are discussed in more detail in the results and discussion section to enable clearer interpretation of the findings.

## 1.5 Antioxidants

The role of different types of antioxidant is often over-simplified because of their broad-based classification based on the basic autoxidation scheme (BAS) (**Figure 1.11**)

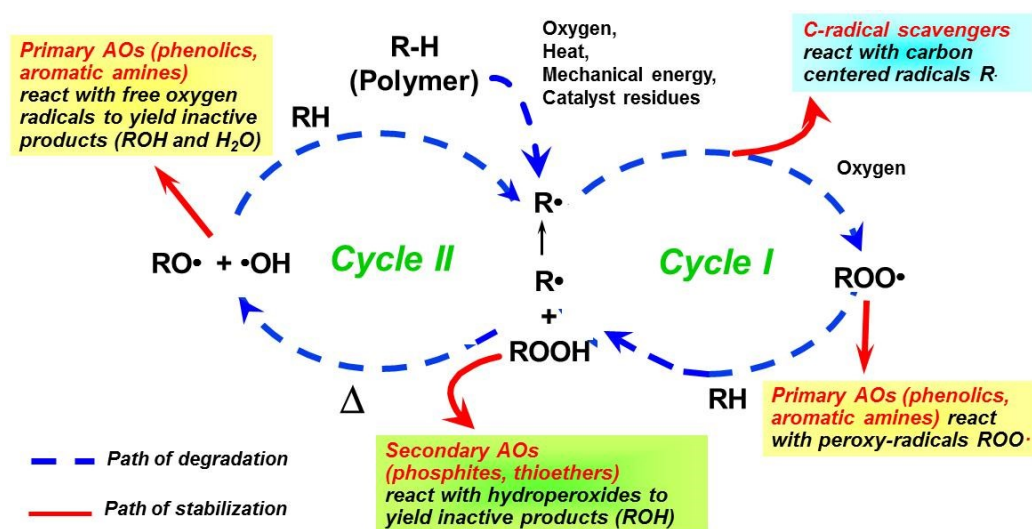


Figure 1.11: (Cycle 1 = Propagation; Cycle II = Chain Branching)<sup>20</sup>

The inhibition of hydrocarbon autoxidation can be achieved by the addition of compounds that interfere with either chain-initiation or chain-propagation. In the latter case, Radical-Trapping Antioxidants (RTAs) possess a labile H-atom and interrupt oxidation by H-atom transfer (HAT). Because the rate constant for HAT with chain-carrying peroxy radicals ( $k_{inh}$ ) is very much greater than the rate constant of propagation ( $k_p$ ), propagation being the rate-determining-step, only small amounts of RTAs (typical 0.05 wt%) are needed to inhibit oxidation in the polymer matrix.

The relative rates/extents of interaction of reactive species from polymer oxidation with the stabiliser classes, as depicted in the BAS given in **Figure 1.11**, are given in **Table 1.7**.

**Table 1.7:** Interaction of reactive species from polymer oxidation with stabilisers<sup>10</sup>

Type of Free Radical	Depiction	Hindered amine >N-H	Nitroxy radical >N-O•	N-Hydroxylamine >N-OH	Hindered phenol >O-H	Aryl Phosphites	Thioesters monosulphides
Hydroperoxide						Reacts	Reacts
Hydroxyl							Reacts
Allyl	R•	Reacts	Reacts				
Alkyloxy	RO•	Reacts very slowly			Reacts	Reacts	
Alkylperoxy	ROO•	Reacts very slowly			Reacts	Reacts	Reacts
Acyl	RC(=O)•		Reacts	Reacts slowly			
Acyloxy	RC(=O)O•	Reacts fast		Reacts fast			
Acylperoxy	RC(=O)OO•	Reacts fast		Reacts fast			

Traditionally, antioxidants have been subdivided into primary antioxidants (chain breaking acceptor (CBA) or chain-breaking donor (CBD)) and secondary antioxidants. Primary antioxidants are considered to scavenge radicals (Radical trapping agents (RTAs) for alkyl, alkoxy and peroxy radicals), whilst secondary antioxidants decompose peroxides. CBD primary antioxidants interrupt chain reactions by hydrogen atom transfer (HAT) and CBA primary antioxidants accept unpaired electrons to form inert compounds. The CBA mechanism usually applies to alkyl radicals and takes place in oxygen deficient environments. The term ‘transformation products’ is frequently used in the literature to describe the intermediate and resultant species formed during such reactions. Because many primary antioxidants can act by both CBD and CBA mechanisms, according to their transformation products, it is implied that inhibition of oxidation of polymers by antioxidants is not the simple process implied by the BAS<sup>17</sup>.

It is likely that this categorization has partly contributed to some of the apparent contradictions regarding the performance of antioxidants across the range of processing and

service-life temperatures. It can be seen in **Figure 1.12** that whilst phenols are relatively efficient antioxidants across the entire range of temperatures, encompassing processing and service-life of polymers, phosphites, thiosynergists and amines are not as successful<sup>20</sup>.

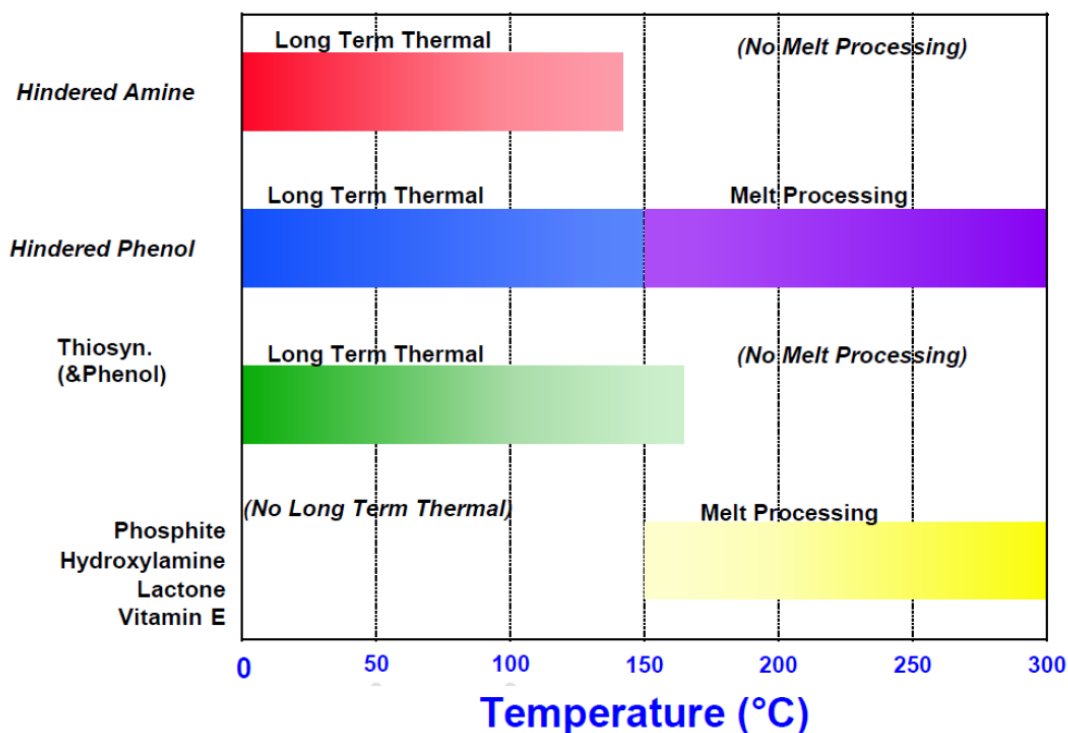
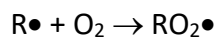


Figure 1.12: Derived from <sup>20</sup>

This poses the question as to why phosphites are good antioxidants at processing temperatures but not at service-life temperatures and *vice-versa* for thiosynergists. Furthermore, why are hydroxylamines more effective at processing temperatures and hindered amines at service-life temperatures?

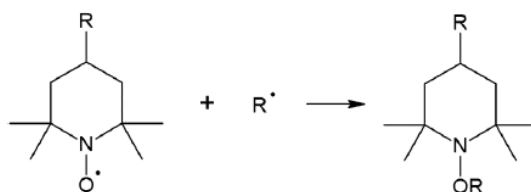
### 1.5.1 Inhibition of oxidation by scavenging alkyl radicals (R•) [CBA Antioxidants]

The high reaction rates of alkyl radicals with oxygen during chain propagation (**Equation 1.3**) means that for the-majority-of processing and service-life situations the concentration of R• is very much less than that of RO<sub>2</sub>•.

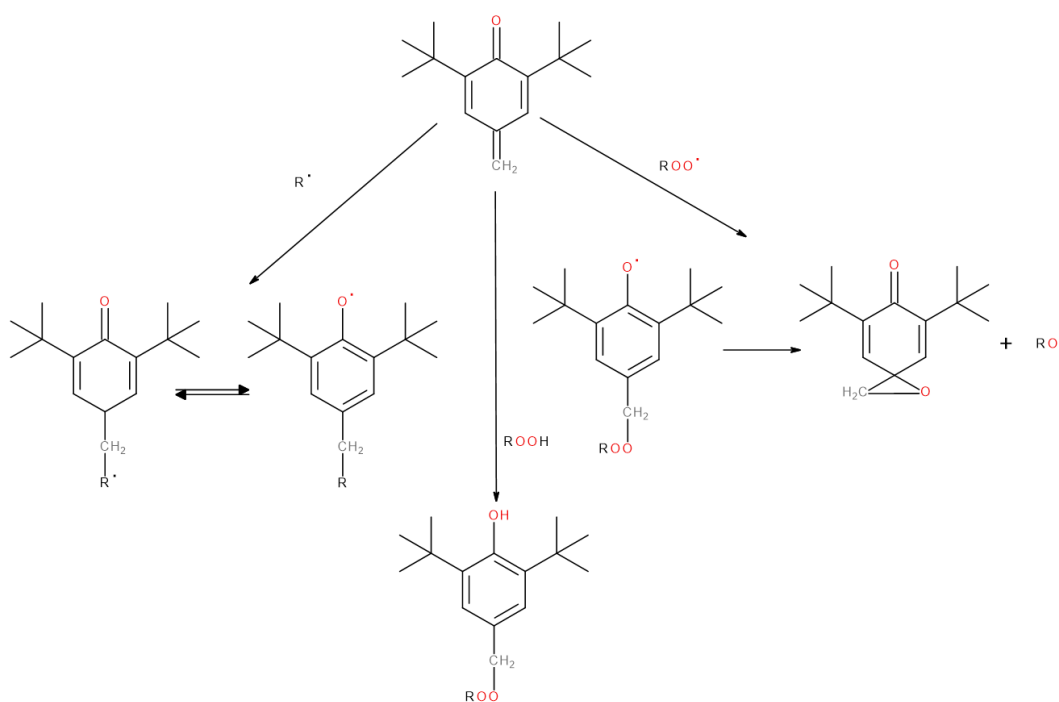


(Equation 1.3)

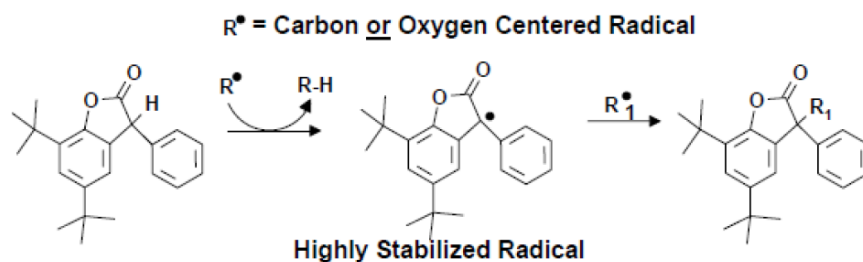
A-number-of antioxidant structures have been examined as inhibitors of alkyl radicals, namely nitroxyls (**Scheme 1.8**), quinones (**Scheme 1.9**) and more recently aryl benzofuranones (lactones) (**Scheme 1.10**). Nitroxyls and quinones are transformation products of aminic and phenolic antioxidants respectively.



**Scheme 1.8:** Reaction of nitroxyl radicals from hindered piperidine with polymer alkyl radicals



**Scheme 1.9:** Reaction of quinone from hindered phenols with polymer alkyl radicals



**Scheme 1.10:** Reaction of aryl benzofuranone with polymer alkyl radicals

Benzofuranones are efficient antioxidants arising from the HAT ability of the parent molecules. The highly stabilised radical intermediate that is formed is a particularly good alkyl radical acceptor. Quinones on the other hand are as efficient since there is a reduced resonance stabilisation of the radical, with scavenging ability dependent on substituents in the phenyl ring. According to the Denisov Cycle<sup>11</sup> there is a catalytic activity of amines/nitroxyls in scavenging radicals. The fact that this is evident at low concentrations of the latter to compete more effectively than oxygen for alkyl radicals makes the Denisov cycle, as it is currently cited in the literature, questionable. Recent molecular modelling studies have extended the Denisov Cycle to account for this<sup>53</sup>.

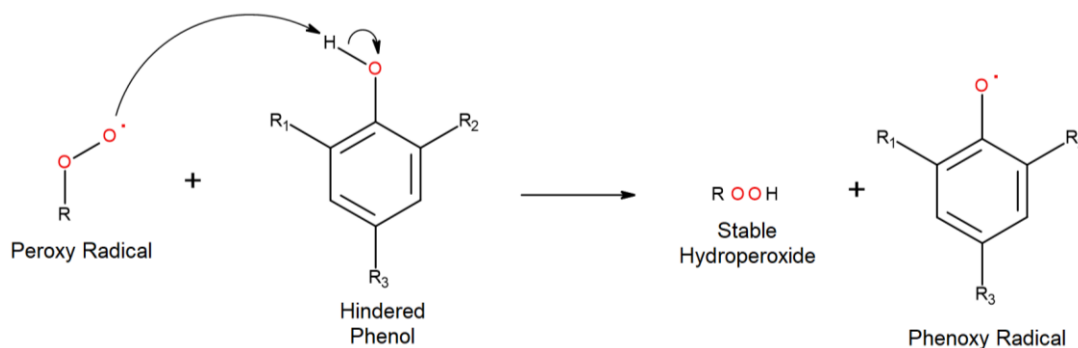
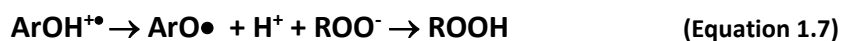
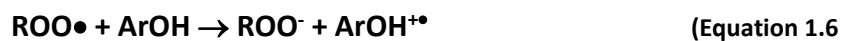
## 1.5.2 Inhibition of oxidation by scavenging peroxy radicals ( $RO_2^\bullet$ )

### 1.5.2.1 Phenolic Antioxidants

Phenols are generally considered to be more reactive with the higher concentrations of peroxy radicals (in comparison to  $R^\bullet$ ). The reaction of phenol with peroxy radicals in non-polar media to give hydroperoxide and phenoxyl radical has been thought for many years to occur by a hydrogen atom transfer (HAT) mechanism (**Scheme 1.11, Equations 1.4 and 1.5**).



As opposed to an initial electron transfer (ET) mechanism followed by proton transfer (**Equations 1.6 and 1.7**).



**Scheme 1.11:** Reaction mechanism between hindered phenol and peroxy radical

Choosing the type of hindered phenol will play a part in the stabilisation of the polyolefin. For example, fully hindered phenols are generally known to be more effective than partially hindered phenols. This is due to fully hindered phenols having two tertiary-butyl groups on the 2- and 6- positions in the benzene ring that can prevent self-condensation of phenols, along with a substituent on the 4- position i.e. they have no hydrogen atom on the  $\alpha$ -carbon (so no tautomeric benzyl radical formation is possible). This in turn, shields the newly formed phenoxyl radical from further degradation. A common example of a fully hindered phenol is Butylated Hydroxytoluene (BHT) (**Figure 1.13**).

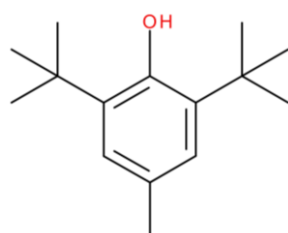


**Figure 1.13:** The structure of BHT

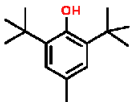
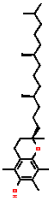
The reason for this is the positioning of the tertiary-butyl groups (*ortho* position) on the aromatic ring, this impacts the bond dissociation energy of the hydroxyl group as hydrogen bonding is increased when substituents are added on to the *ortho* and *para* positions. This is evidenced by many commercial hindered phenolic antioxidants, which have two tertiary-

butyl groups on the *ortho* position, followed by a substituent group on the *para* position. This makes the resulting phenoxy radical, relatively stable, so that it does not contribute further to polymer oxidation via electron delocalisation or resonance, this in turn prevents further abstraction of hydrogen from the polymer.

However, some studies have shown that high steric hindrance is also responsible for a low radical scavenging rate and by decreasing the steric hindrance, more radicals can be scavenged more efficiently. This is mainly effective during processing conditions, where the oxygen concentration is lower, and the life span of alkyl radicals is increased long enough for the hindered phenol to react with the radical. After the processing stage, where oxygen concentration is increased dramatically, the lifetime of alkyl radicals is reduced long enough that alkyl radical scavenging will not be possible, so in this instance, fully hindered phenols are more effective than less hindered phenols<sup>54</sup>.

The ability of an antioxidant to act as HAT agents is linked to its bond dissociation energy (BDE). Because of the highly delocalised electron in the phenoxyl radical, the driving force for HAT means that phenols have relatively weak O-H bonds. The BDEs are close to the values of the O-H of a hydroperoxide but can be improved by substitution of electron-donating (e.g. tertiary butyl) groups, which decrease the BDE and lead to faster HAT reactions with peroxy radicals. For example,  $\alpha$ -tocopherol reacts approximately 1000x faster with peroxy radicals than most phenols and its BDE is significantly lower.

**Table 1.8:** Antioxidant HAT rate constants ( $k_{inh}$ ) and bond dissociation energies (BDEs)

						
	BHT		$\alpha$ -tocopherol (Nature's limit)			
$k_{inh}$ ( $M^{-1} s^{-1}$ )	$10^4$	$10^5$	$10^6$	$10^7$	$10^8$	$10^9$
BDE (kcal/mol)	79.9		77.2			



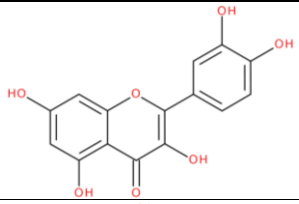
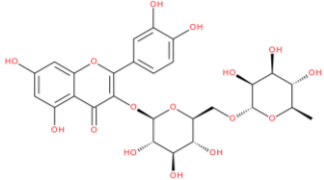
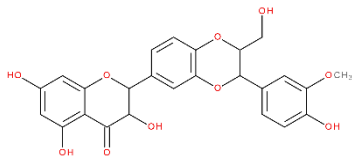
Barrierless H-atom transfer

Although the chemistry of synthetic antioxidants in polyolefins is a mature field, the chemistry of natural phenols has been of interest relatively recently. The impetus for this is more stringent requirements to meet environmental concerns, especially low toxicity. As a whole, most journals agree HAT from the phenolic hydroxyl group is the main reaction pathway to effective radical scavenging<sup>55</sup>. However, the hydrogen atom transfer is dependent on a few factors: such as the number and position of the phenol group, the solubility of the AO in the reaction solvent and the bond dissociation energy (BDE) between the oxygen atom and the hydrogen atom.

The table below illustrates various examples of natural phenols and their BDE. Initial observations from the table suggests that, as the number of hydroxyl groups increase in the compound, the activation energy of hydrogen abstraction decreases allowing easier hydrogen atom transfer. However, this decrease in the energy barrier is only observed if the additional hydroxyl groups are in the *ortho* position, only a small change in energy was observed if the hydroxyl groups were situated in the *meta* and *para* position<sup>56</sup>.



**Table 1.9:** Physical properties of selected natural phenols

Natural AO	Structure	No of OH groups	BDE (kcal/mol)	Mp (°C)	Solubility in PE (ppm)
Quercetin		5	72.9	316	19
Rutin		10	80.4	135	24
Silymarin		5	87.9	167	54

#### 1.5.2.2.1 $\alpha$ -Tocopherol

Vitamin E is the most commercialised natural hindered phenolic antioxidant and the one that is most widely used<sup>57</sup>. It is mainly found in majority of oils in vegetables, Vitamin E refers to eight different molecules, half consists of tocopherols and the other half is tocotrienols, which are all very similar in terms of structure.

In terms of the most efficient and active antioxidant out of all eight variations of vitamin E, goes to ' $\alpha$ -tocopherol'<sup>58</sup>. Apart from aqueous solutions, the antioxidant is easily soluble in oils and many organic solvents. One of the advantages of  $\alpha$ -tocopherol is that only very low concentrations are needed for it to improve polymer performance significantly<sup>59</sup>. The excellent performance of  $\alpha$ -tocopherol is linked with its chemical structure in comparison to many synthetic fully hindered phenols such as **Phenol 5** (industry standard), Irganox 1330™, 3114™ etc. These synthetic phenol AO are highly reliant on their BHT (**Figure 1.13**) functionality for their AO properties, however, due to their higher molecular weight, their volatility decreases with respect to BHT. This is why  $\alpha$ -tocopherol has improved HAT ability compared to its synthetic analogues.

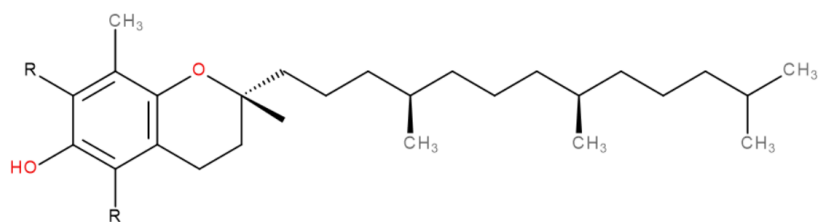
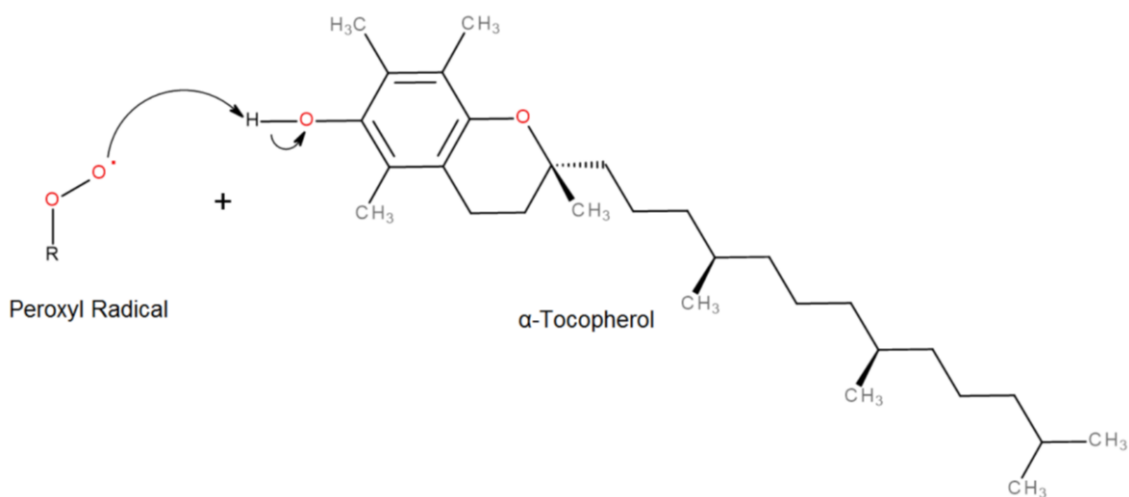
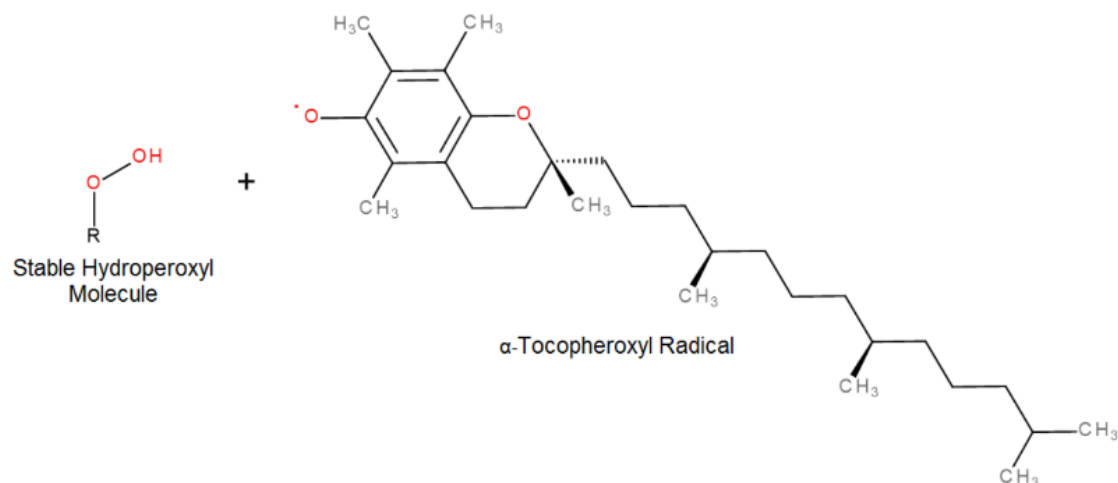


**Figure 1.14: Structure of  $\alpha$ -tocopherol.**

One of the reasons why  $\alpha$ -tocopherol is an effective AO is because of its high reactivity (due to the compound being highly soluble in oil, acetone, ethanol, ether and various other organic solvents) with fatty acid peroxy radicals, this is why it is known as the best lipid soluble antioxidant.  $\alpha$ -tocopherol is classed as a primary antioxidant; as mentioned above, this means that during the primary oxidation cycle, the AO disrupts the free-radical chain of oxidative reactions by having its hydrogen abstracted from the phenolic hydroxyl group and being donated to the free peroxy radicals. This stabilises the reaction and prevents the reaction to propagate or initiate further oxidation of lipids as illustrated below.



**Scheme 1.12:** Reaction mechanism between Peroxyl radical and  $\alpha$ -tocopherol. Peroxyl radical abstracting Hydrogen from  $\alpha$ -tocopherol. 'R' group represents the Polymer.



**Scheme 1.13:** Reaction showing  $\alpha$ -tocopheroxyl radical being formed with stable Hydroperoxyl molecule as a result of the reaction in **Scheme 1.12**.

The reaction with the peroxy radicals and the  $\alpha$ -tocopherol happens extremely fast that it strips the radicals from the molecule, ensuring that further reactions are prevented.

Another reason why  $\alpha$ -tocopherol is an effective antioxidant, according to Wijtman *et al*, is because it is a relatively stable radical with low reactivity. This is due to the delocalization of the unpaired electrons over the aromatic ring. The natural AO will only react with either a Peroxyl radical or another tocopheroxyl radical to form inert stable molecules<sup>60</sup>. However, it has been found from Houlihan *et al*, that synthetic AO's can better  $\alpha$ -tocopherol in terms of effectiveness<sup>61</sup>.

Al-Malaika with others have carried out extensive studies on the mechanisms and performance of  $\alpha$ -tocopherol, the studies concluded that the performance of  $\alpha$ -tocopherol surpasses the effect of synthetic phenolic AO<sup>62</sup>. However, which particular functional group of the  $\alpha$ -tocopherol that gives the strong antioxidant effect is open to question. One widely used commercial synthetic antioxidant such as **Phenol-5** depends on its 'BHT' functional group to impart its antioxidant effect on to the polymer. In terms of major structural differences between  $\alpha$ -tocopherol and BHT is that, BHT lacks a long carbon chain that  $\alpha$ -tocopherol has. And BHT has two tertiary-butyl groups surrounding the hydroxyl group whilst  $\alpha$ -tocopherol has only methyl groups surrounding its hydroxyl group<sup>63</sup>.

One particular study, by Howard and Ingold, aimed to establish which group on the aromatic ring of the  $\alpha$ -tocopherol gave the greatest AO effect during the reaction with peroxy

radicals. They discovered that the AO effect of  $\alpha$ -tocopherol was significantly improved by the presence of the oxygen in the *para* position along with the surrounding methyl groups in proximity to the hydroxyl group. In comparison to the tertiary-butyl groups on the BHT molecule, the AO effect was much greater; this could be due to steric hindrance of the tertiary-butyl groups surrounding the hydroxyl group<sup>64</sup>. In addition, further evidence from other authors who found this increase in AO activity from the *para* oxygen have been reported. However, BHT was only compared to BHA, the BHA molecule has an oxygen in the *para* position to the hydroxyl group which is responsible in its increased AO effect compared to BHT<sup>65</sup>.

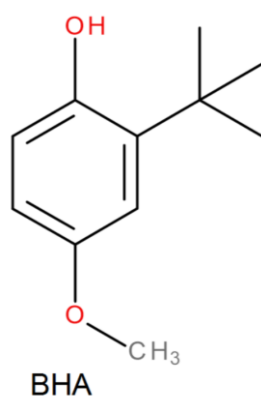


**Figure 1.15:** BHA compound

Ingold *et al* also went on to investigate the effects of the long carbon chain on the  $\alpha$ -tocopherol. The comparison was between the  $\alpha$ -tocopherol and 2,2,5,7,8-Pentamethyl-6-chromanol (PMHC), PMHC is an identical molecule to the  $\alpha$ -tocopherol only without the long alkyl tail. They discovered that the carbon tail had no effect on AO reactivity and that only the *para* Oxygen and the methyl groups in proximity to the hydroxyl group led to increased AO activity<sup>66</sup>.

#### 1.5.2.2.2 Quercetin

Quercetin is a particularly efficient flavanol found in red onion<sup>67</sup>, tea<sup>68</sup> and grapes<sup>69</sup>. What makes Quercetin appealing in the polymer industry is the fact that it has already been proven as an AO in the human body; the mechanism that exhibits the AO effect could be similar to that of  $\alpha$ -tocopherol reported. Another unique property of Quercetin is that it has many hydroxyl groups, which can aid in the transfer of hydrogen abstraction to peroxy radicals forming stable hydroperoxides.

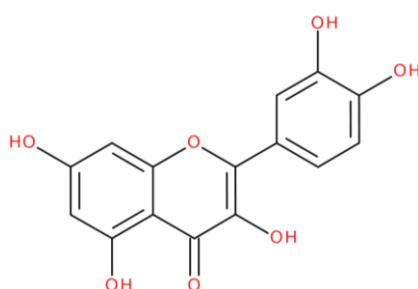


**Figure 1.16:** Structure of Quercetin

In terms of stability of polyolefins, Quercetin has shown promise as an AO, being used successfully in low-density polyethylene (LDPE) by increasing the thermal stability with small additions of about 0.20 wt.%. Pukánszky *et al*<sup>70</sup>, have likened Quercetin to the industry's synthetic equivalent of **Phenol-5** (used in the present study). The comparison was made in terms of stability as individual phenolic AO and also with PE as a combination with secondary phosphorous stabilisers. They reported that even at low concentrations of 50 ppm, Quercetin prevents the formation of long chain branches and at 250 ppm, it renders the polymer sufficient for long term stability. The only disadvantages of Quercetin is that it highly colours the polymer, as do most natural AO, the solubility in PE is low and has a high melting temperature. If these problems were addressed, Quercetin could be seen as a long-term replacement for **Phenol-5**<sup>70</sup>.

Another study by Samper *et al*<sup>71</sup>, studied the effects on the stabilisation of PP using Quercetin and other flavonoids such as Chrysin, Hesperidin, Naringin and Silibinin. To measure the thermal stability of the polymer, the PP was assessed in an oxidising atmosphere using DSC

(differential scanning calorimetry). Concerning the flavonoids themselves, the effectiveness as thermal stabilisers was quantified using TGA (thermogravimetric analysis). These workers found that out of all the flavonoid compounds used, Quercetin and Silibinin provided the best thermal stability in PP<sup>71</sup>.

#### 1.5.2.2.3 Rutin

Rutin is another member of the flavonoid family; more specifically this natural AO is classed as a flavonoid glycoside. Rutin is closely related to Quercetin as it is the glycoside of the Quercetin formed with the rutinose disaccharide. As for Rutin, it is found in fruits such as citrus based fruits and apples<sup>72</sup>. In bio-systems Rutin has been found to protect the heart and arteries<sup>73</sup>.

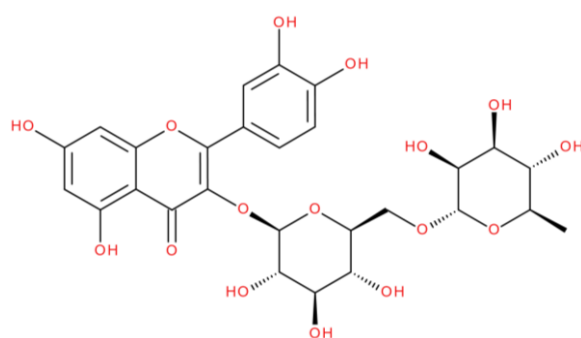
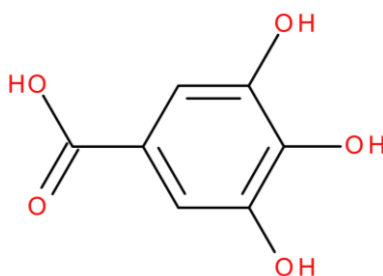


Figure 1.17: Rutin structure

Kirschweng *et al*<sup>74</sup>, studied the effects of Rutin as a processing stabiliser in PE aiming to circumvent the drawbacks of many natural AOs: high melting temperature, low solubility a high yellowness. Using melt flow index measurements (MFI), Rutin proved to be just as efficient as a stabiliser as Quercetin. This was mainly due to the identical hydroxyl groups found in both compounds. However, with regards to solubility, very little difference was observed. This may stem from the increased amount of hydroxyl groups in the compound, especially in the saccharide groups, which may not enable the solubility in polyolefins. The other major disadvantage of using Rutin was that it was prone to partially decompose at high processing temperatures<sup>74</sup>.

#### 1.5.2.2.4 Gallic acid

Unlike Quercetin and Rutin, Gallic acid does not have many members within their group. In fact, phenolic acids can only be divided into two subgroups; these can be hydrobenzoic acids or hydrocinnamic acids, where, gallic acid is based on the hydrobenzoic acid structure. The radical scavenging mechanism is similar to the flavonoids, where HAT occurs from the phenol group. However, the efficiency of the phenolic acid depends on the actual structure of the compound<sup>75</sup>.

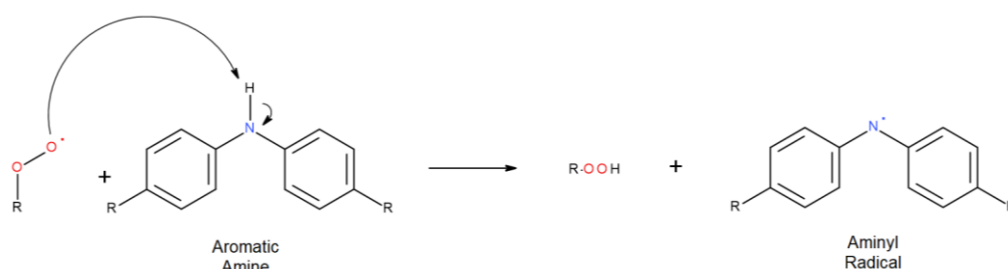


**Figure 1.18:** Gallic acid structure

Normally, most phenolic acids have limited thermo-oxidative stability and practically zero solubility in non-polar polymer matrices, this can lead to poor processing stabilisation effects<sup>76</sup>. However, one study measured the thermal stability, AO activity and photo-oxidation stability of standard polyphenol solutions. Using Catechin, Gallic Acid and Vanillic Acid as the chosen natural AO, these AO were subjected to exposure at increasing temperatures of 60°C, 80°C and 100°C for four hours and then analysed after the exposure times. The natural AO with the highest radical scavenging ability was the Gallic acid followed by the catechin and vanillic acid, the stability against UV radiation was high in general for all AO, however the highest stability under UV light was observed for Gallic acid followed by vanillic acid.

### 1.5.2.3 Aminic Antioxidants

Diphenylamines and hindered amine light stabilisers [HA(L)S] are commonly added to petroleum-based products. Like phenols, amines transfer their iminic H-atom to peroxy radicals via a *syn*-transition-state. This allows the interaction of  $\pi$ -HOMO of the diphenylamine and the  $\pi^*$ -SOMO of the peroxy (**Scheme 1.14**). Compared with phenols, amplifying the HAT reactivity of aromatic amines is more challenging.



**Scheme 1.14:** Reaction mechanism between aromatic amine and peroxy radical

### 1.5.2.4 Organosulfur Antioxidants

Relative to phenols and amines the HAT chemistry of organosulfur compounds is less-well explored.

It has recently been shown that precursor polysulfides and their oxides can undergo (non-HAT) homolytic substitution reactions with peroxy radicals.

**Table 1.10:** Organosulphur HAT rate constants ( $k_{\text{inh}}$ ) and bond dissociation energies (BDEs)<sup>53</sup>

	RSSH	RSH	RSOH	RSO <sub>2</sub> H	RSO <sub>3</sub> H
$k_{\text{inh}}$ ( $\text{M}^{-1} \text{s}^{-1}$ )	$\sim 10^6$	$< 10^3$	$\sim 10^7$	$\sim 10^1$	—
BDE (kcal/mol)	$\sim 70$	$\sim 89$	$\sim 72$	$\sim 78$	$\sim 107$



Sulfur has a high nucleophilicity and oxidizability resulting in the formation of sulfur acids. This sequence of events is important. Although thiols have relatively weak S-H bonds and in this respect are used to reduce alkyl radicals in synthetic reactions, they are not particularly efficient HAT reagents to peroxy radicals. However, sulfenic acids are very effective HAT agents, approximately 10000x better than thiols. The preferred geometry for this reaction is via a *syn* transition-state (**Figure 1.19**).

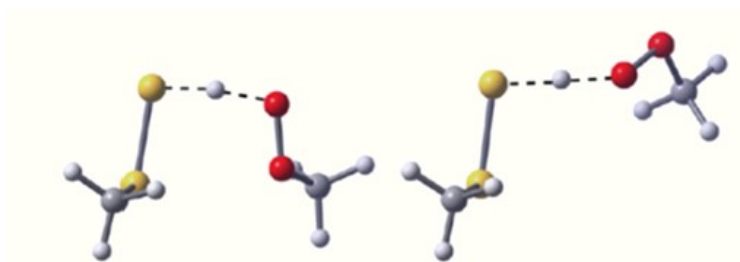
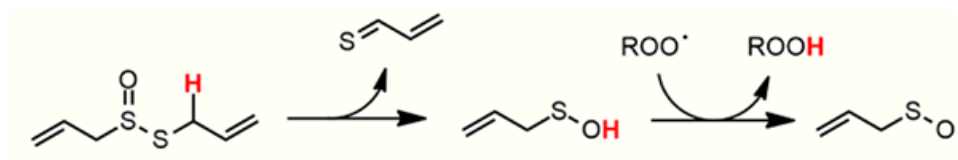
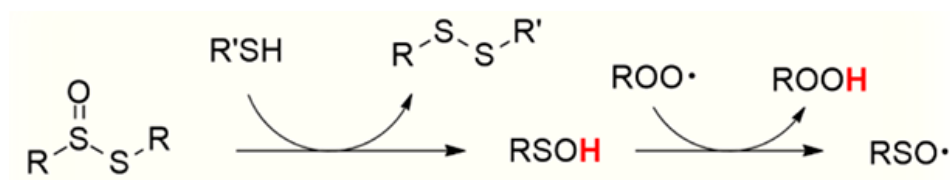


**Figure 1.19:** *syn* versus *anti* HAT transition-state structures<sup>53</sup>

The variety of reactions that may result from this (**Schemes 1.15 to 1.17**)

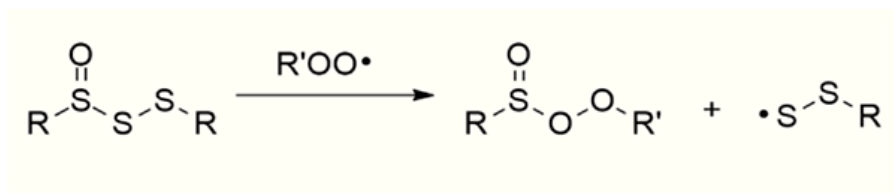


**Scheme 1.15:** Cope-type elimination followed by HAT<sup>53</sup>



**Scheme 1.16:** Nucleophilic substitution followed by HAT<sup>53</sup>

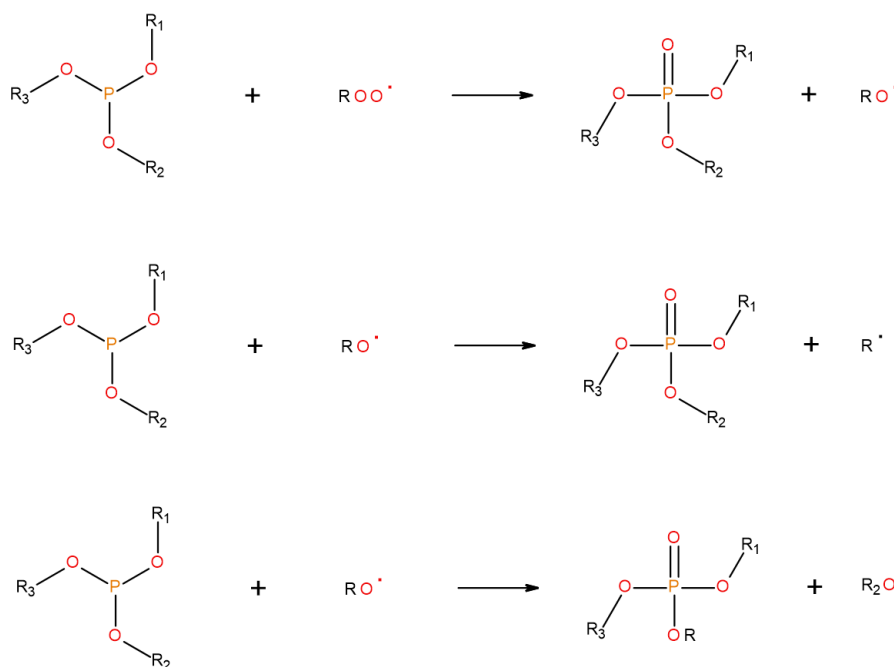
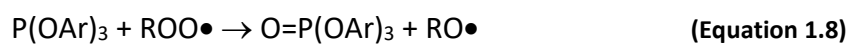




**Scheme 1.17:** Bimolecular homolytic substitution<sup>53</sup>

### 1.5.2.5 Organophosphite Antioxidants

At polymer processing temperatures, the RTA activity of aromatic phosphites is comparable<sup>27</sup>. If not better than, hindered phenolic antioxidants, although further polymer radicals are generated as part of this activity, so chains are not effectively terminated (**Equations 1.8 to 1.10** and **Scheme 1.18**).



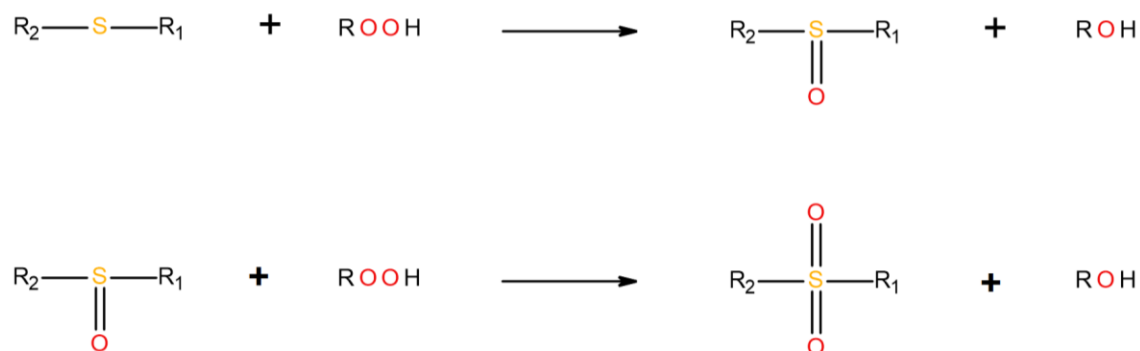
**Scheme 1.18:** Phosphite reactions with peroxy and alkoxy radicals.

### 1.5.3 Inhibition of oxidation by decomposing polymer hydroperoxides (ROOH)

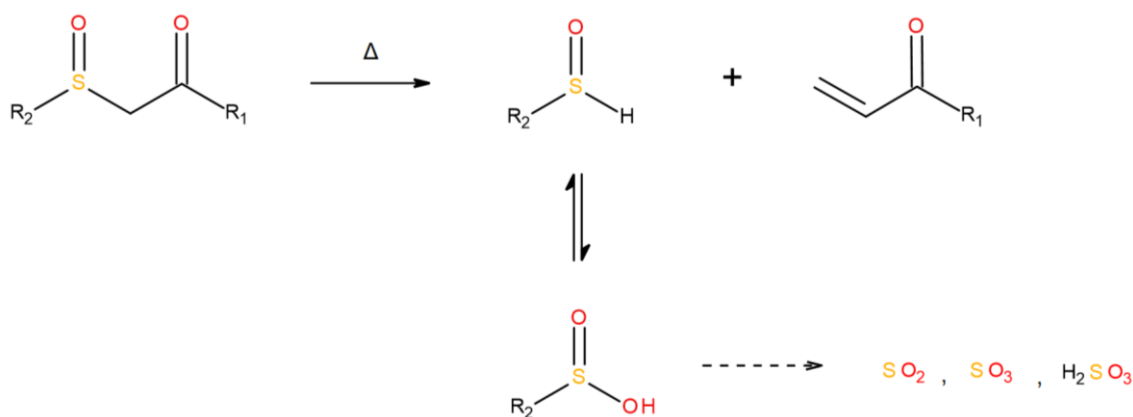
Because the formation and decomposition of polymer hydroperoxides initiates oxidation of new chains (i.e. is a degenerate chain-branching process) then inhibition is key to suppressing overall oxidation rate. Here sulphides/sulphoxides/thioesters and phosphites/phosphonates are effective in converting ROOH to non-radical products (ROH) by a redox mechanism and as such are termed preventive antioxidants.

#### 1.5.3.1 Organosulfur Antioxidants

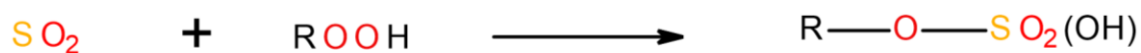
The sulfur reacts stoichiometrically with hydroperoxide forming the sulfur oxide. Sulfenic acid is then formed through thermal decomposition. Another possible reaction is the formation of the dioxide. Starting with sulfenic acid and other sulfur containing oxidation products, further oxidation with hydroperoxide may lead to sulfuric acid. The overall reaction sequence contributes over-stoichiometrically with respect to the used thiosynergist, because sulfur containing acids act catalytically in the decomposition of hydroperoxides (**Schemes 1.19 to 1.21**).



**Scheme 1.19:** Mechanism of thioethers as hydroperoxide decomposers



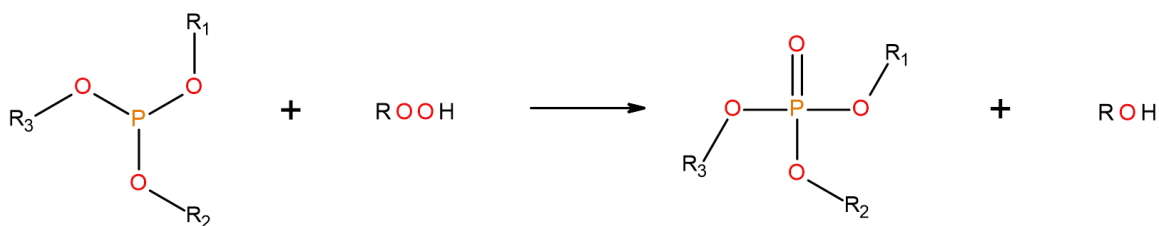
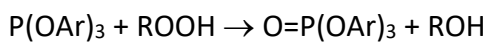
**Scheme 1.20:** Thermolysis of thioethers to form sulphenic acid



**Scheme 1.21:** Reaction of sulphur dioxide decomposing hydroperoxides

### 1.5.3.2 Organophosphite Antioxidants

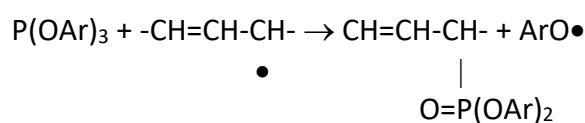
Hindered aromatic phosphites function as stoichiometric decomposers of hydroperoxides



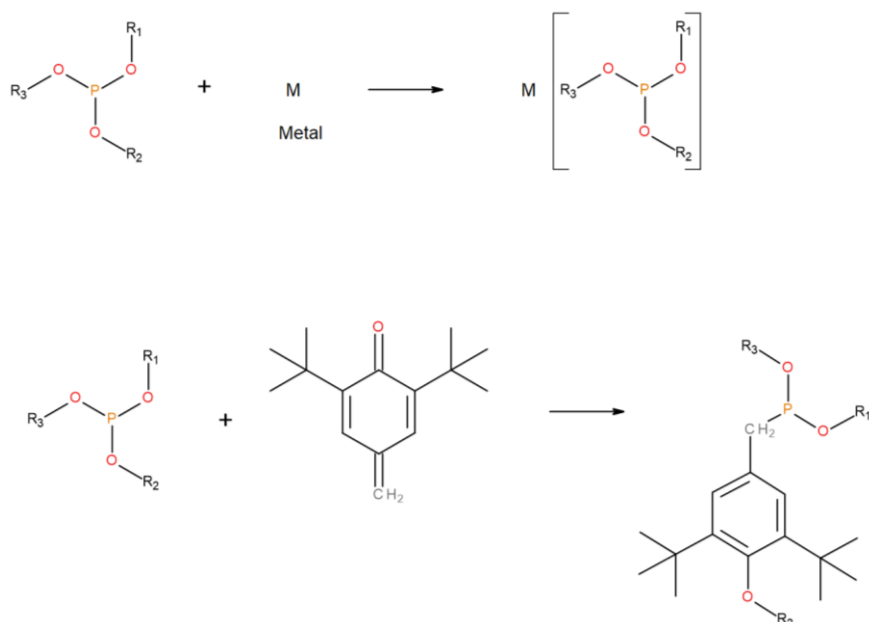
**Scheme 1.22:** Decomposition reaction of a typical phosphite with hydroperoxide.

They can also:

- React with unsaturated (vinyl) groups in the polymer



- Prevent discolouration by coordination with transition metal complexes and reaction with quinonoid species generated as transformation products from phenols



**Scheme 1.23:** Mechanisms of phosphite reactions, which improves colour

#### 1.5.4 Issues with Antioxidants

##### 1.5.4.1 Colour formation from Antioxidant Transformation Products

Another common issue hindered phenols experience is its propensity to undergo colour changes, mainly a yellowish tint colouring on the polymer. Once the phenols have donated their hydrogens to the peroxy radicals, the newly formed phenoxy radicals can be transformed into conjugated quinoidal compounds, such as a stilbene quinone structure, which are highly conjugated and yellow to orange in colour<sup>77</sup>.

#### 1.5.4.2 Loss of Antioxidants and Antioxidant Transformation Products: Volatiles and Extractables

It is one of the ironies of polymer stabilisation is that the very reactions required to inhibit oxidation may lead to loss of transformation products of antioxidants as volatiles or as low molecular weight species that can be leached or extracted to the environment. Strictly, extractables are species are potentially released to the environment and leachates represent those species that are released to the environment in practice, from this point they will be referred as extractables.

More recently, studies that examine the potential toxicity of fragments arising from AOs and leached to the environment, under both processing and service-life conditions have become of interest. Arvin and co-workers have been key investigators in this field and a class of fragments are now recognised as Arvin structures<sup>78</sup>. Fragments from key phenolic and phosphite AOs are given in **Figure 1.20** and **Figure 1.21**. Such fragments may be produced from the transformation products of antioxidants during their role as inhibitors of oxidative degradation or from products of their hydrolysis.

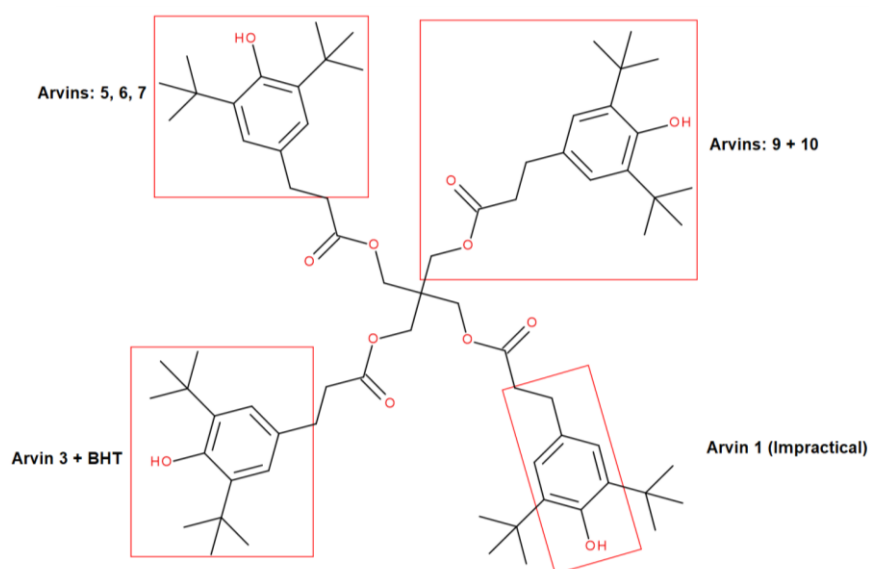


**Figure 1.20:** Formation of potential Arvins from phenolic AO

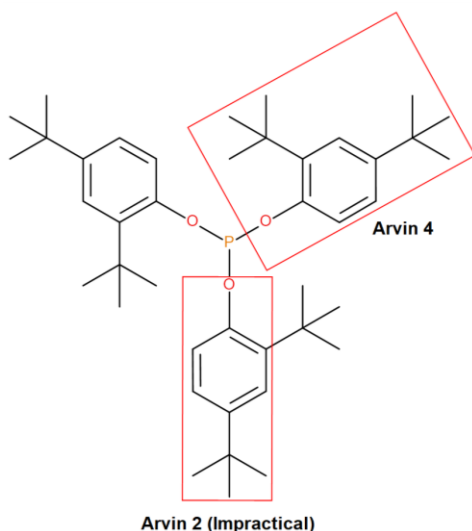


**Figure 1.21:** Formation of potential Arvins from phosphite AO

Irrespective of degradation of the polymer matrix a significant source of V-L-E (Volatiles, Leachates and Extractables) arise from the fragmentation (and/or transformation products) of antioxidants. If the polymer industry is to maintain its commitment to environmental sustainability, then this must be addressed as part of a wider understanding of the performance of additive formulations.

## 1.6 Aims and objectives

Although there has been considerable work performed to date by industrial and academic researchers in the field of polyolefin stabilisation, further progress to enhance the performance of antioxidant packages is still limited by our understanding of the details of polymer degradation and stabilisation mechanisms. The generic BAS of polymer oxidation presents limits to the interpretation of the degradation and stabilisation processes taking place in polyolefins. This may be one reason why kinetic models, aimed at predicting the lifetime of polymers containing specified stabiliser formulations, deviate from actual performance.

In this context, the main aim of this project is to examine the BAS of polymer degradation to account for the key species that contribute to the evolution of CL as a measure of oxidative

induction time (OIT) and how this influences the generation of volatile and extractable oxidation products. In this respect, the main objectives will be to:

- Characterise volatiles and extractables as a function of chain-branching and the incorporation of antioxidant packages in PP, PP-HD and PE-LLD polyolefins; and
- Examine the role of peroxy/polymer hydroperoxide species by CL and how they behave for antioxidant packages in PP, PP-HD and PE-LLD polyolefins

By assimilating the data from these objectives, it is hoped to achieve a holistic approach to polyolefin stabilisation. This will provide information that allows optimisation of antioxidant packages that are able to increase the lifetime of the polyolefins and suppress the formation of the volatiles and extractables that have the potential to be toxic to the environment.



## **2 Experimental**

### **2.1 Materials**

#### **2.1.1 Polymer Resins**

A number of polymer resins were selected for illustrative purposes, the aim being to assess how chain branching and polymer type influenced the evolution of volatiles and extractables from the non-stabilised and stabilised polymer matrix'. The formulations (polymers with antioxidants) were supplied from the sponsoring company in pellet form following multiple extrusions to give materials at Pass 5. The samples had previously been made for use in other in-house projects and had been stored in a refrigerated room to prevent degradation prior to analysis (which was undertaken within 12 months of provision of samples). Samples were stored in glass jars rather than plastic bags to prevent any cross-contamination from volatile and extractable species.

A non-disclosure agreement in place with the sponsoring company prevents the exact quantities of antioxidant in specified formulations and in some cases specific grades of polymers being provided. In this thesis, Antioxidants (AO's) are referred to by their IUPAC names and number codes rather than trade names.

The polymer types were as follows:

- **Polypropylene**

Ziegler-Natta PP (grades undisclosed) was extruded at temperatures of 190-230°C under nitrogen at pass 0 to pass 5 and subsequently under air to produce formulated pellets that were supplied by SONGWON.

- **Polyethylenes**

Both PE-HD and PE-LLD (grades undisclosed) extruded at temperatures of 180-205°C under nitrogen at pass 0 to pass 5 and subsequently under air to produce formulated pellets that were supplied by SONGWON.

The PE-HD was produced using Phillips-based catalyst (chromium oxide on an amorphous support) The PE-LLD was produced using Ziegler- Natta catalysts (e.  $\text{TiCl}_3\text{-Al}(\text{C}_2\text{H}_5)_3$  on  $\text{MgCl}_2$  support).

### **2.1.2 Antioxidants**

Because samples obtained from the industrial sponsor were pre-prepared, and selections were made from a wider range of formulations, antioxidants were grouped to allow easier comparison of their typical behaviours and attempt an experiment design that would limit the number of samples to be tested. Antioxidants were grouped as phenolic, phosphite, thioester and aminic based AOs and used alone or in combination. For phenolic antioxidants both synthetic and natural types were evaluated (the latter limited to PE-HD as the polymer matrix). This was due to the relatively high cost of natural antioxidants, so the HDPE samples were subsequently produced on a small scale (20g in total weight). All samples were combined with an acid scavenger (calcium stearate) as protection from acid residues in the same amounts for all samples. The total stabiliser level was fixed for all samples for both PP and PE as well as the relative concentration (not greater than 1000 ppm). As mentioned in **Section 2.1.1**, a non-disclosure agreement prevents the exact concentration to be revealed in this study.

#### **2.1.2.1 Rationale for selection of the AO formulation**

Over the last 30 years, the use of AOs in commercial polyolefins has been limited to a few 'set packages' of AOs, based mainly on their processing performance (radical scavenging ability and hydrogen atom transfer). These include the combination of hindered phenols with phosphites, (also including an acid scavenger). Although this package is the 'workhorse' of the industry, during processing, these synthetic AOs tend to fragment to give rise to volatiles and extractables. Ever more stringent requirements from environmental legislation means that a better understanding of mechanisms leading to fragmentation is required. This has led to several studies, which examine the potential toxicity of fragments arising from AOs, and leached to the environment, under both processing and service-life conditions. Arvin and co-

workers have been key investigators in this field and a class of fragments are now recognised as Arvin structures (derived from key phenolic and phosphite AOs **Figures 1.2** and **1.21**).

### 2.1.3 Formulations

The formulations selected for this study are given in this section. The full names of the AOs used are given in **Table 2.1** and the corresponding structures and physical properties are given in the **Appendix**.

**Table 2.1:** IUPAC names and corresponding structure codes for antioxidants

Structure Code	IUPAC Name
<b>Acid scavenger</b>	Calcium octadecenoate
<b>Phenol-1</b>	octadecyl 3-(3,5-ditert-butyl-4-hydroxyphenyl)propanoate
<b>Phenol-2</b>	4-methylphenol;tricyclo[5.2.2.0 <sup>2,6</sup> ]undecane
<b>Phenol-3</b>	(2 <i>R</i> )-2,5,7,8-tetramethyl-2-[(4 <i>R</i> ,8 <i>R</i> )-4,8,12-trimethyltridecyl]-3,4-dihydrochromen-6-ol ( <b><math>\alpha</math>-tocopherol</b> )
<b>Phenol-4</b>	1,3,5-tris[(4- <i>tert</i> -butyl-3-hydroxy-2,6-dimethylphenyl)methyl]-1,3,5-triazinane-2,4,6-trione
<b>Phenol-5</b>	[3-[3-(3,5-ditert-butyl-4-hydroxyphenyl)propanoyloxy]-2,2-bis[3-(3,5-ditert-butyl-4-hydroxyphenyl)propanoyloxymethyl]propyl] 3-(3,5-ditert-butyl-4-hydroxyphenyl)propanoate
<b>Phenol-6</b>	[2-[3-[1-[3-(3- <i>tert</i> -butyl-4-hydroxy-5-methylphenyl)propanoyloxy]-2-methylpropan-2-yl]-2,4,8,10-tetraoxaspiro[5.5]undecan-9-yl]-2-methylpropyl] 3-(3- <i>tert</i> -butyl-4-hydroxy-5-methylphenyl)propanoate
<b>Phenol-7</b>	2-(3,4-dihydroxyphenyl)-3,5,7-trihydroxychromen-4-one
<b>Phenol-8</b>	2-(3,4-dihydroxyphenyl)-5,7-dihydroxy-3-[(2 <i>S</i> ,3 <i>R</i> ,4 <i>S</i> ,5 <i>S</i> ,6 <i>R</i> )-3,4,5-trihydroxy-6-[[[(2 <i>R</i> ,3 <i>R</i> ,4 <i>R</i> ,5 <i>R</i> ,6 <i>S</i> )-3,4,5-trihydroxy-6-methyloxan-2-yl]oxymethyl]oxan-2-yl]oxychromen-4-one
<b>Phenol-9</b>	3,4,5-trihydroxybenzoic acid
<b>Phosphite-1</b>	tris(2-nonylphenyl) phosphite
<b>Phosphite-2</b>	3,9-bis(2,4-ditert-butylphenoxy)-2,4,8,10-tetraoxa-3,9 diphosphaspiro[5.5]undecane
<b>Phosphite-3</b>	triphenyl phosphite
<b>Phosphite-4</b>	3,9-bis[2,4-bis(2-phenylpropan-2-yl)phenoxy]-2,4,8,10-tetraoxa-3,9-diphosphaspiro[5.5]undecane
<b>Thioester-1</b>	dodecyl 3-(3-dodecoxy-3-oxopropyl)sulfanylpropanoate
<b>Thioester-2</b>	octadecyl 3-(3-octadecoxy-3-oxopropyl)sulfanylpropanoate
<b>Thioester-3</b>	[3-(3-dodecylsulfanylpropanoyloxy)-2,2-bis(3-dodecylsulfanylpropanoyloxymethyl)propyl] 3-dodecylsulfanylpropanoate
<b>Amine-1</b>	Amine, bis(Hydrogenated rape-oil alkyl) methyl, N-oxide
<b>Amine-2</b>	Bis (octadecyl) hydroxylamine
<b>Amine-3</b>	4-(2-phenylpropan-2-yl)- <i>N</i> -[4-(2-phenylpropan-2-yl)phenyl]aniline
<b>Amine-4</b>	<i>N</i> , <i>N'</i> , <i>N''</i> , <i>N'''</i> -tetrakis(4,6-bis(butyl-( <i>N</i> -methyl-2,2,6,6-tetramethylpiperidin-4-yl)amino)triazin-2-yl)-4,7-diazadecane-1,10-diamine

The formulations of the stabiliser combinations in the selected polyolefins are given in **Tables 2.2 to 2.8** encompass phenols, phosphites, thioester and aminic antioxidants in PP, PE-HD and PE-LLD.

**Table 2.2:** PP formulations PP-A, PP-B, PP-D and PP-F

	PP-A	PP-B	PP-D	PP-F
PP (homopolymer, Z-N)				
Calcium Stearate				
<b>Phosphite-3</b>				
<b>Amine-2</b>				
<b>Amine-4</b>				
<b>Phenol-3</b>				
<b>Phenol-5</b>				
<b>Phenol-6</b>				
<b>Thioester-2</b>				
<b>Thioester-3</b>				

**Table 2.3:** PP formulations PP-A, PP-C, PP-E and PP-G

	PP-A	PP-C	PP-E	PP-G
PP (homopolymer, Z-N)				
Calcium Stearate				
<b>Phosphite-3</b>				
<b>Amine-2</b>				
<b>Amine-4</b>				
<b>Phenol-3</b>				
<b>Phenol-5</b>				
<b>Phenol-6</b>				
<b>Thioester-2</b>				
<b>Thioester-3</b>				

**Table 2.4:** PP formulations PP-H, PP-I, PP-J and PP-K

	PP-H	PP-I	PP-J	PP-K
PP (homopolymer, Z-N)				
Calcium Stearate				
<b>Phosphite-3</b>				
<b>Amine-2</b>				
<b>Amine-4</b>				
<b>Phenol-3</b>				
<b>Phenol-5</b>				
<b>Phenol-6</b>				
<b>Thioester-2</b>				
<b>Thioester-3</b>				

**Table 2.5:** PP formulations PP-L, PP-M and PP-O

	PP-L	PP-M	PP-O
PP (homopolymer, Z-N)			
Calcium Stearate			
<b>Phosphite-3</b>			
<b>Amine-2</b>			
<b>Amine-4</b>			
<b>Phenol-3</b>			
<b>Phenol-5</b>			
<b>Phenol-6</b>			
<b>Thioester-2</b>			
<b>Thioester-3</b>			

**Table 2.6:** PE-LLD formulations LLD-A, LLD-B, LLD-C and LLD-D

	LLD-A	LLD-B	LLD-C	LLD-D
PE-LLD (Z-N)				
<b>Phenol-1</b>				
<b>Aminic-1</b>				
<b>Phosphite-1</b>				

**Table 2.7:** PE-HD formulations HD-A to HD-F

	HD-A	HD-B	HD-C	HD-D	HD-E	HD-F
PE-HD (homopolymer, Cr)						
Calcium Stearate						
<b>Quercetin</b>						
<b>Rutin</b>						
<b><math>\alpha</math>-tocopherol</b>						
<b>Gallic acid</b>						

**Table 2.8:** PE-HD formulations HD-G to HD-K

	HD-G	HD-H	HD-I	HD-J	HD-K
PE-HD (homopolymer, Z-N)					
Calcium Stearate					
<b>Quercetin</b>					
<b>Rutin</b>					
<b><math>\alpha</math>-tocopherol</b>					
<b>Gallic acid</b>					
<b>Phosphite-4</b>					
<b>Phosphite-3</b>					
<b>Phenol-5</b>					

## 2.2 Sample analysis

Due to the large number of samples evaluated, testing has been limited to selected test methods. These were:

- Chemiluminescence (CL) for insight into mechanisms of termination in the presence of AO's.
- Gas chromatography-mass spectroscopy (GC-MS) analysis for insight into mechanisms underpinning production of volatiles and extractables.

### 2.2.1 Chemiluminescence methodology

CL spectroscopic analysis involves simultaneous thermal oxidation in the melt-state (to reduce the irregularities that occur in solid-state samples) and detection of emissions, by ageing in a furnace installed in the instrument equipped with thermal and pneumatic controls allowing sample degradation to take place under a range of ageing environments, e.g. nitrogen, air and vacuum etc. For each formulation using either PP or PE-LLD, a 0.5 mg of the sample was placed in a stainless-steel dish and aged at 180-200°C in presence of air at a flow rate of 50 ml min<sup>-1</sup>. With regards to sample analysis, three replicates per run was completed for increased reliability, the comparison was then made to a control sample which was sample PP-A and in between samples, blanks were also run to remove any background noise. The selection of high ageing temperature, and oxidation environment was made to allow high CL emissions. The emissions from the samples were recorded in qualitative as well as quantitative mode, commonly known as CL emission spectra and integral CL emission, respectively. The instrument used was an ultra-high sensitivity CLA-FS3 model CL spectrophotometer depicted in **Figure 2.1**. The detectors in the spectrophotometer are photomultiplier tubes working for a wavelength range of 300-850 nm. Unlike IR analysis that involves ageing samples prior to their analysis, the CL spectroscopic analysis involved simultaneous ageing of the samples, and detection/measurement of the subsequently generated emissions.

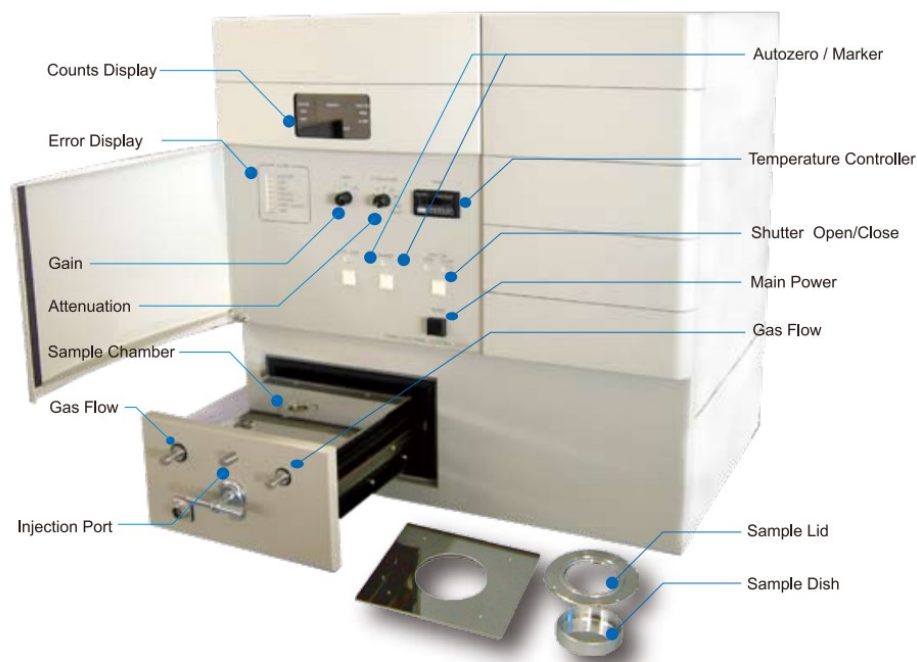


**Figure 2.1:** Typical CL spectrophotometer and accompanying integral spectra obtained (above) and spectrum obtained at given time of ageing from the integral curve

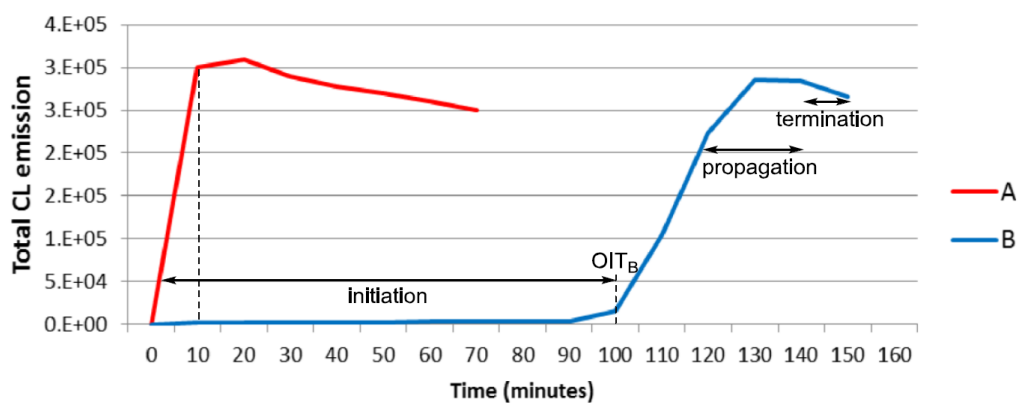


**Figure 2.2:** An example of a CL spectrum, where A is an unstabilised polymer and B is a stabilised polymer<sup>52</sup>

At each point on the integral CL curve individual wavelengths were selected by 20 different cut-off filters. Spectra under the integral curves were then recorded in the wavelength range 300-700 nm.

## 2.2.2 GC-MS methodology

### 2.2.2.1 Sample Preparation for Detection of Volatiles

Here a dynamic Solid-phase Microextraction (SPME) adsorption unit was fabricated modelled on that used in a previous study (**Figure 2.3**)<sup>52</sup>.

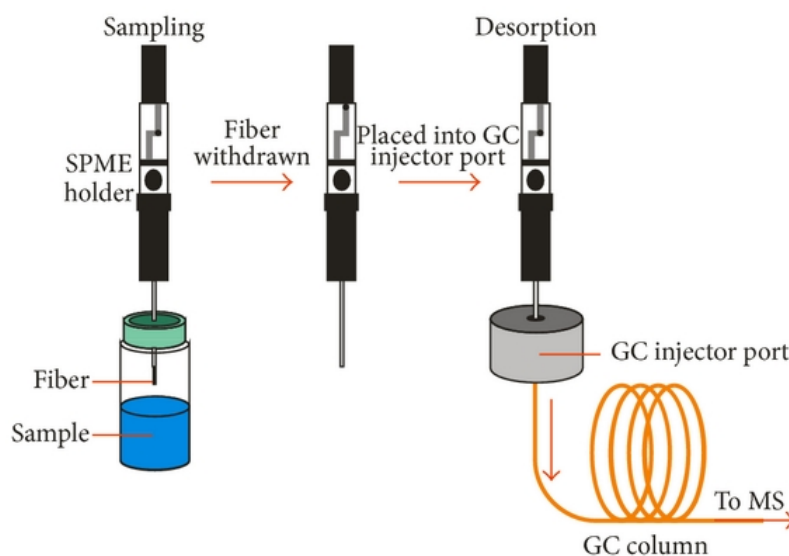


**Figure 2.3:** Dynamic SPME adsorption unit to enable identification of volatiles by GC-MS<sup>79</sup>

The unit consisted of a cartridge heater with a replaceable glass-lining. The rear of the tube (sample housing) was thermally controllable from ambient to 500°C, whilst the rear of the unit remains at ambient temperature (SPME fibre-housing). The sample was swapped with air while it was aged at a given temperature for a predetermined period. Air was used to facilitate thermo-oxidative degradation of the polymer as well as flow of the sample emissions situated at the other end of the sample tube, counter-clockwise to the air-current. To avoid contamination caused by surrounding environment and any contaminants inside the adsorption unit, process-blanks and fibre-blanks were run regularly. For the fibre-blank, the SPME fibre was desorbed in the GC-liner at 300°C for 10 min. The cleaned fibre was then analysed to ensure it was free of contaminants. Potential contamination from the adsorption unit was tested by running a blank on the fibre under the experimental conditions without any sample inside the tube.



#### 2.2.2.2 Sample Preparation for Detection of Extractables

Samples of PP, PE-HD and PE-LLD were Soxhlet extracted using hexane and ethanol. Hexane was used as a 'model' solvent for PP, PE-HD and PE-LLD, since the polarity of Hexane is comparable to that of the polymers. Many food packaging studies claim the use of Ethanol as a solvent, yielding migration results similar to results into oil and fat in polyolefins<sup>80</sup>.

The only salient difference between the two sets of samples was that a total weight of 25 g of the PP and PE-LLD sample was used in a 100 mL of either Hexane or Ethanol. Whilst, as mentioned above regarding the small amount of natural AO sample produced, the experiment had to be scaled down to match the amount of sample being used. For this batch, only 5 g of sample was used in 20 mL of either Hexane or Ethanol to match the same ratio of sample to solvent as the PP samples (1:4).

Once the experiment was complete, the newly refluxed solvent was transferred into glass vials and kept away from sunlight at room temperature to prevent any thermal or photo degradation of extracts. Prior to analysis samples were further concentrated by Nitrogen blowdown.

In order to obtain the maximum extraction from the samples, all solvent samples were concentrated further by evaporation. A 6-port Mini-Vap Evaporator from Supelco was used to achieve this; the solvent samples that was transferred into clean glass vials would then be placed under the 6-needle station (**Figure 2.4**) where a steady constant stream of Nitrogen gas would be blown on the samples encouraging evaporation of the samples. Nitrogen was used as the chosen gas as it is relatively inert compared to normal air-drying, which has Oxygen and water vapour in the atmosphere. The latter environment has the potential to hydrolyze and oxidize the extracts leading to incorrect product assignments.



**Figure 2.4:** 6-port Mini-vap Evaporator

A GC-MS instrument works on the principle that organic compounds such as the PE/PP and AO, undergo fragmentation that is unique to their structure and can be used to identify the parent compound as mentioned above. Advances in the field of mass spectrometry research has allowed better spectral and library databases which makes it easier to identify unknown compounds. The GC-MS instrument is defined as a semi-quantitative method, for example, in an MS based spectrum, peak area is directly proportional to the total count of ions generated during ionization and fragmentation stages of a compound which, is affected by volatility and the thermal lability of a compound<sup>81-83</sup>.

However, although identification of simple substances is relatively straight-forward, for complex mixtures such as polymer-additive matrices, an underlying appreciation of structure and stability is required to confidently assign peaks and resolve any potential mis-assignment of peaks due to different compounds with the same mass. This was the case in the current project where degradation fragments from the polymer matrix and various stabilisers had the same or similar masses and sometimes, similar retention times. In addition, due to the limitations of the current work (small-scale experiment) the concentration of the expected leachates and further volatiles is expected to be within the ppb range. Therefore, the need to introduce a highly sensitive technique that is able to detect these leachates from the polymer matrix with limited interruptions from extrinsic factors is key to this project.

### **2.2.2.3 GC-MS Instrumentation**

The GC-MS analysis was conducted on an Agilent 7890B GC with a 5977B MSD mass spectrometer in combination with a 7693 auto sampler in order to increase the efficiency of sample injection. The column used to separate the analytes was a non-polar HP-5ms column, 30 m long with a diameter of 0.25 mm along with a 0.25 mm film thickness. The GC vials used to store the sample is a 1.5 mL SureStop amber glass vial from Thermo Scientific. All spectra was processed using the Agilent MassHunter software and samples were characterized under the built in, MassHunter Library. Helium is the chosen gas for the mobile phase.

### **2.2.2.4 GC-MS Sample Preparation**

Once all the various solvent samples evaporated, a dry concentrated residue was left remaining. From this, 2 mL of the original solvent was added back into the glass vial containing the residue in order to re-dissolve the solid and was left to stand for 30 minutes to ensure a homogenous liquid. After half an hour, the solvent was transferred and filtered into the glass amber vials to avoid any solid contamination in the GC liner. Since the GC-MS instrument is extremely sensitive, spectra are easily confused by contamination with plasticizers from any additional plastic equipment used during this process. Therefore, in order to eliminate the potential development of unwanted plasticizers from the lab equipment, glass syringes were used in order to transfer the solvent to the glass vials. However, simply transferring the pure solvent that contains the small amounts of solid residue into the glass vials and then subsequently into the GC, can cause the column to clog up and cause damage on to the GC instrument. To avoid this potential issue, the solvent was filtered through Polytetrafluoroethylene (PTFE) filters and then transferred into the glass vials, which contained the pure liquid solvent without any residue. The PTFE syringe filters supplied by Cole-Parmer, had a membrane diameter of 25 mm and a pore size of 0.45  $\mu\text{m}$ . Once the solvent was transferred through to the vials, they were ready for analysis. The same procedure above was also used for a pure solvent blank.

As this study looked at two solvents (ethanol and hexane) a suitable method is required to analyse each of these solvents with both sets of polymers.

#### **2.2.2.2 Hexane – PP**

As the GC-MS was attached to an auto sampler, all PP samples including the 1 ppm Hexane stock solution and a hexane blank was ready to be automatically injected into the GC. Prior to injection of the samples, the injection needle was manually removed from the holder and cleaned thoroughly with Hexane to ensure no previous contaminants will affect the spectra. Once this was complete, solvent washes (in this case Hexane) was programmed to be done three times pre and post injections, in between the washes, an injection volume of 3  $\mu$ l was taken for all samples. The inlet temperature was programmed at 280°C at a pressure of 7.1psi in split less mode with Helium flowing through the column at a rate of 1ml/min. The oven temperature of the GC was set between 40°C-325°C and was held for 2 minutes initially, followed by a ramp rate of 60°C/min until it reached 120°C. After it reached 120°C, the temperature ramp rate decreased to a steady 10°C/min to 240°C until finally it ramped back again to 60°C/min until it reached a final temperature of 300°C. The total time for the experiment took 16 minutes. The MS was set in a full scan mode for an m/z range of 45-350 amu, with a gain factor of 5.000. The solvent delay was set at 4 minutes with the MS source at 300 and the MS quad at 150.

#### **2.2.2.3 Hexane – HDPE (Natural AO)**

In order to keep the results reliable as possible over all samples and solvents, majority parts of the method will remain the same. However, there will be necessary adjustments needed so that the method is compatible with the solvent. In this case for the natural HDPE samples in Hexane, the method in **section 2.2.2.2**, remained largely the same, however, the oven temperature was set between 40°C-310°C with a ramp rate of 25°C/min to 310°C and held for 5 minutes. The MS was set to scan for masses between 45-700amu, in order to capture the masses of the various natural AO's that may not fragment. The total time for this experiment was 19.5 minutes.

#### 2.2.2.4 Ethanol – PP

Again, similarly to **section 2.2.2.2**, the method was identical, however, the only factor that changed was the solvent delay, this was altered to 6 minutes to remove traces of Ethanol from the system.

#### 2.2.2.5 Ethanol – HDPE (Natural AO)

Originally, the method was set as it was in **section 2.2.2.3**, with the adjustments made on the solvent delay. However, the peaks in were extremely broad as evidenced in **Figure 2.5**, therefore, the final ramp rate was adjusted to 10°C/min to 300°C rather than 60°C/min.

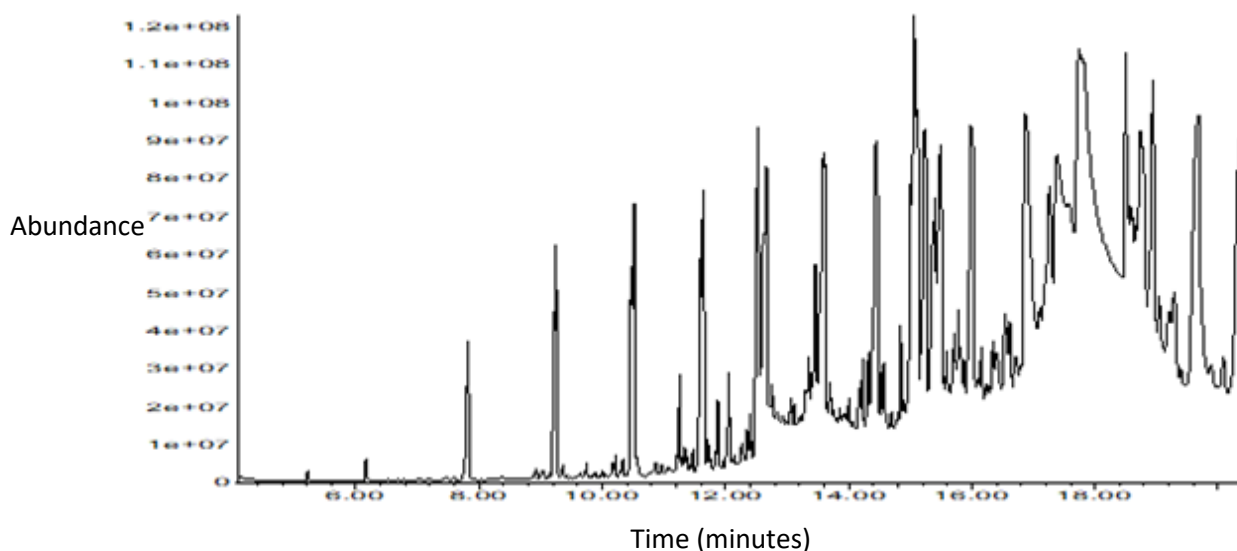


**Figure 2.5:** Example of a sample under the same method as section 2.2.2.5

### 3 Results and Discussion

#### 3.1 Chemiluminescence

Although there is much debate as to the origins of chemiluminescence (CL) the following data will be evaluated in the context of mechanisms from high-level *ab initio* calculations undertaken by Coote and co-workers<sup>17</sup>. This work postulates, contrary to the literature (Russell mechanism), that primary and secondary as well as tertiary tetroxides form a transition state cage. Furthermore, that this can be used to explain why secondary alkylperoxyl bimolecular self-reactions occur on timescales, which are, orders of magnitude faster than for tertiary analogues. Please note all AO structures are denoted in the **Appendix**.

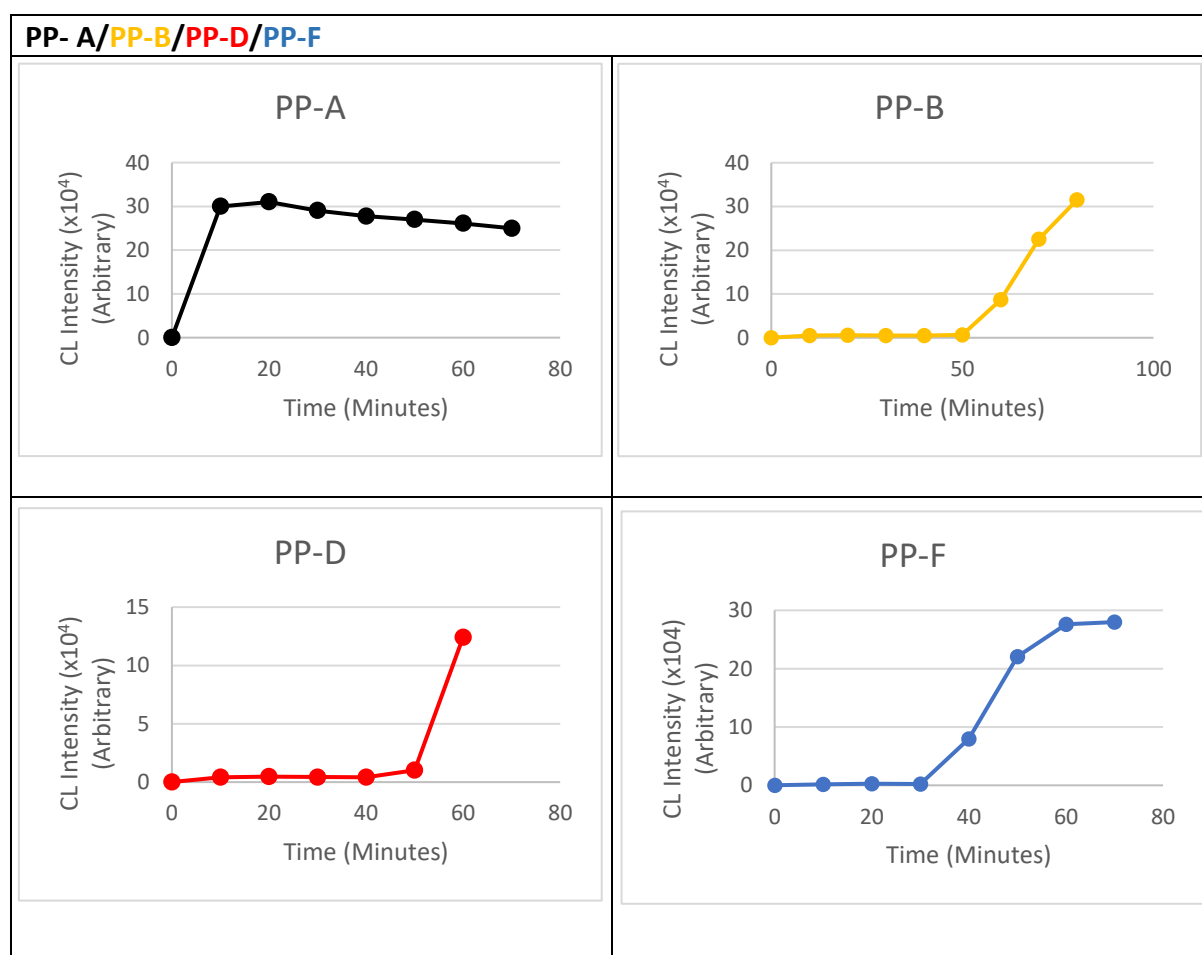


**Figure 3.1:** Chemiluminescence intensity (arbitrary) for polypropylene in melt at 180°C stabilised with formulations A, B, D and F

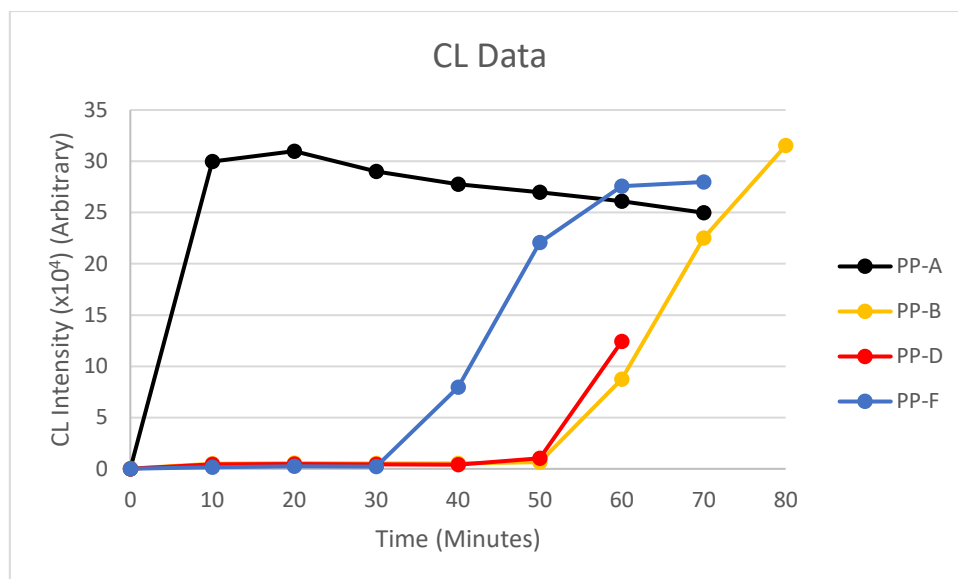


**Figure 3.2:** Overall CL intensities for formulations A, B, D and F

The oxidation induction times (OIT) as measured by CL are given in **Figure 3.1** and **Figure 3.2**. The OIT increases in the order PP-A < PP-F < PP-B  $\cong$  PP-D. The low induction time to oxidation supports the data from evolution of volatiles in that this sample exhibits the largest quantity of oxidised species, principally ketones and smaller amounts of aldehydes, though significant quantities of CO<sub>2</sub> are evolved suggesting the conversion of a much larger amount of aldehydes were initially generated by the sample. The phosphite (**Phosphite-3**) has a hydrogen acceptor bond count of three but a hydrogen bond donor count of zero. It has been put forward that, for primary and secondary peroxy radicals, the transition state cage for the recombination of peroxy radicals is stabilised by C- $\alpha$  hydrogens on carbon atoms (**Structure 1.1** and **Structure 1.2** (page 19)). If this were the case, then with a lack of hydrogen bond donors the phosphite would be unable to 'stabilise' the transition state. However, for tertiary peroxy radicals, the slower reaction makes it likely that tertiary peroxy radicals will escape the cage to form alkoxy radicals. If this occurs, reaction with the phosphite (**Equations 1.8 to 1.10** (page 41)) would then effectively reduce alkoxy radical concentration and chain-branching but be unable to prevent chain propagation because alkyl radicals would be products of these reactions.

The OIT is extended from 10 to 50 minutes on the addition of the phenol (**Phenol 5**). The phenol has 12 hydrogen bond acceptors and 4 hydrogen bond donors. From the literature, it is known that phenols are more resourceful in the reaction with peroxy radicals. For this phenol, free-rotation about bonds (the structure has 32 rotatable bonds) would allow

hydrogen atoms from the O-H groups to position in proximity to the oxygens within the stabilised transition-state. The relatively low bond-dissociation energy (BDE) would then permit HAT to generate peroxides from the collapse of the cage structure. Dissociation of the peroxides would then allow the resultant alkoxyl radicals to be scavenged by the phosphite. In fact, synergism between phenols and phosphites is widely reported in the literature, where this has been explained by the phosphite protecting the phenol by reducing the concentration of peroxide. However, as stated by Gijsman, peroxides are short-lived at processing temperatures and it is more likely that the phosphite is scavenging alkoxyl radicals.

On addition of thioesters, the OIT remains at 50 minutes for **Thioester-2** but is reduced to 30 minutes for **Thioester-3**. Like phosphites, thioesters also display synergism with phenols. However, in this case it may be that as the S-H is oxidised to the sulfenic acid S-OH, i.e. that **Thioester-3** is competing with the phenol in HAT. Whilst S-H is not a good HAT agent to peroxy radicals, because of a tendency to dimerize and react with oxygen, sulfenic acids do have potential to be good hydrogen-atoms donors. However, the **Thioester-3** structure does not favour dimerization.



PP- A/PP-C/PP-E/PP-G

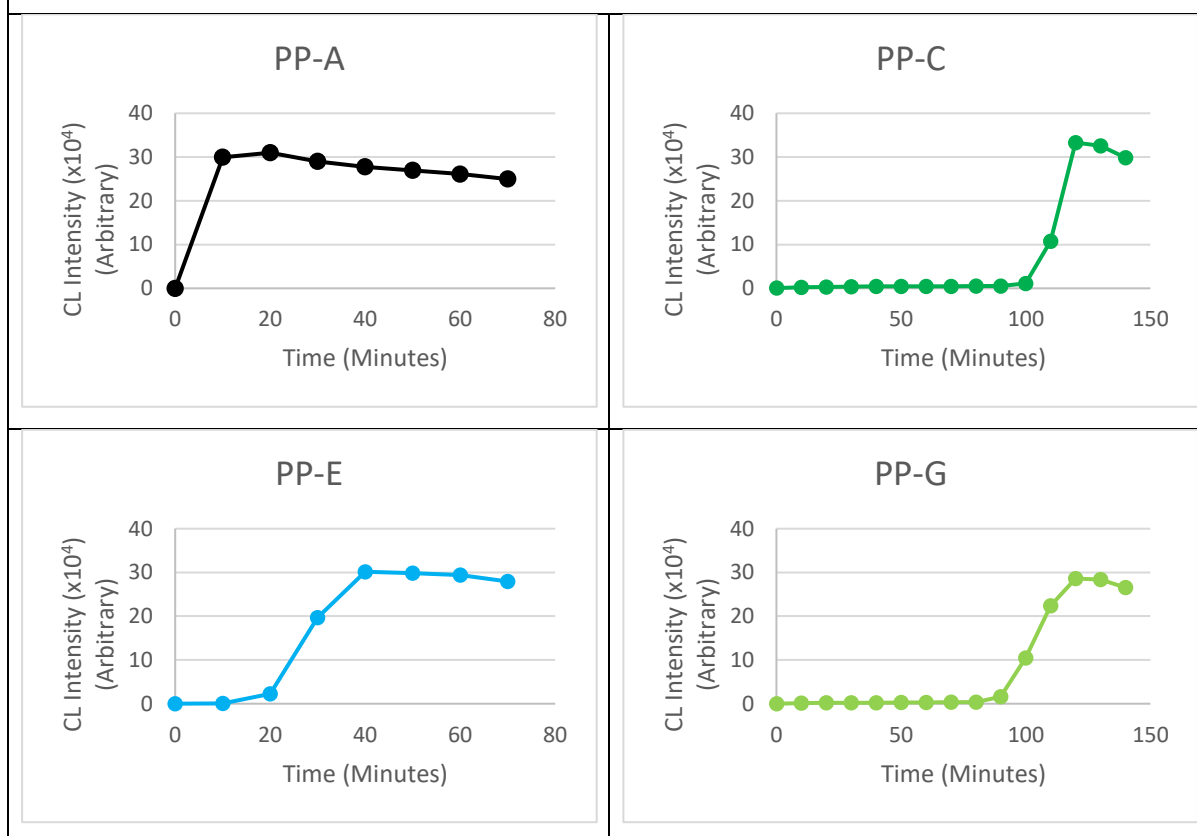


**Figure 3.3:** Chemiluminescence intensity (arbitrary) for polypropylene in melt at 180°C stabilised with formulations A, C, E and G

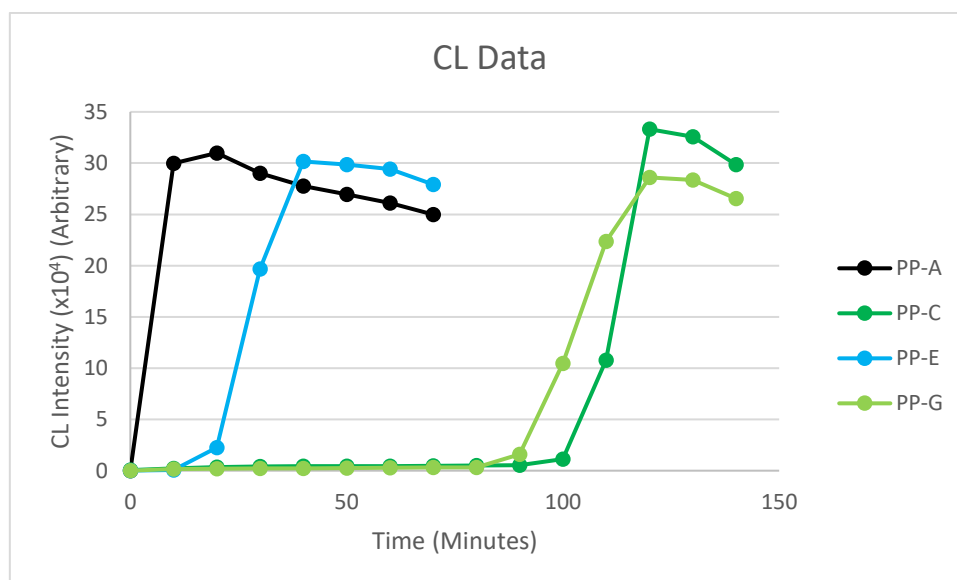


**Figure 3.4:** Overall CL intensities for formulations A, C, E and G

The CL oxidation induction times (OIT) for the second set of samples (A, C, E, G) are given in **Figure 3.3** and **Figure 3.4**. The OIT increases in the order PP-A < PP-E < PP-C  $\cong$  PP-G. Here the replacement of the previous phenol with **Phenol-6** increase the OIT to 100 minutes, the longest OIT of all the PP stabiliser formulations (PP-C). This phenol has a hydrogen bond acceptor count of 10 and a hydrogen bond donor count of two, i.e. half that of the previous phenol. However, **Phenol-6** is less hindered and it is known that under processing conditions by decreasing the steric hindrance, radicals can be scavenged more efficiently. Rather, in this case the, lower steric hindrance would permit the hydrogen atom on the O-H of the phenol to position itself in an improved conformation in order to facilitate HAT. In sample PP-G, the addition of the thioester with **Thioester-3** maintains the OIT at a value of 100 minutes. For sample PP-E, the OIT is reduced to 20 minutes for **Thioester-2**. In this case, the observation of improvements in OIT on addition of the individual thioesters is reversed. Again, this is likely due to interplay between the two AOs in ‘stabilising’ the bimolecular peroxy cage.

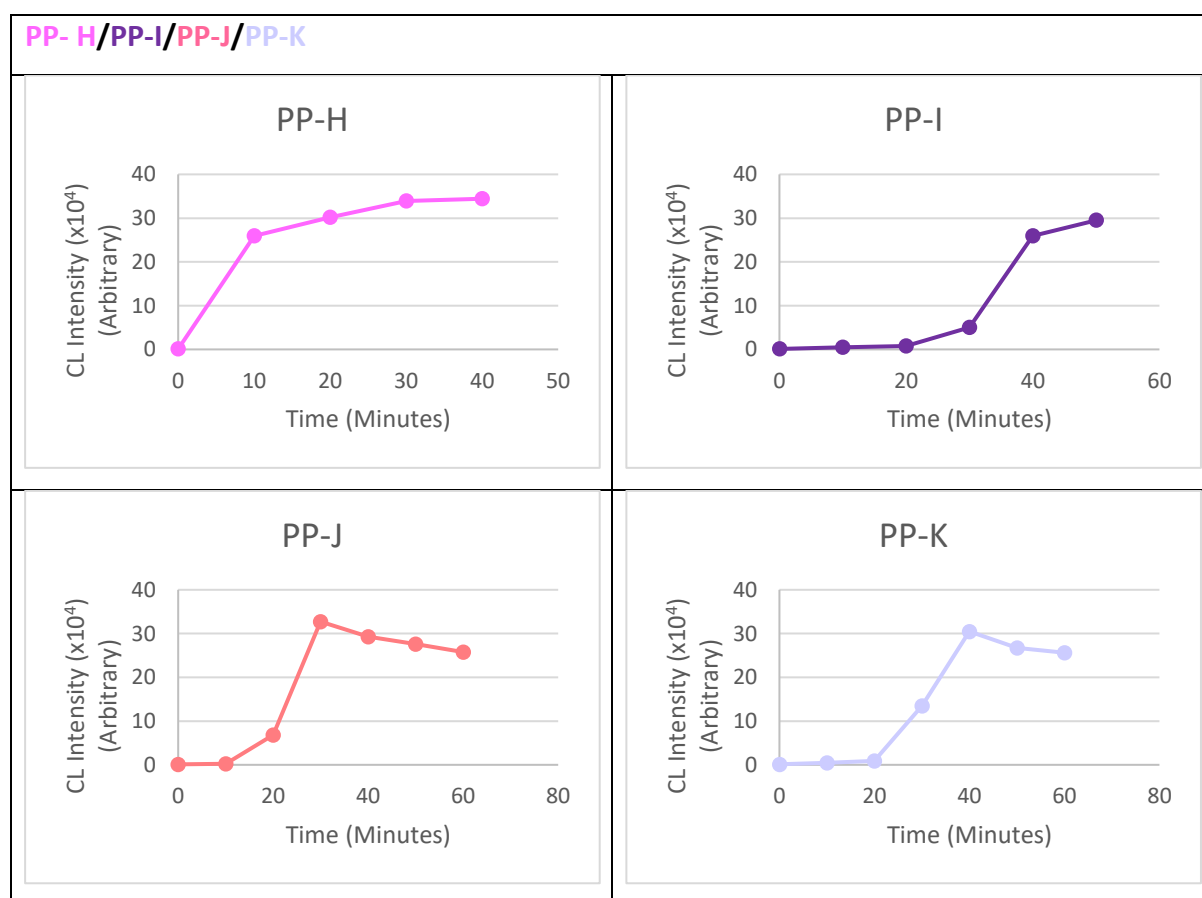


**Figure 3.5:** Chemiluminescence intensity (arbitrary) for polypropylene in melt at 180°C stabilised with formulations H, I, J and K.

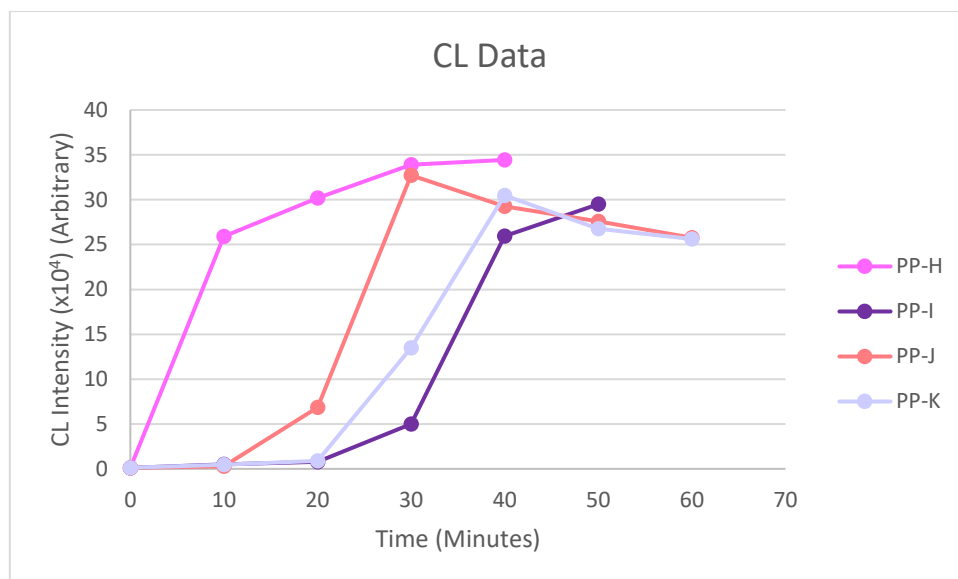


**Figure 3.6:** Overall CL intensities for formulations H, I, J and K

The replacement of the phosphite with hydroxylamine (**Aminic-2**) as 'base' stabiliser demonstrates that although hydroxylamines are reported as good radical scavengers *per se*, the hydroxylamine when used alone appears to be a more effective alkyl radical scavenger than it is a peroxy radical HAT operator (formulation PP-H, **Figure 3.5**). On addition of the **Phenol-5** it is seen that the OIT is increased by only 20 minutes. This small increase is seen for all the stabiliser formulations in this group PP-H to PP-K. It is known in the field of stabiliser chemistry that the nitroxyl generated from the hydroxylamine can complex with the phenol, thereby preventing its HAT activity. The addition of the thioester serves to deactivate the amine (by formation amine sulphates or sulphonates). All samples have rapid rates of increase in CL.

PP-L/PP-M/PP-O

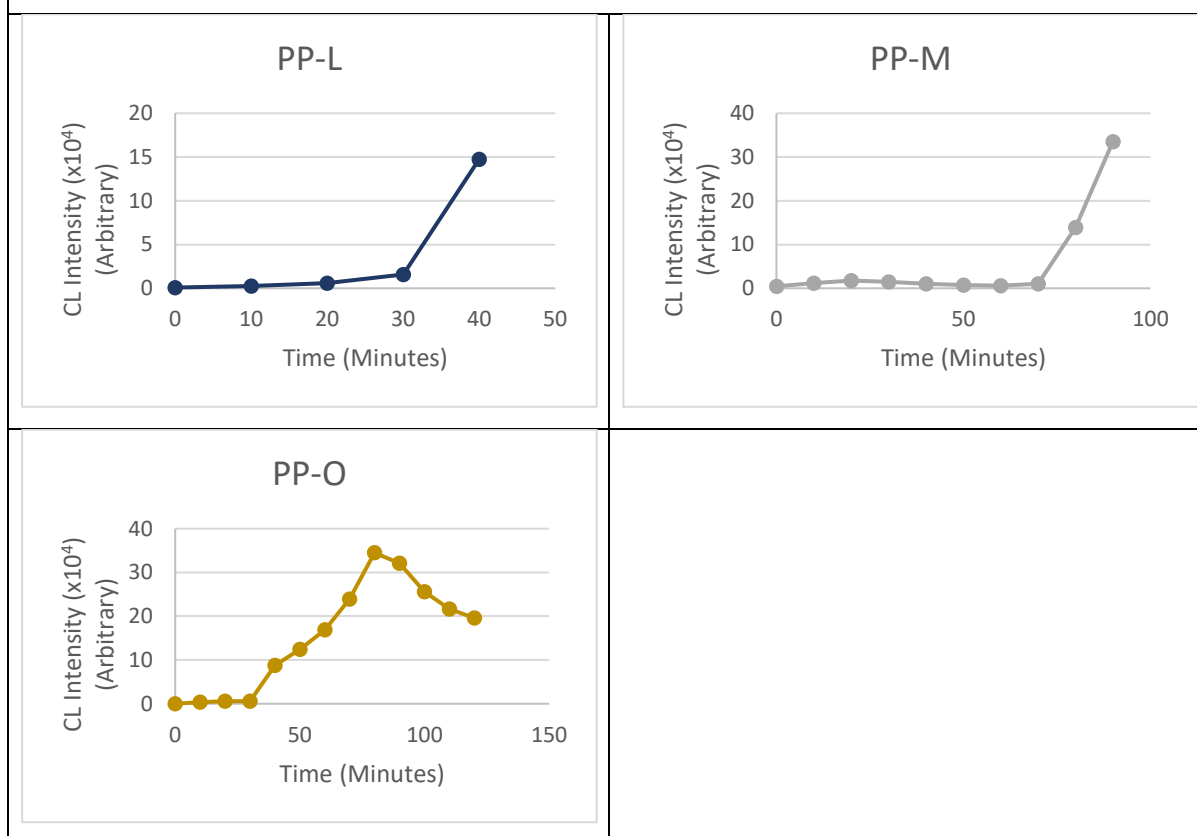


**Figure 3.7:** Chemiluminescence intensity (arbitrary) for polypropylene in melt at 180°C stabilised with formulations L, M and O

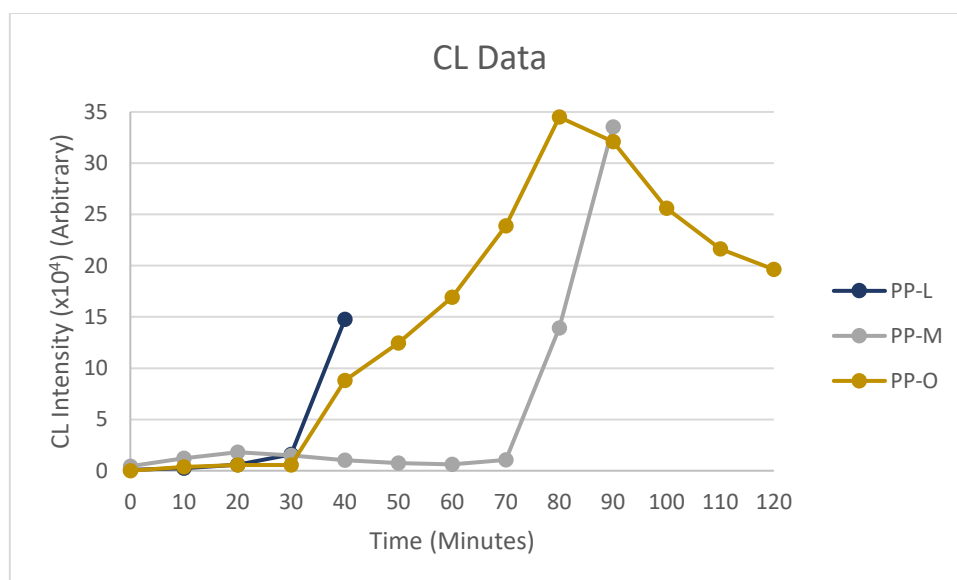


**Figure 3.8:** Overall CL intensities for formulations L, M and O

Sample PP-L also contains the hydroxylamine as ‘base’ stabiliser but compared to its counterpart (sample PP-K) there is a slight improvement from 20 to 30 minutes in the OIT by CL (**Figure 3.7** and **Figure 3.8**). This may be due to poorer complex stability between the nitroxyl of the hydroxylamine and **Phenol-6**, leaving a greater proportion of the available phenol to participate in HAT. Often the interaction between amines and phenols depends on their relative acid and base character.

Replacement of the hydroxylamine with  $\alpha$ -tocopherol (PP-M) increases the OIT to 70 minutes from 20 minutes when compared to the ‘equivalent’ formulation PP-J, though when the phosphite is the base stabiliser in the comparable formulation the OIT is 50 minutes. This suggests the phenol (**Phenol-5**) and the tocopherol work cooperatively. The latter had a hydrogen bond acceptor count of three and a hydrogen bond donor count of one.

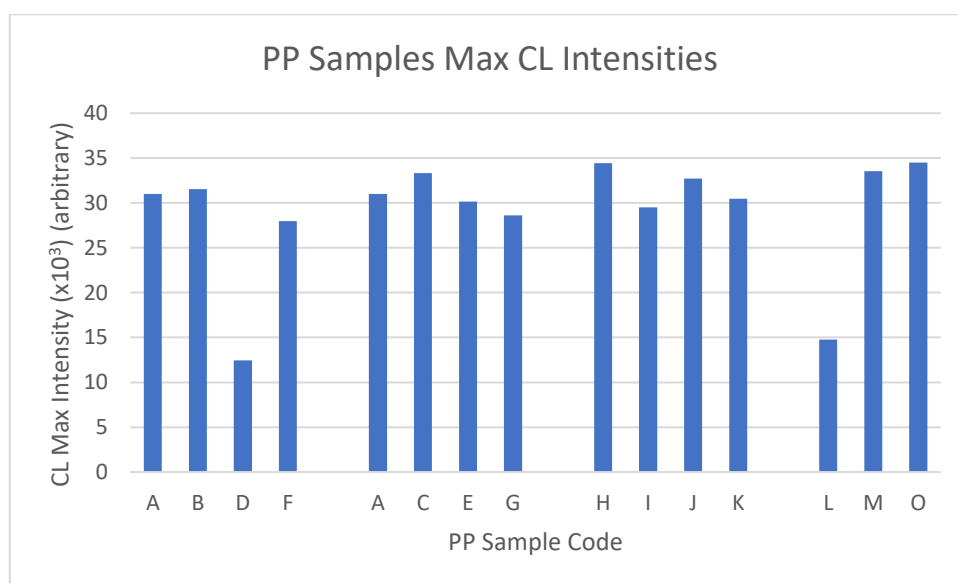


**Figure 3.9:** Maximum CL intensity (arbitrary) from PP (extrusion pass 5) containing stabiliser formulations A to O

The maximum CL intensity for all stabiliser formulations is depicted in **Figure 3.9**. This emphasises the data discussed previously. In general, for all samples containing phosphite as base stabiliser along with a phenol, the maximum CL intensity is substantially lower than that of samples containing aminic antioxidants. If there is a correlation between the concentration

of peroxy radicals and CL intensity, the phenol-phosphite formulation is much more successful in suppressing or converting these species.

A more detailed inspection of changes in CL intensity is seen in **Figures 3.10 to 3.13**. These figures examine the CL ‘spectra’ as a function of wavelength for each data point on the integrated CL curves. It is observed that for all OIT curves obtained by the CL method, there is a characteristic pattern in the sequence of spectral changes.

For sample PP-A (**Figure 3.10**) there is a negligible induction period prior to onset of oxidation. The end of the induction period is associated with a sudden and mostly rapid increase in CL intensity until a maximum value is reached. At this point, the shape of the CL spectrum changes suddenly a marked curvature and drop in intensity at wavelengths above 500 nm (signified by the boxed spectra in the figures).

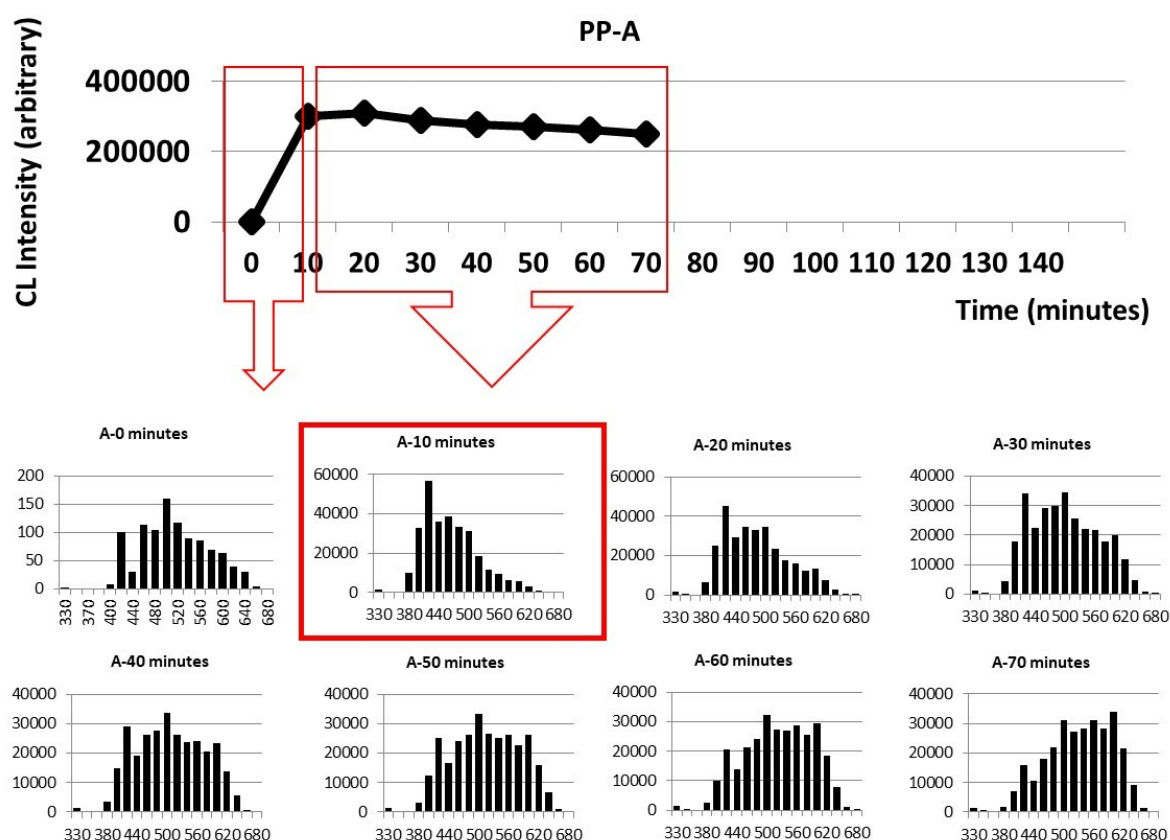


**Figure 3.10:** CL spectra in the wavelength range 380-620 nm under each data point in the CL versus time OIT plot for formulation PP-A. Data obtained in air at 180°C

At longer time periods the longer wavelengths increase in intensity and the shorter wavelength CL emissions (below 500 nm) begin to decrease.

This is more easily understood if it is compared with **Figure 3.11**. Here an induction period is evident for 50 minutes and at the point at which the OIT is exceeded (60 minutes) there is the characteristic change in the CL spectrum.

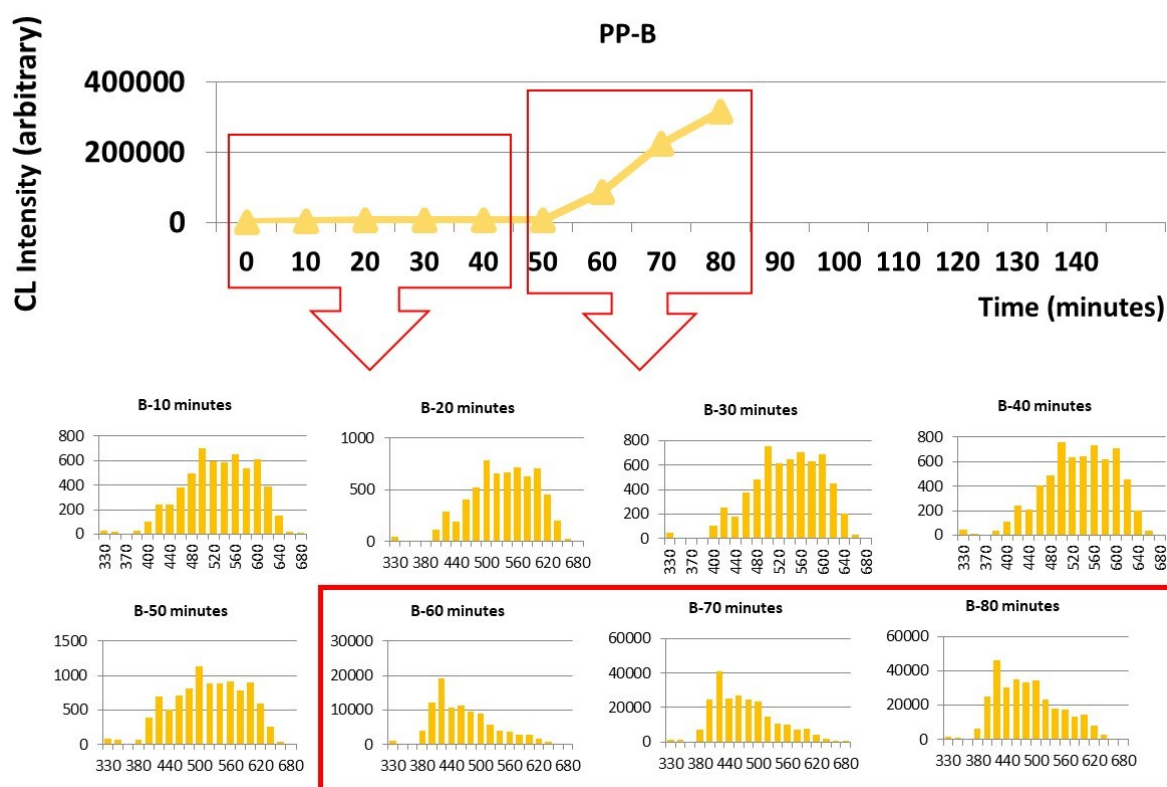


**Figure 3.11:** CL spectra in the wavelength range 380-620 nm under each data point in the CL versus time OIT plot for formulation PP-B. Data obtained in air at 180°C

This phenomenon is further confirmed in **Figure 3.12** for sample PP-D which also has an OIT of 50 minutes. Again, there is a characteristic change in the CL spectrum under the 60-minute data point for the integral CL curve at 60 minutes.

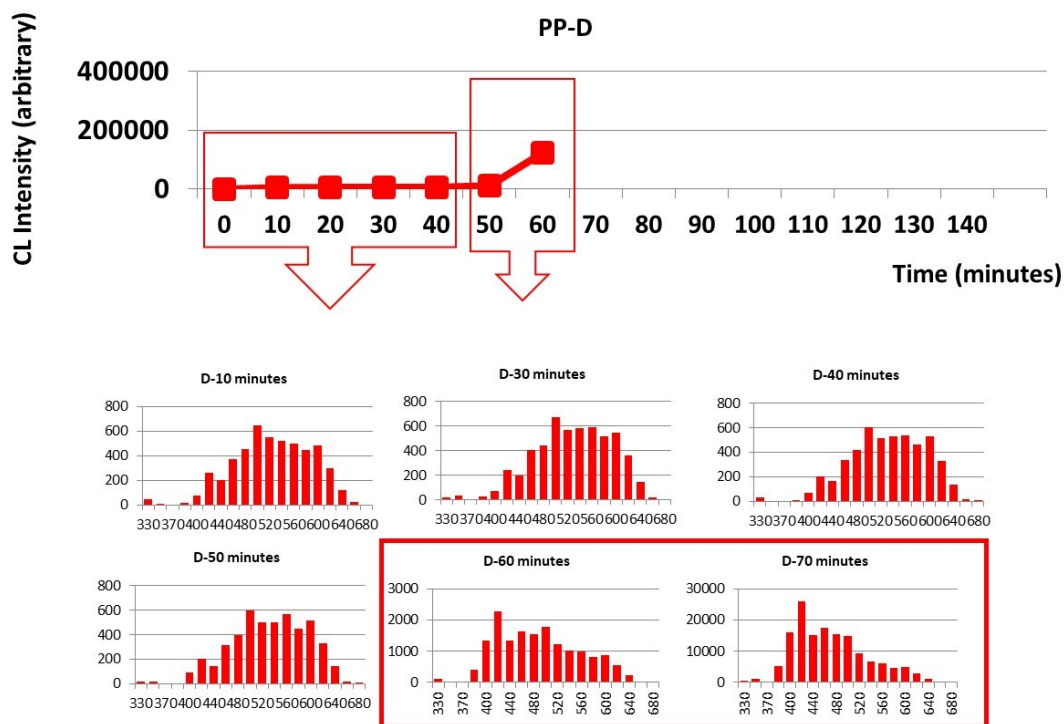


**Figure 3.12:** CL spectra in the wavelength range 380-620 nm under each data point in the CL versus time OIT plot for formulation PP-D. Data obtained in air at 180°C

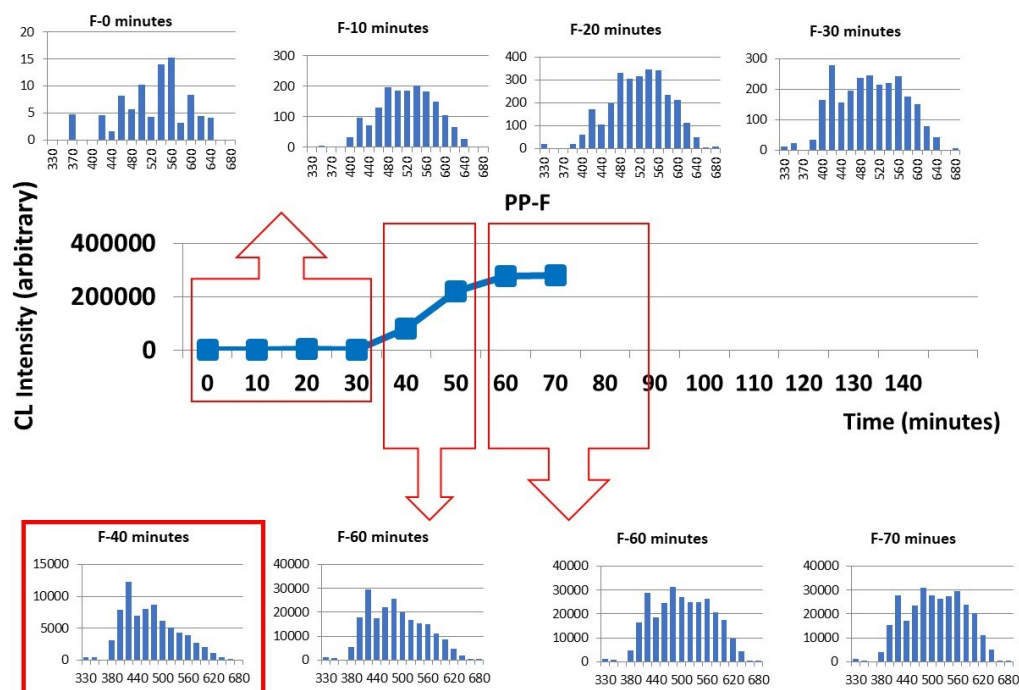


**Figure 3.13:** CL spectra in the wavelength range 380-620 nm under each data point in the CL versus time OIT plot for formulation PP-F. Data obtained in air at 180°C



This characteristic feature in the CL spectrum is confirmed further by sample PP-F (**Figure 3.13**) where the OIT is reduced to 30 minutes the sudden changes in the CL spectrum is seen at 40 minutes.

The end of the induction period coincides with depletion of the antioxidant. During the induction period, there is a build-up of oxidised species (peroxyls).

It has been proposed in the literature<sup>84</sup> that in the luminescence range 350-500 nm is reported to be excited-state carbonyl, and the band at 500-680 nm to singlet oxygen. Two distinct components to the overall CL spectrum are observed in all the CL spectra in this study. The sudden increase in CL intensity following the induction period coupled with a rapid reduction in the longer wavelength band suggests that the route involving singlet oxygen is no longer available at the point at which the AO is depleted. At longer times, the CL band shifts to longer wavelength suggesting this route is again available as the sample becomes more oxidised.

Because real changes in luminescence might be masked by changes in colour of the sample (yellowing due to transformation products of the AO) then care should be taken when interpreting CL spectra in the presence of AOs. Fortunately for the formulations used in this study none of the samples are very yellow, except that containing  $\alpha$ -tocopherol (formulation PP-M).

These features are again observed for formulations PP-C to PP-G. **Figures 3.14 to 3.16**. This reinforces the premise that AOs are blocking a specific route to degradation and that the **Phenol-6** is more effective in this than the **Phenol-5**.

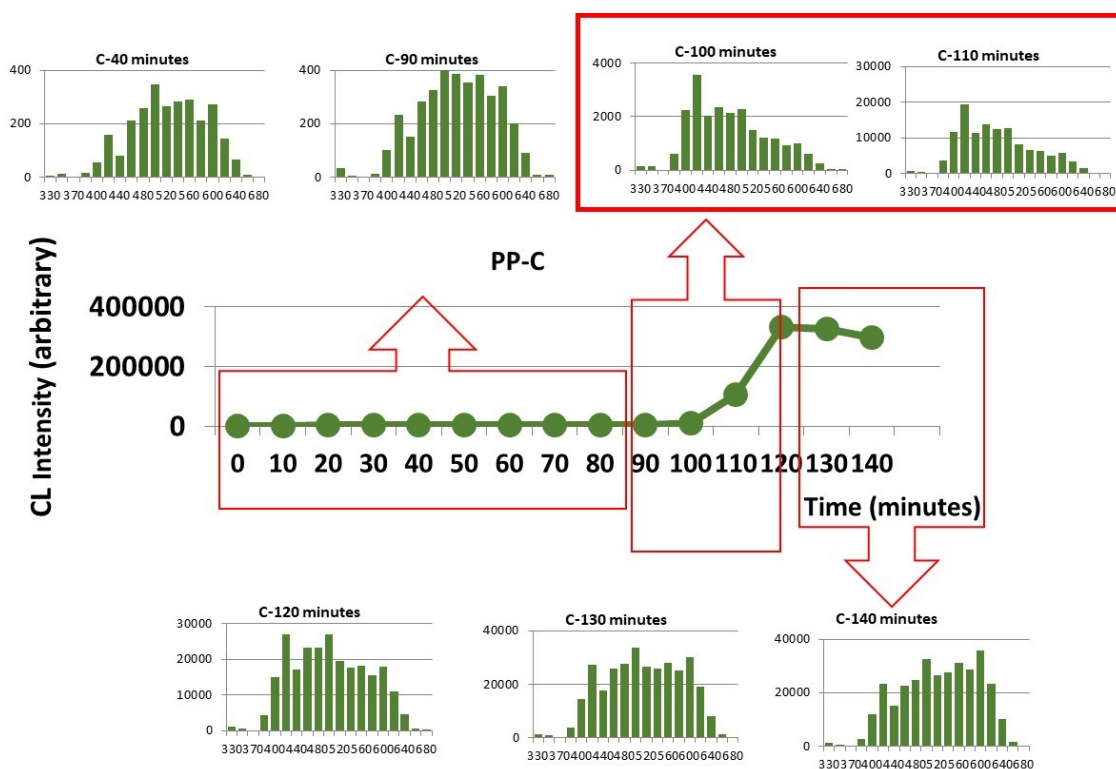


**Figure 3.14:** CL spectra in the wavelength range 380-620 nm under each data point in the CL versus time OIT plot for formulation PP-C. Data obtained in air at 180°C

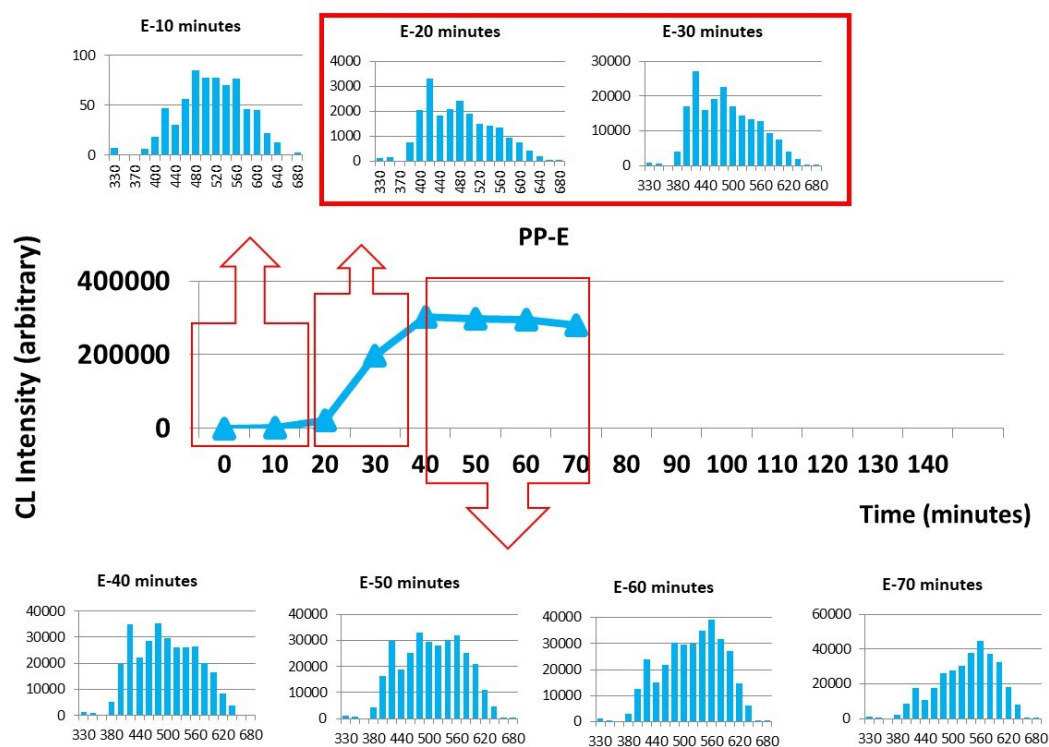


**Figure 3.15:** CL spectra in the wavelength range 380-620 nm under each data point in the CL versus time OIT plot for formulation PP-E. Data obtained in air at 180°C

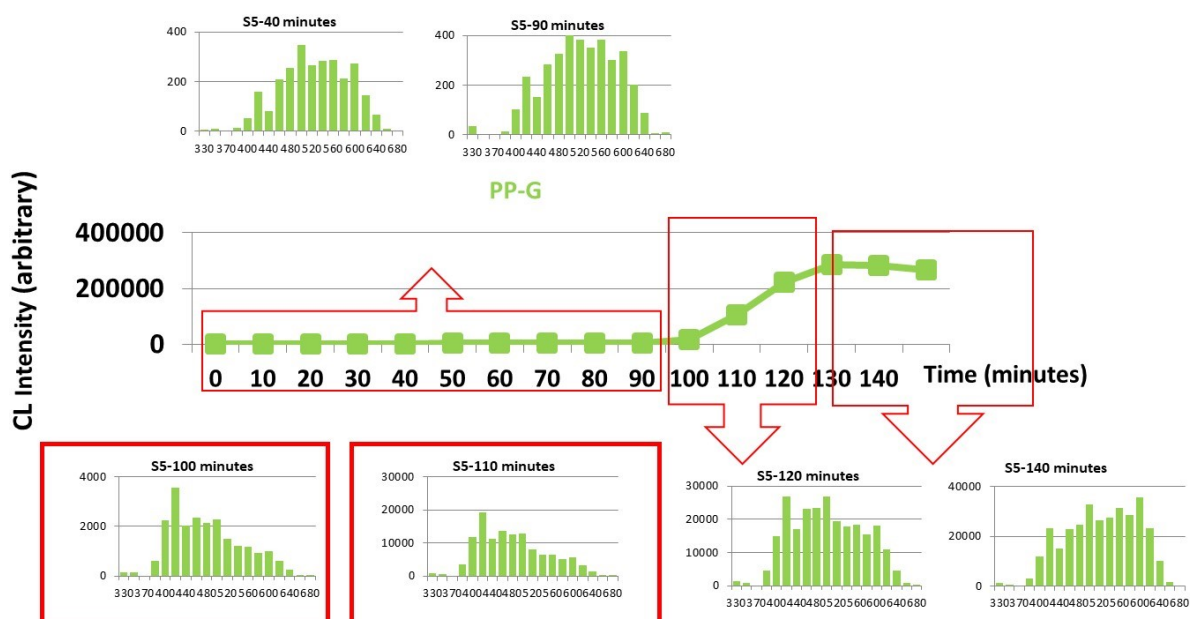


**Figure 3.16:** CL spectra in the wavelength range 380-620 nm under each data point in the CL versus time OIT plot for formulation PP-G. Data obtained in air at 180°C

For the hydroxylamine (**Figure 3.17**) the CL behaviour mirrors that for sample PP-A (**Figure 3.10**). As seems to be the case base stabilisers when used alone have little capacity to inhibit cage decomposition.

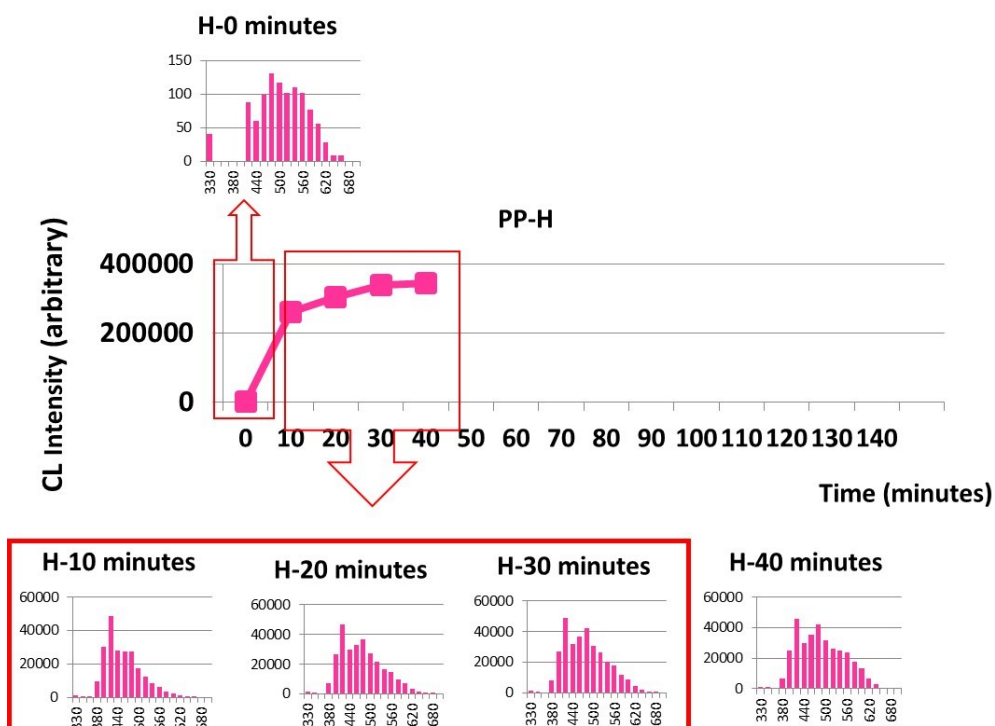


**Figure 3.17:** CL spectra in the wavelength range 380-620 nm under each data point in the CL versus time OIT plot for formulation PP-H. Data obtained in air at 180°C

For samples PP-I, PP-J and PP-K (**Figure 3.18, Figure 3.19, Figure 3.20**) the induction period is only extended to 20-30 minutes as mentioned previously. For sample PP-K after 50 minutes, when the CL has reached its maximum intensity that the shorter wavelength band 350-500 nm attributed to excited-state carbonyls has diminished and the longer wavelength band 500-680nm has again increased.

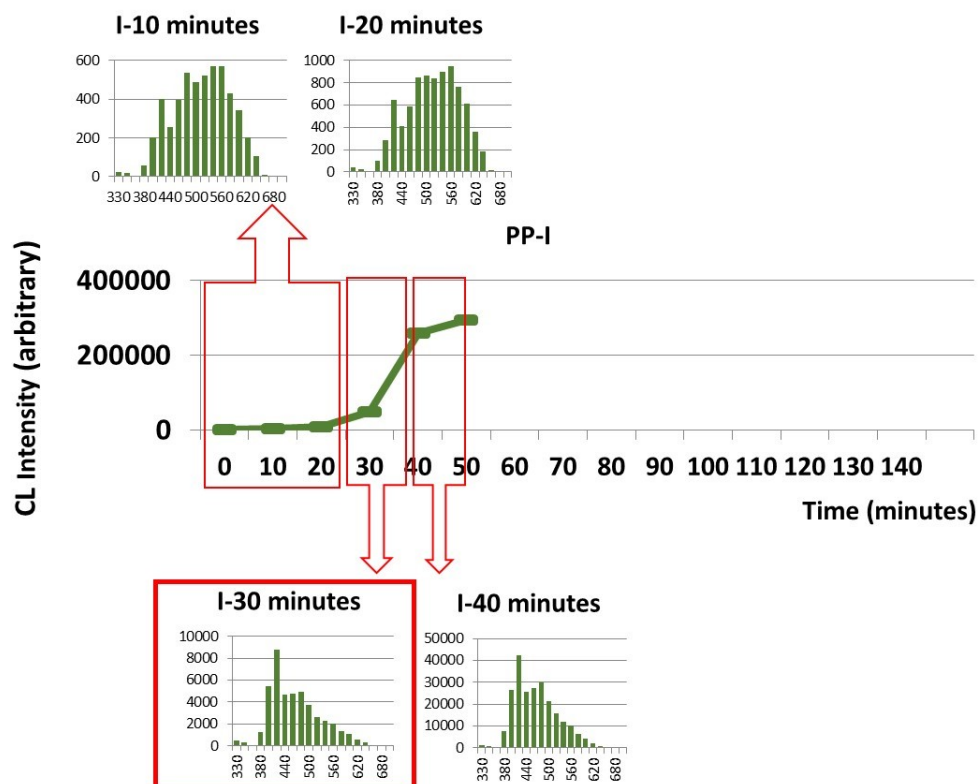


**Figure 3.18:** CL spectra in the wavelength range 380-620 nm under each data point in the CL versus time OIT plot for formulation PP-I. Data obtained in air at 180°C

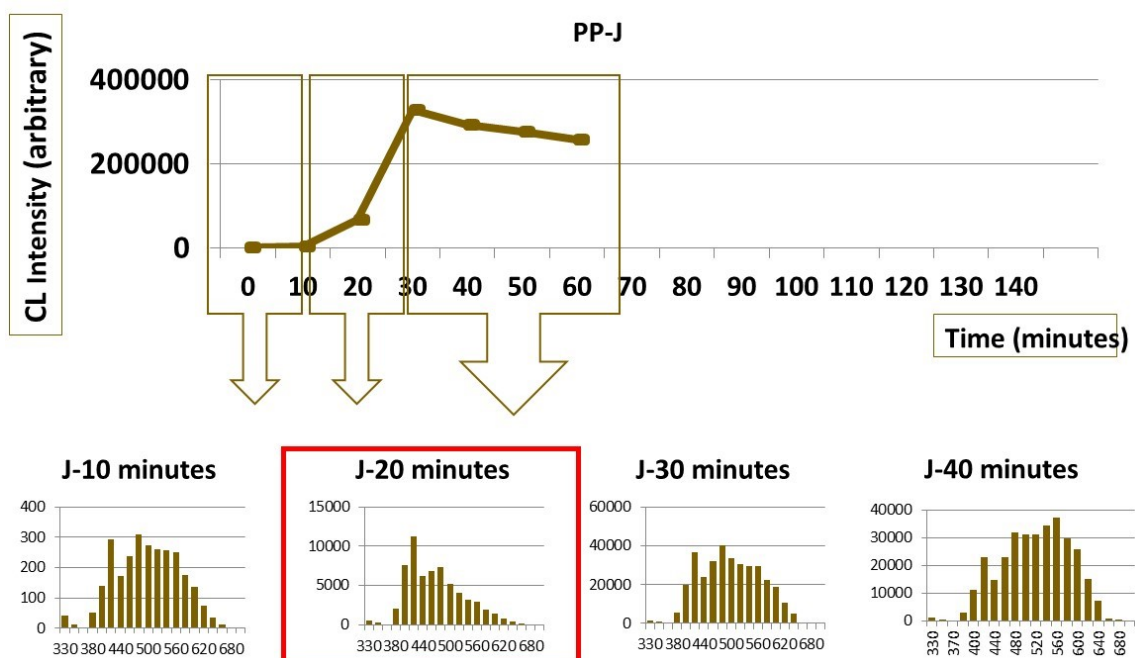


**Figure 3.19:** CL spectra in the wavelength range 380-620 nm under each data point in the CL versus time OIT plot for formulation PP-J. Data obtained in air at 180°C

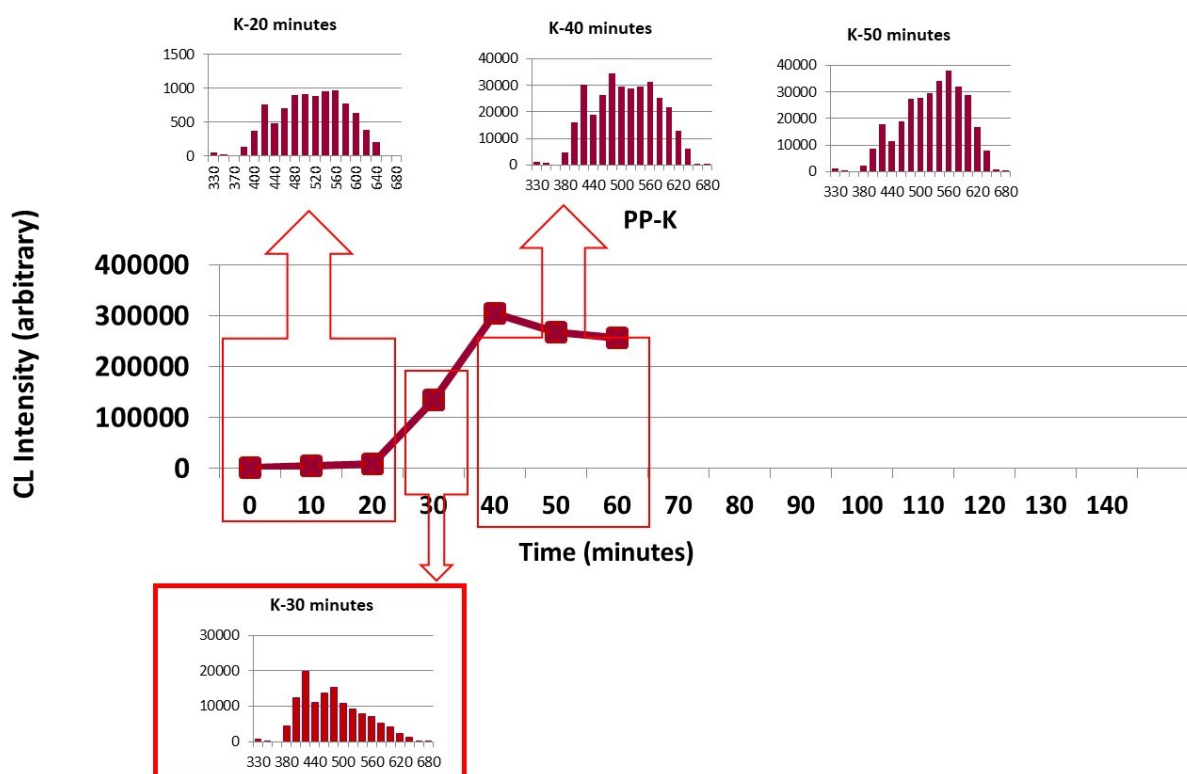


**Figure 3.20:** CL spectra in the wavelength range 380-620 nm under each data point in the CL versus time OIT plot for formulation PP-K. Data obtained in air at 180°C

The CL spectra arising from antioxidant formulations PP-J to PP-M (**Figures 3.18 to 3.22**) further support this theory. However, there are some subtle differences in the spectra for sample PP-O (**Figure 3.23**). For this sample, the transition to a sudden change in the CL spectrum at the end of the induction period proceeds at a much slower rate. Following the maximum CL intensity at 80 minutes there is a marked decrease in the CL intensity below 500 nm. Although this feature is less evident in the spectra of other samples, for those samples where the CL is monitored beyond its maximum intensity a similar pattern of changes emerges. Sample PP-O contains a hindered amine stabiliser and hindered amines are known to quench singlet oxygen<sup>85</sup>. In fact, the longer wavelength band 500-680 nm is suppressed from the onset of oxidation for this sample but following depletion of the AO grows back sharply as the CL decays after achieving its maximum intensity.

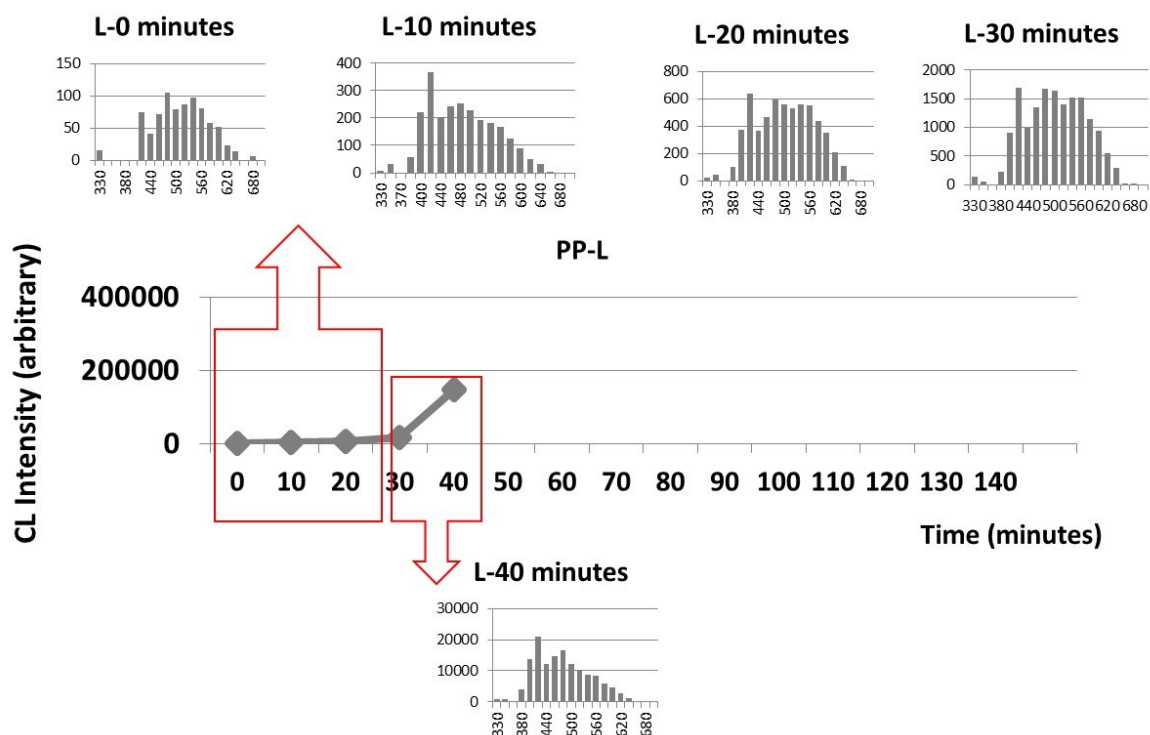


**Figure 3.21:** CL spectra in the wavelength range 380-620 nm under each data point in the CL versus time OIT plot for formulation PP-L. Data obtained in air at 180°C

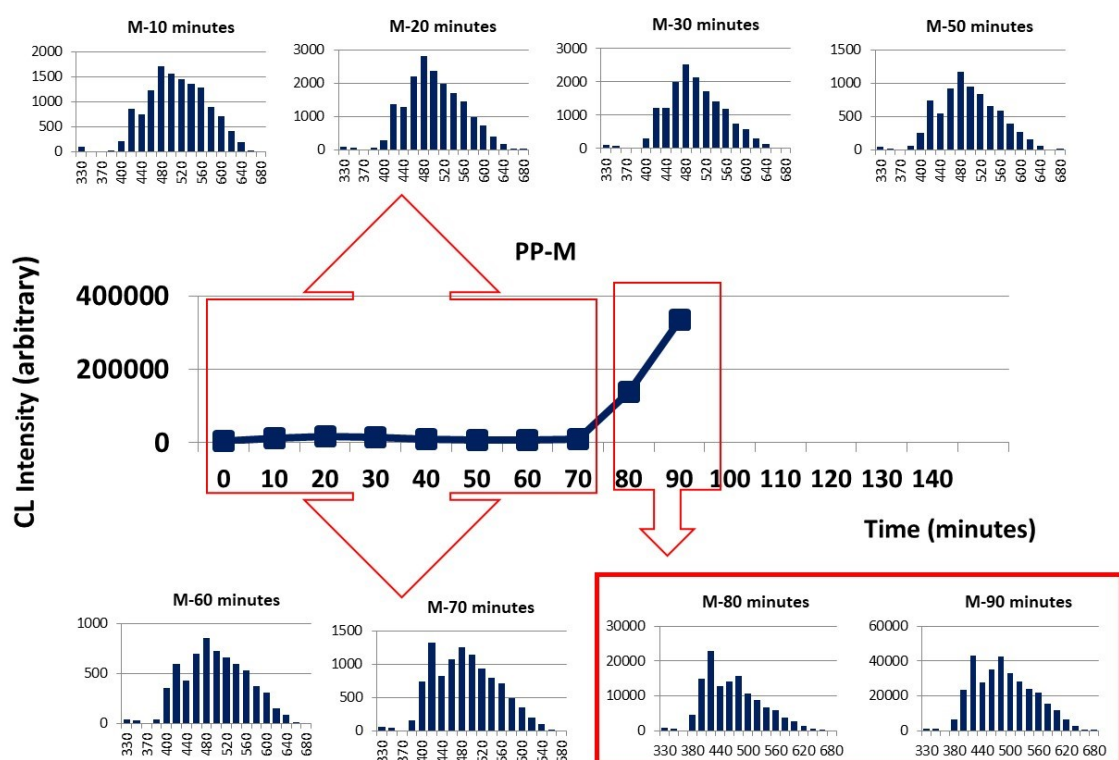


**Figure 3.22:** CL spectra in the wavelength range 380-620 nm under each data point in the CL versus time OIT plot for formulation PP-M. Data obtained in air at 180°C

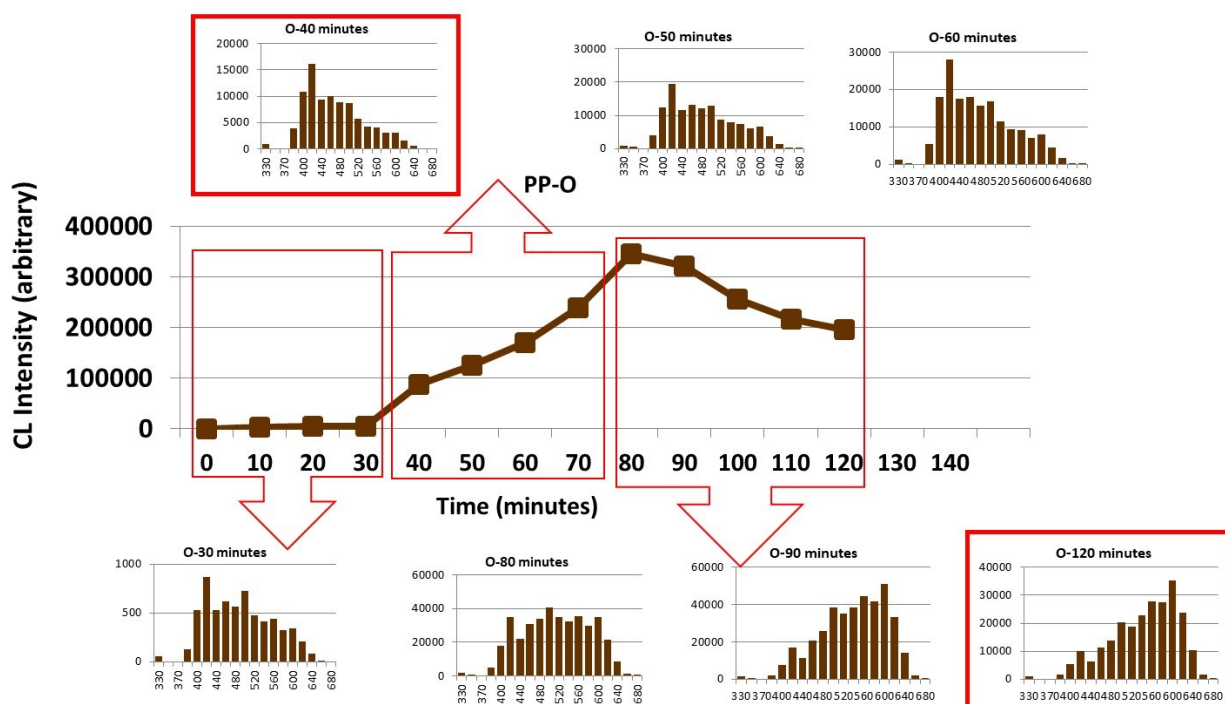


**Figure 3.23:** CL spectra in the wavelength range 380-620 nm under each data point in the CL versus time OIT plot for formulation PP-O. Data obtained in air at 180°C

If, as it is considered in the literature, the induction time to oxidation by CL measurements provides a much better indicator of polymer degradation than other techniques then it is clear that for a stabilised polymer this relates to an ability to control the concentration of excited-state carbonyls and singlet oxygen. If this is the case, then CL is essentially measuring routes to the bimolecular recombination of alkyl peroxy.

It is known that the rates of radical termination for primary and secondary alkyl peroxy radicals is very much faster than for tertiary alkyl peroxy radicals. If the Russell mechanism for the bimolecular recombination of peroxy radicals via an intermediate tetroxide is correct, then this discrepancy is unlikely. If it is accepted that cage recombination of radicals is taking place, leading to carbonyl group excited states that decay by emitting their energy as CL, then it is possible that there is some process that stabilises the transition state to facilitate this.

Recent molecular modelling studies have shown<sup>1</sup> that the activation energy barriers to the formation of the tetroxide in the Russell mechanism are too high to be applicable from a kinetic viewpoint. Instead it is proposed that the cage breaks down asymmetrically with the alkoxy radicals that are formed undergoing  $\alpha$ -hydrogen transfer to give the detected products of ketone, alcohol and oxygen. In the case of tertiary peroxy radicals such a hydrogen transfer



reaction is not possible (the nearest transferable being  $\beta$ -hydrogens) and so the alkoxyl radical would escape the cage, again consistent with observations in practice for chain termination.

If it is accepted that the  $\alpha$ -hydrogens are highly acidic and that the RO• is strongly electron-withdrawing, then this would be a suitable environment for hydrogen transfer via hydrogen bond donors. Here  $\alpha$ -hydrogens would bond to both the oxygen atoms associated with O<sub>2</sub> evolution, as would AOs with appropriate structures.

This changes the currently accepted perception of stabilisation and supports the work of others<sup>1</sup>. The work described in this thesis suggests that the CL species do indeed arise from primary and secondary alkyl peroxy radicals and that for effective stabilisation the control of these routes as a termination process is promoted at the expense of controlling the tertiary peroxy pathways that promote cage escape and propagation.

**Scheme 3.1** sketches the potential pathways for these processes. It is claimed by the authors undertaking the molecular modelling work that *“the same asymmetric cleavage process B that is known to occur for tertiary radicals, in which consecutive single bond cleavage leads to the formation of overall singlet cage containing <sup>3</sup>O<sub>2</sub> (spin up) and two same-spin RO• (spin down)...for primary and secondary alkyl radicals the two RO• can undergo alpha hydrogen transfer H to yield the experimentally observed products oxygen, alcohol and ketone. The direct reaction yields triplet ketone and triplet oxygen. For tertiary radicals, this hydrogen transfer reaction is, of course, not available. Moreover, the same-spin RO• radicals cannot yield ROOR without first undergoing a spin-flip E. This makes cage escape D a more likely possibility for the t-RO• pair and is consistent with experimental observation that a significant fraction of t-ROO• pairs do not terminate oxidation chains”*.

That is pathways G, H and I in **Scheme 3.1**, are not open to tertiary peroxy.



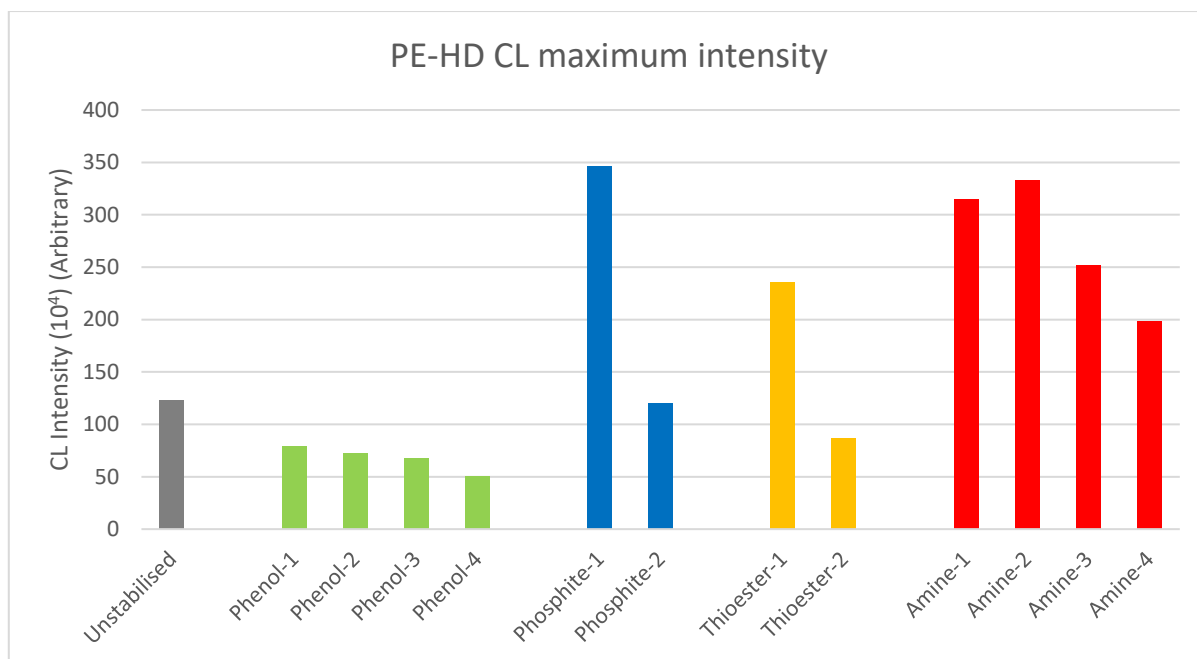


**Figure 3.24:** Maximum CL intensity (arbitrary) from PE-HD (extrusion pass 5) containing phenol, phosphite, thioester and amine antioxidant formulations

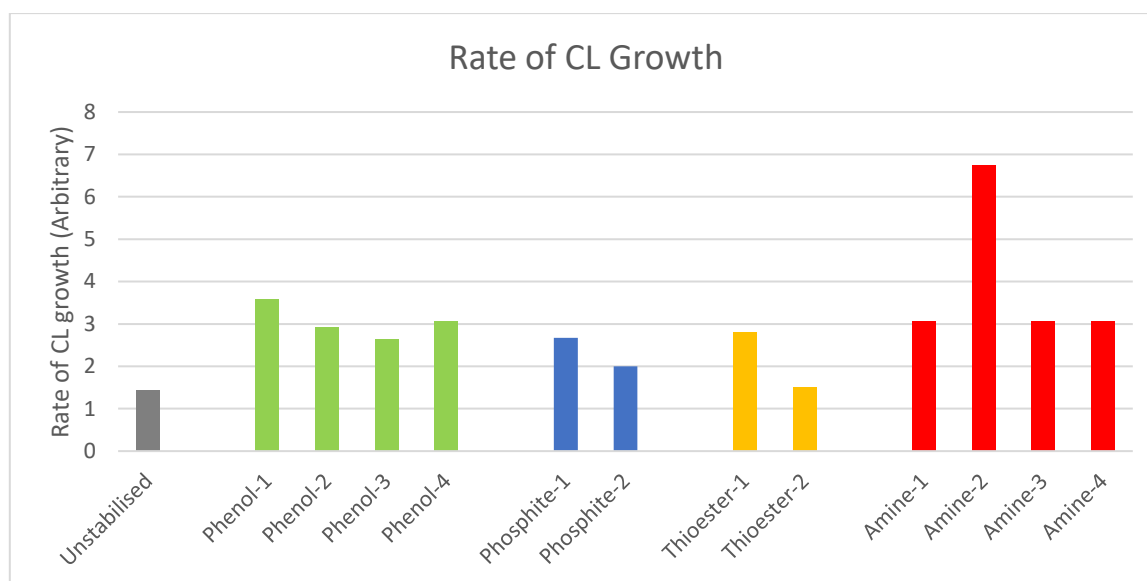


**Figure 3.25:** Rate of growth in CL intensity (arbitrary) from PE-HD (extrusion pass 5) containing phenol, phosphite, thioester and amine antioxidant formulations

## 3.2 Volatiles

As stated in the introduction, although numerous studies have been undertaken to identify VOCs originating from PP and PE, the nature of species can vary through some key products recur in all studies. This makes it difficult to draw conclusion about how AOs might interact with chain radicals to inhibit specific pathways during oxidative degradation. Because most studies on VOCs are for 'non-stabilised' polymer, the present study seeks to understand the pathways to their production by the inclusion of specific AO formulations.

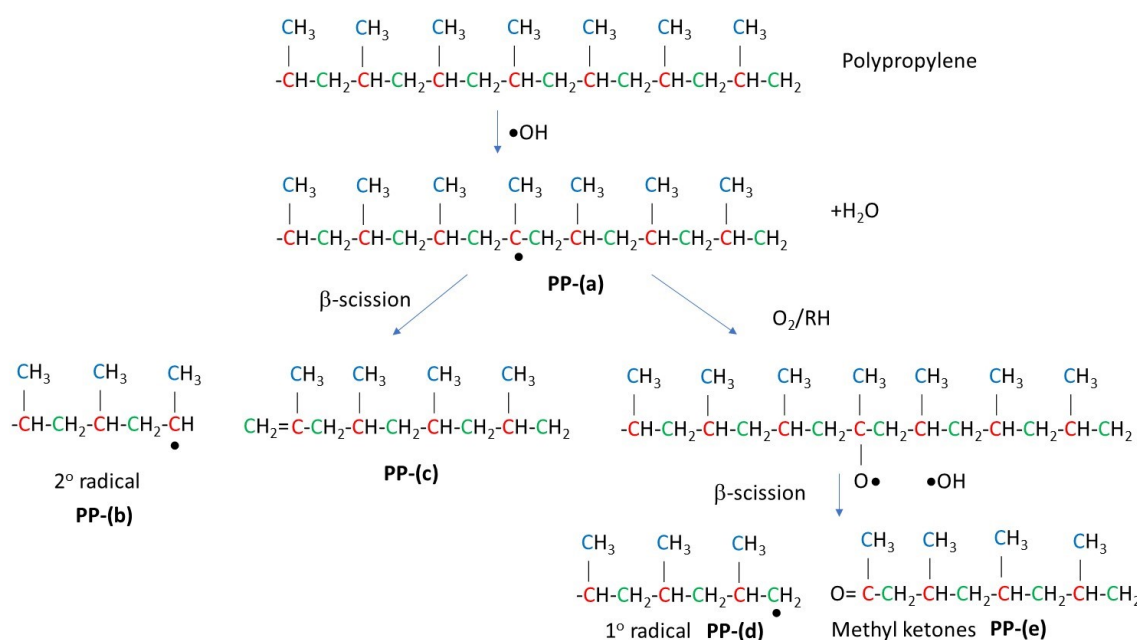
Based on previous studies<sup>43-45</sup> for PP, typical VOC's such as hydrocarbons (alkanes and alkenes), aldehydes, ketones, acids, alcohols and ethers would all be predicted to be seen in support of mechanisms proposed in this study. For PE-HD and PE-LLD<sup>46</sup>, long unsaturated alcohols, linear alkanes and branches alkanes would also be produced. However, the following data demonstrates that ketones were not present for PP and aldehydes were not present for PE for the stabilised compositions evaluated here.

In previous studies undertaken at Manchester Metropolitan University on the evolution of volatiles from the thermal oxidation of PP, PE-HD and PE-LD, interpretation of information was limited by the resolution of the mass spectrometer used<sup>52</sup>. In this study, the use of a different mass spectrometer has enabled the resolution of different isomers to provide information of specific degradation pathways. To affect a comparison with the literature, structures drawn in the schemes throughout this section have been colour highlighted according to primary, secondary and tertiary carbons in blue, green and red respectively. This corresponds to the coding presented in the work of Bernstein and others, where carbons were isotopically labelled<sup>49, 50</sup>.

### 3.2.1 Volatiles from Polypropylene

**Scheme 3.2** outlines the initial steps during degradation of PP. Although there is residual oxygen present in reactor powders, processing usually take place under nitrogen, until the PP exits the extruder and is again contacted with air. This means that there will be a mixture of products emanating from both oxidative routes and mechano-thermal scission. Assuming that there are peroxy or hydroxyl radicals already present in the reactor powders, as

suggested in the introduction, then initial hydrogen abstraction is likely to take place at tertiary sites (**PP-(a)**) resulting in direct  $\beta$ -scission and the formation unsaturated end groups (**PP-(c)**) and secondary radicals (**PP-(b)**). In the presence of oxygen and further hydrogen abstraction (by intra- or inter- molecular processes) the formation of peroxides and their breakdown to alkoxyl radicals will facilitate  $\beta$ -scission to primary radicals (**PP-(d)**) and methyl ketones (**PP-(e)**).



**Scheme 3.2:** Initial degradation pathways for generation of primary and secondary alkyl radicals in PP during polymer processing

Because the samples were air oxidised at 150°C following extrusion under nitrogen a relatively high percentage of hydrocarbons (alkenes and alkanes) were observed as a relative percentage of the total volatiles detected. The relative amounts of alkanes and alkenes are given in **Figure 3.26** and **Figure 3.27**. It is notable that more alkanes are evident across all formulations than alkenes, likely due to the fact that the alkenes are more readily oxidised and so their concentration is depleted as they are converted to oxidised fragments.

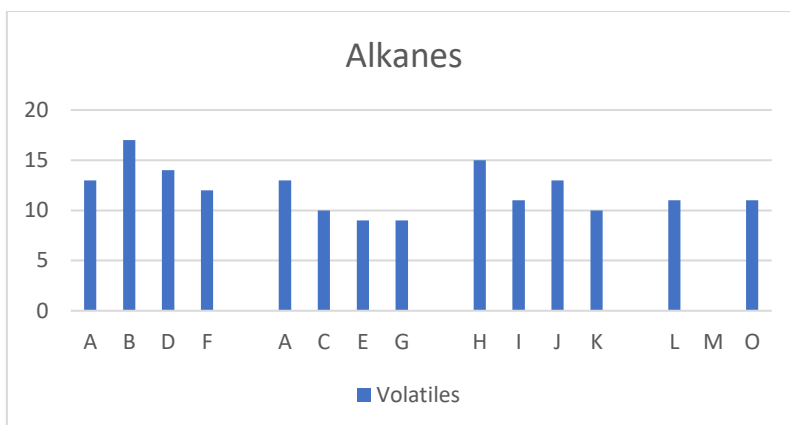


**Figure 3.26:** Alkanes as relative % total of volatiles from stabilised PP (extrusion pass 5) formulations A to O during air oxidation at 150°C for 2-20 hours by SPME GC-MS

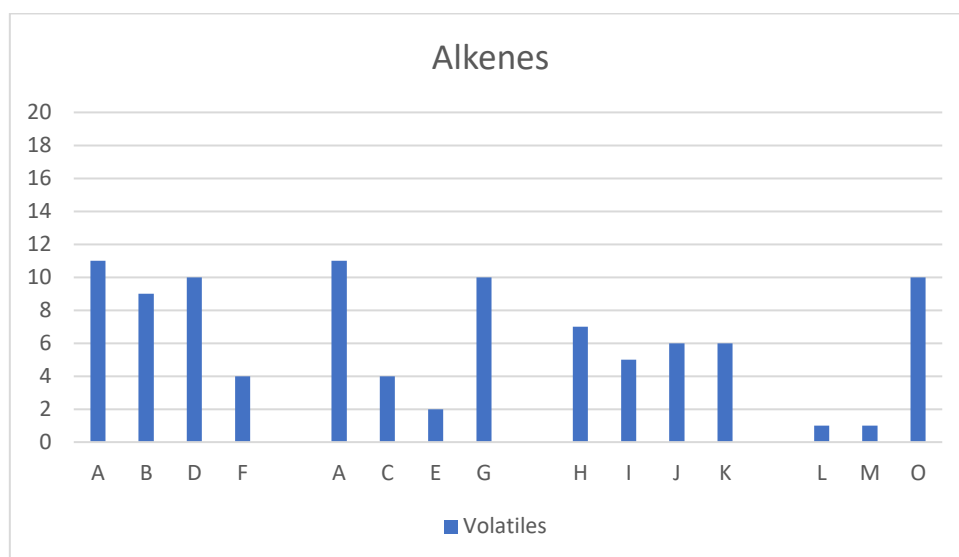
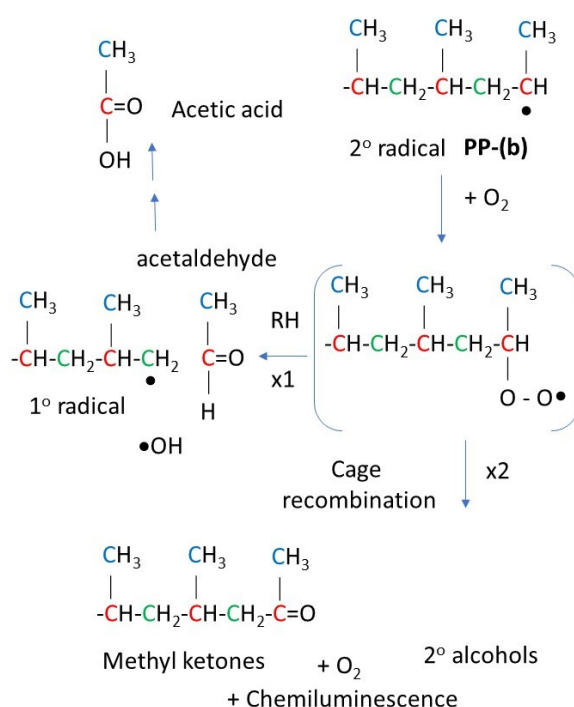


**Figure 3.27:** Alkenes as relative % total of volatiles from stabilised PP (extrusion pass 5) formulations A to O during air oxidation at 150°C for 2-20 hours by SPME GC-MS

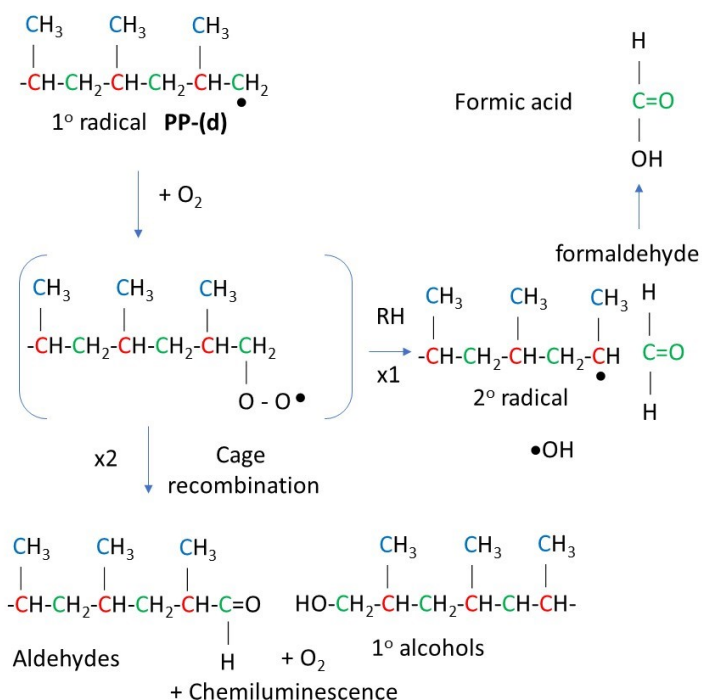
At first glance, it is difficult to discern an overall pattern in the performance of the individual formulations, so the data has been broken down to give more detail and interpreted in the context of potential mechanistic schemes and specific volatiles.

Following from **Scheme 3.3**, the primary and secondary alkyl radicals can further oxidise. If the secondary alkyl radicals are unable to escape the cage, then recombination will take place (x2 pathway **Scheme 3.3**) causing chain-termination and the production of further methyl ketones and secondary alcohols. If there is no cage recombination (x1 pathway **Scheme 3.3**), then the decomposition of resultant alkoxy radicals will result in the production of further

primary alkyl radicals and the production of acetaldehyde. The acetaldehyde is likely to oxidise readily to acetic acid, though in the presence of peroxy radicals and further oxidation, it may also offer a pathway to the production of carbon dioxide. The carbon dioxide that results will have then originated from methine sites rather than methylene sites (tertiary versus secondary carbon). For primary radicals (**Scheme 3.4**) a similar series of pathways may result in the formation of aldehydes, primary alcohols and formaldehyde. Again, the formaldehyde can readily oxidise to formic acid and potentially to carbon dioxide but in this case from methylene carbons.



**Scheme 3.3** Breakdown products resulting from the oxidation of secondary alkyl radicals in PP during polymer processing



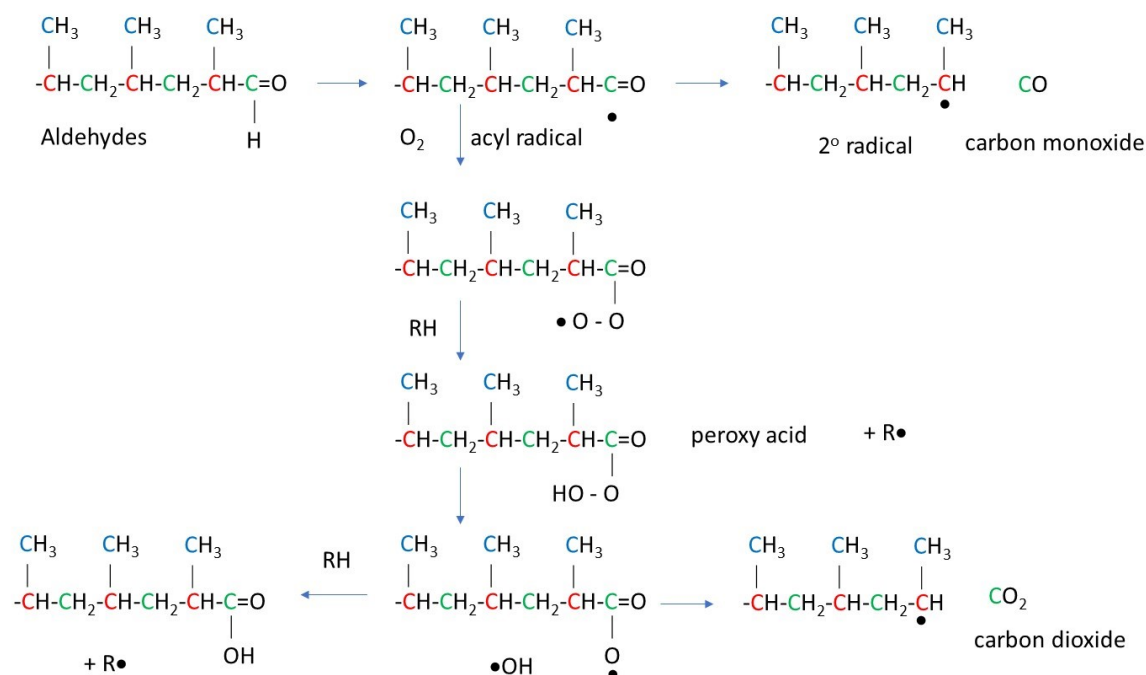
**Scheme 3.4:** Breakdown products resulting from the oxidation of primary alkyl radicals in PP during polymer processing

Any aldehydes formed will be susceptible to hydrogen abstraction to form acyl radicals, which are known to readily decompose to carbon monoxide. In the presence of oxygen, the acyl radicals could further oxidise to peroxy acids, generating carboxylic acids or further secondary radicals and carbon dioxide (**Scheme 3.5**).

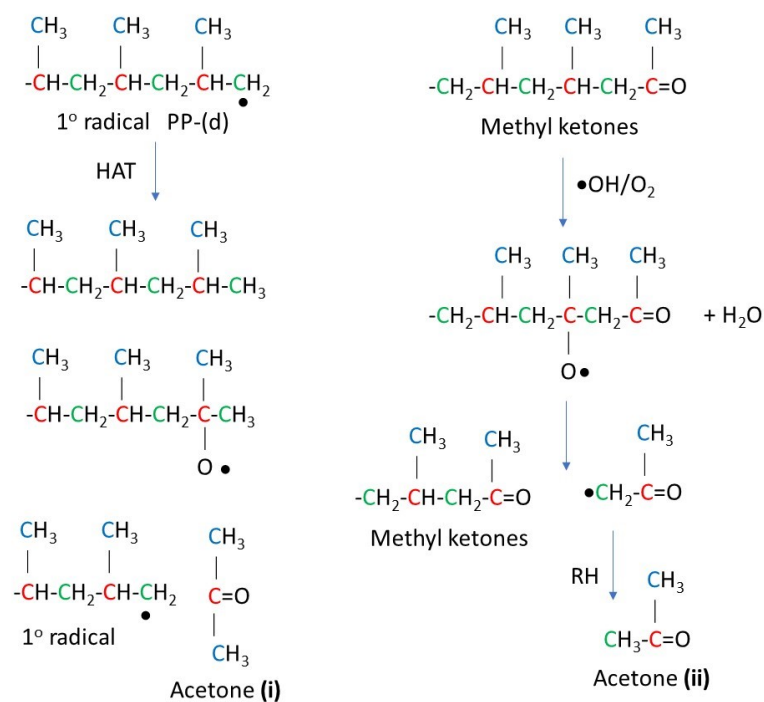
The literature also reports that acetone is formed in significant quantities compared to other volatiles. A potential mechanism that could account for this by an unzipping process has also been proposed by in the literature by Francis-Heude *et al.* (**Scheme 3.6**)<sup>47</sup>. An alternative scheme has been proposed by Bernstein *et al.*<sup>49</sup>. In this study, the carbons in PP have been subjected to isotopic labelling and volatiles determined by SPME GC-MS. The work shows that the acetone contains all three types of carbon atoms (primary, secondary and tertiary), so is more likely to originate via further scission of a methyl ketone (**Scheme 3.6 (ii)**). Given that acetone is seen mainly in the first two groups of formulations (samples PP-A to PP-G) then this latter mechanism seems more likely because there is relatively little acetone produced in formulations PP-H to PP-L which contains hydroxylamine as the base stabiliser and PP-M which contains tocopherol, both of which are capable of scavenging alkyl radicals and so



inhibiting the direct  $\beta$ -scission reactions that would facilitate the pathway proposed by Heude and co-workers.

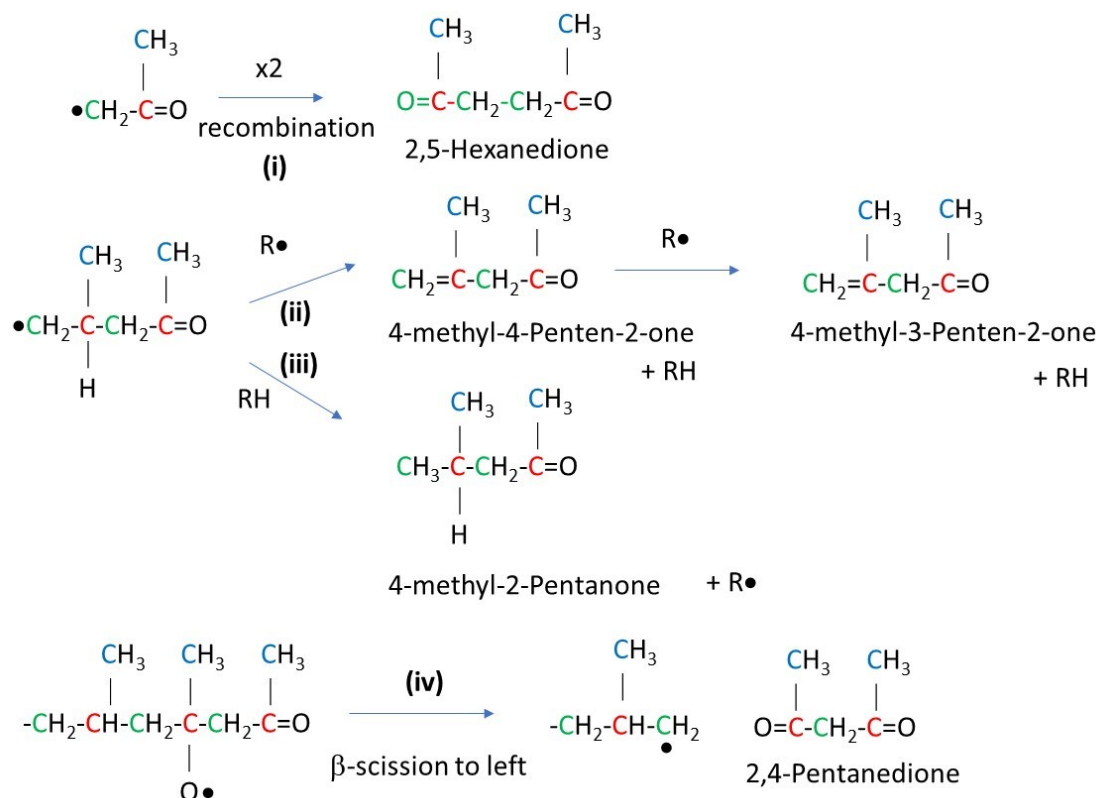


**Scheme 3.5:** Further oxidation of Aldehydes to generate carbon monoxide, carbon dioxide and carboxylic acids from PP during polymer processing



**Scheme 3.6:** Further oxidation of Aldehydes to generate carbon monoxide, carbon dioxide and carboxylic acids from PP during polymer processing





**Scheme 3.8:** Further oxidation of Aldehydes to generate carbon monoxide, carbon dioxide and carboxylic acids from PP during polymer processing

**Figure 3.28** and **Figure 3.29** summarise the low-molecular weight fragments produced during oxidation of PP containing formulations A, B, D and F. This group of samples all contain ‘base’ stabiliser (an aryl phosphite, **Phosphite-3**). PP-A contains the base stabiliser alone, PP-B also includes a phenol (**Phenol-5**) and samples PPD and PP-F the phenol along with two different thioesters (**Thioester-2** and **Thioester-3**).

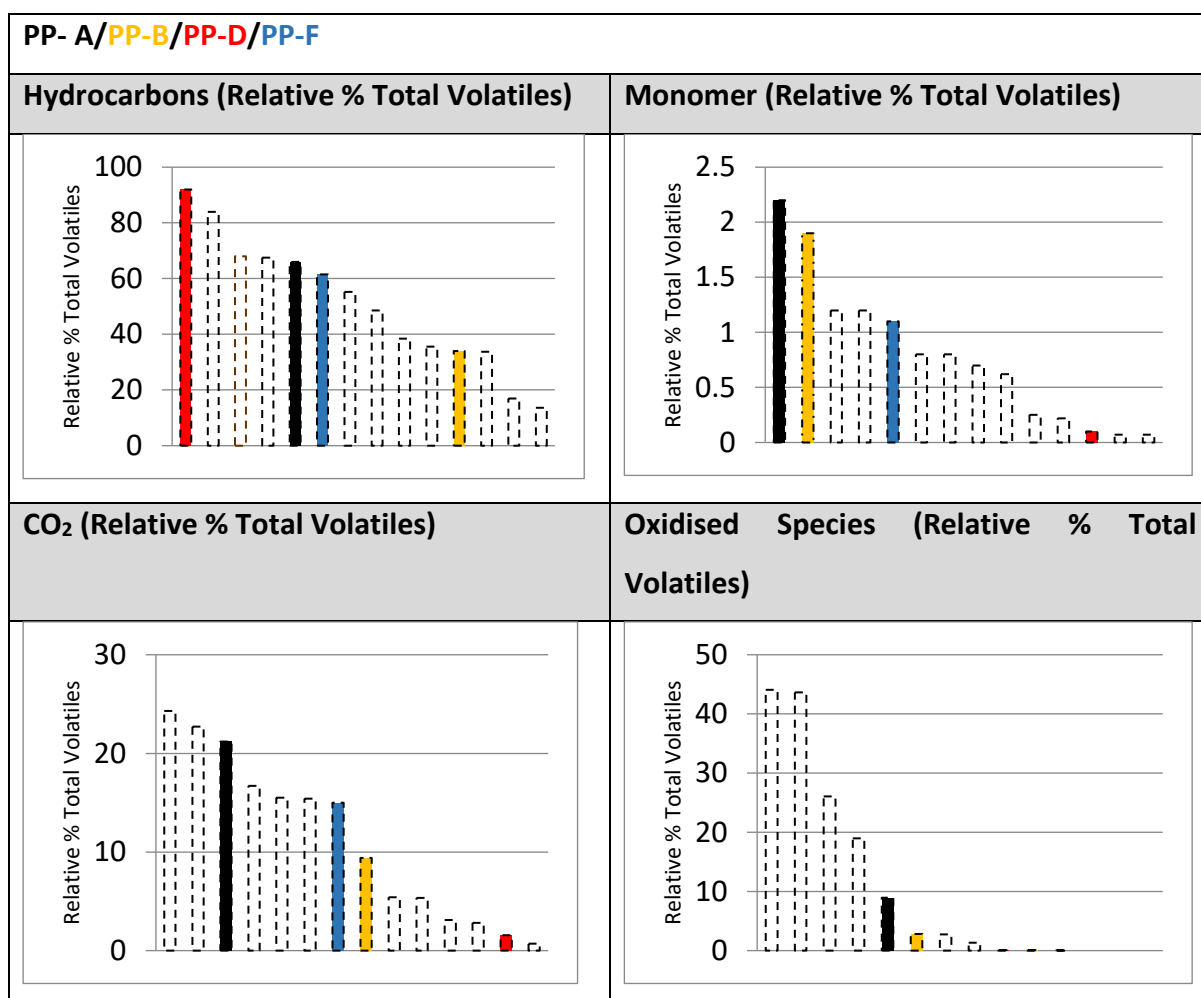


**Figure 3.28:** Volatiles as relative % total for polypropylene, stabilised with formulations A, B, D and F, in air at 150°C for 2 hours by dynamic SPME-GC-MS

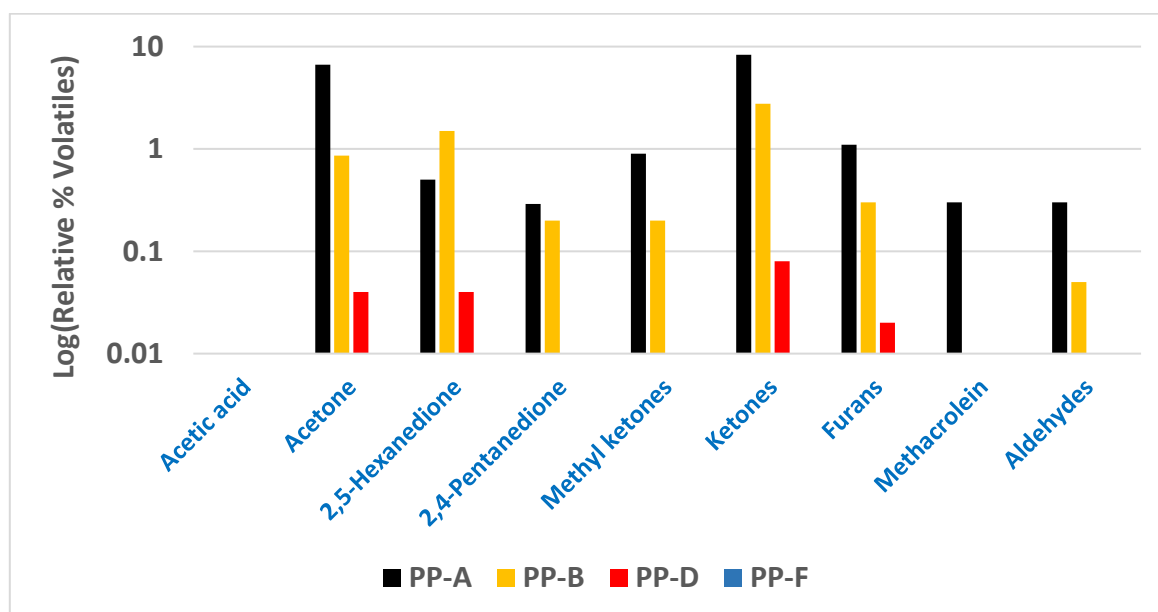


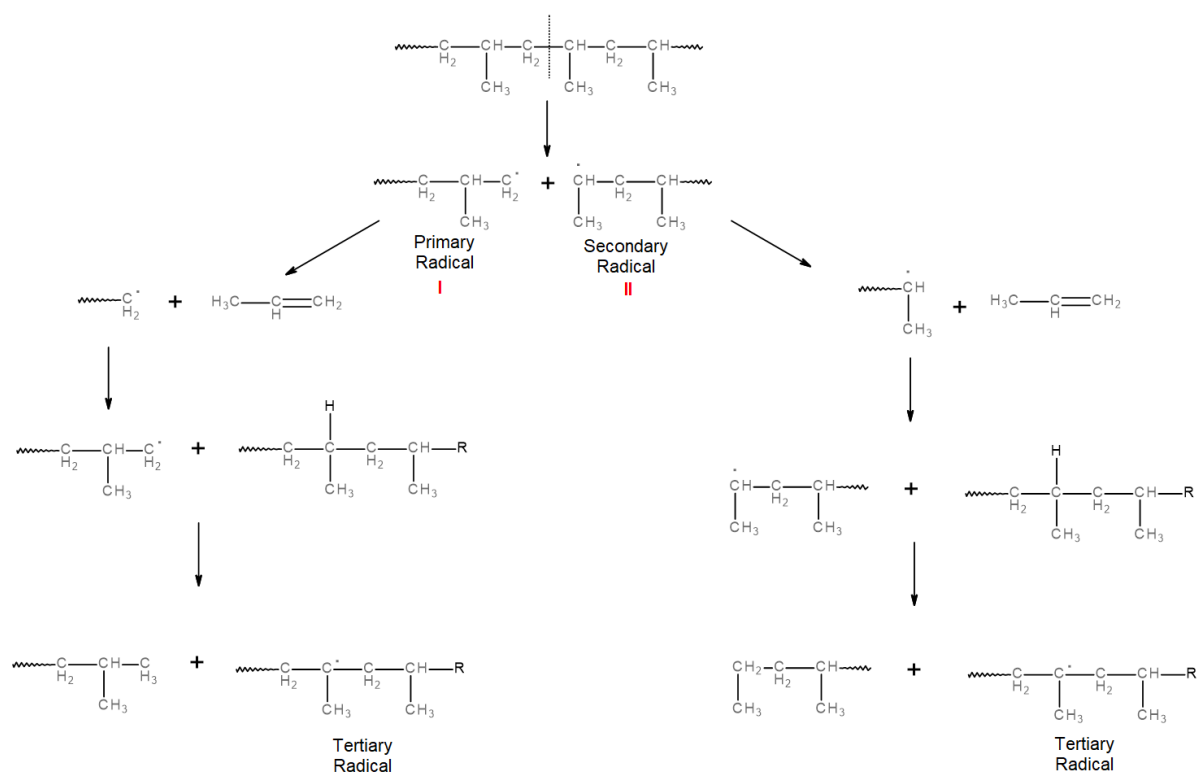
**Figure 3.29:** Oxidised species as Log of relative % total volatiles for polypropylene stabilised with formulations A, B, D and F, in air at 150°C for 2 hours and by dynamic SPME-GC-MS

Within this group of samples PP-A produces the highest amount of monomer and relatively large amounts of hydrocarbons and CO<sub>2</sub>, and lower, but noticeable amounts of oxidised species. The oxidised species contain smaller amounts of methacrolein and aldehydes and comparatively large amounts of ketones (including acetone).

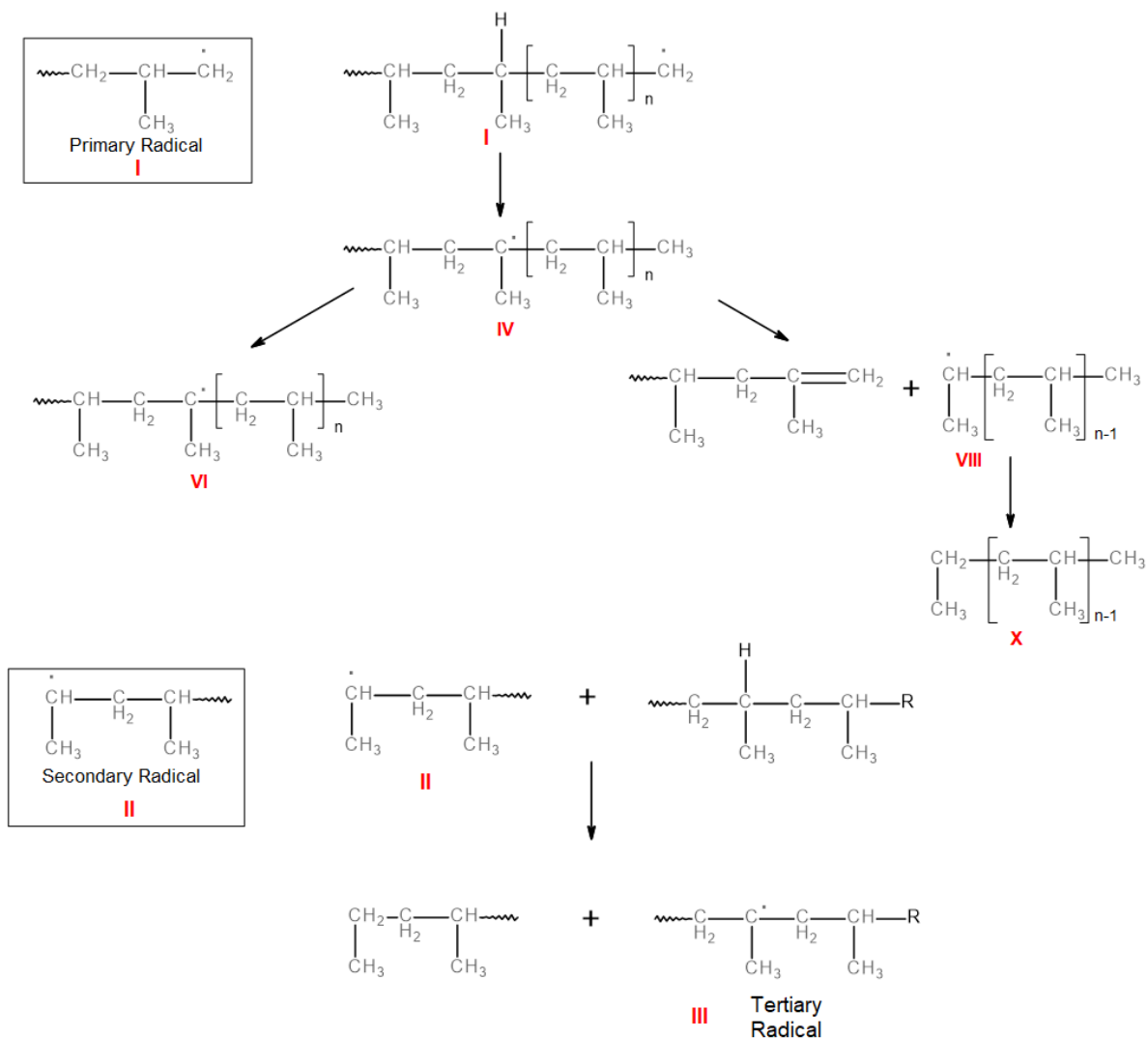
From the literature, attempts have been made to rationalise hydrocarbon degradation products from PP by selective labelling and pyrolysis<sup>49, 50</sup>. Although there are some differences between these studies and thermal oxidation processes (namely that volatile degradation products with methyl groups or double bonds at either or both ends due to higher radical concentrations and scission) they do provide a possible insight into potential pathways to fragmentation.

In summary proposals in these publications are in line with statements made by Bernstein and others<sup>49</sup> that *“Degradation products of PP having more than two directly-bonded carbon atoms, which form a simple pathway of two chain cleavages, without any other rearrangement, will always have an odd number of carbon atoms in their length”* and *“For degradation products of PP having more than two interconnected carbon atoms, the occurrence of an even number of carbon atoms along the chain length is indicative of formation via a radical-radical coupling reaction”*.

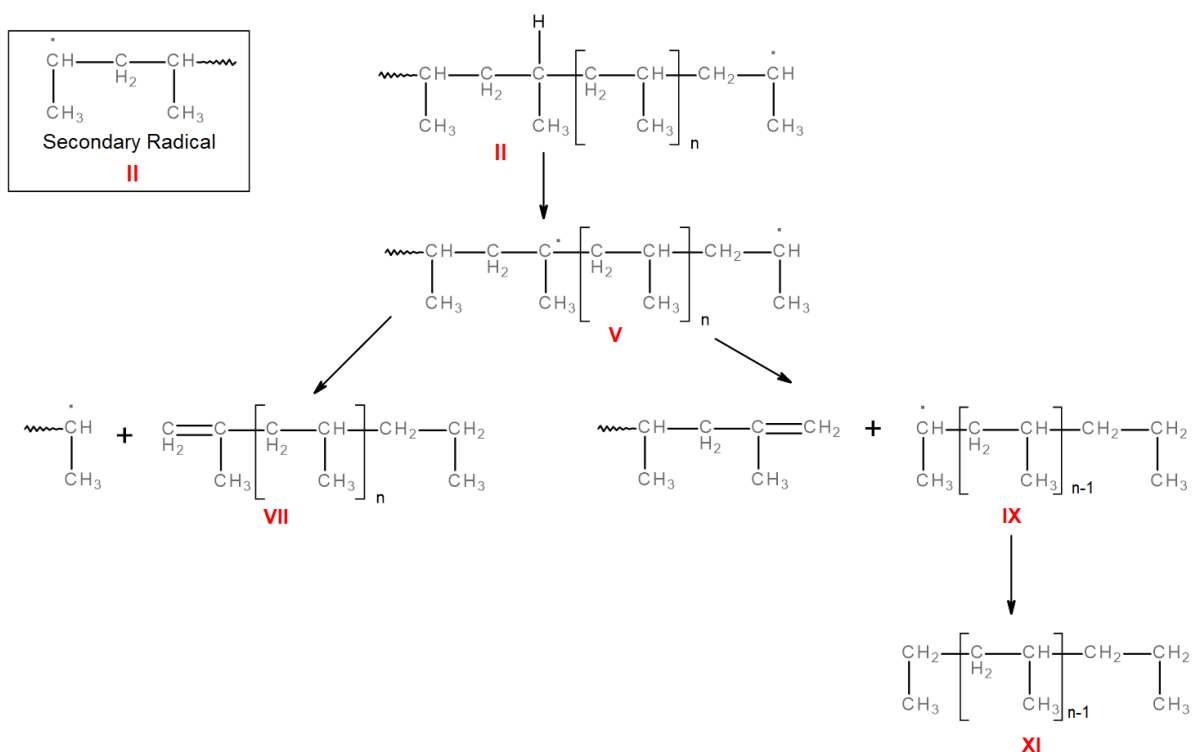
For PP, once primary and secondary alkyl radicals have been formed, either by **Scheme 3.2** or mechanically induced chain-scission in the extruder (**Scheme 3.9**), small amounts of monomer will be formed followed by intramolecular radical transfer reactions to yield tertiary radicals. The tertiary radicals so formed can undergo  $\beta$ -scission. If this occurs to the right of the radical followed by hydrogen abstraction, then the resultant products will be alkanes and if scission is to the left of the radical then the products will be alkenes (**Scheme 3.9** and **Scheme 3.10**).



**Scheme 3.9:** Mechanistic pathway for production of monomer and rearrangement of primary and secondary radicals to tertiary radicals



**Scheme 3.10:** Mechanistic pathway for the further rearrangement of primary and secondary radicals to tertiary radicals and for the further rearrangement of primary radicals to allow for the generation of alkanes and alkenes



**Scheme 3.11:** Mechanistic pathway for the further rearrangement of secondary radicals to allow for the generation of alkanes and alkenes.

**Table 3.1** and **Table 3.2** gives the molecular weight and assignments for alkanes produced by pathways I to IV to VII to X in **Schemes 3.8** to **3.11** arising from primary alkyl radicals.

**Table 3.1:** Assignments for volatile alkanes from stabilised PP formulations in air at 150°C for pathways I to IV to VII to X (outlined in Schemes 3.8 to 3.10)

n	Mw	C-atoms	Assignment
2	86	5	2-methylpentane
3	128	7	2,4-dimethylheptane
4	170	9	2,4,6-trimethylnonane
5	212	11	2,4,6,8-tetramethylundecane
6	254	13	2,4,6,8,10-pentamethyltridecane
7	296	15	2,4,6,8,10,12-hexamethylpentadecane



**Table 3.2:** Assignments of volatile alkanes from stabilised PP formulations in air at 150°C for pathways I to IV to VII to X (outlined in Schemes 3.8 to 3.11)

C-atoms	A	B	D	F		A	C	E	G		H	I	J	K		L	M	O
5																		
7																		
9																		
11																		
13																		
15																		

For the range of alkanes exhibited in **Table 3.2**, it is evident that the stabiliser formulations are unable to inhibit volatiles that originate from primary alkyl radicals. Comparing this with alkanes originally emanating from secondary radicals (**Table 3.3** and **Table 3.4**), it is clear that more of the formulations are effective as inhibitors for this route.

**Table 3.3:** Assignments for volatile alkanes from stabilised PP formulations in air at 150°C for pathways II to V to IX to XI (outlined in Schemes 3.8 to 3.11)

n	Mw	C-atoms	Assignment
1	72	5	pentane
2	114	7	4-methylheptane
3	154	9	4,6-dimethylnonane
4	198	11	4,6,8-trimethylhendecane
5	240	13	4,6,8,10-tetramethyltridecane
6	282	15	4,6,8,10,12-pentamethylpentadecane
7	324	17	4,6,8,10,12,14-hexamethylheptadecane

**Table 3.4:** Assignments for volatile alkanes from stabilised PP formulations in air at 150°C for pathways II to V to IX to XI (outlined in Schemes 3.8 to 3.11)

C-atoms	A	B	D	F		A	C	E	G		H	I	J	K		L	M	O
5																		
7																		
9																		
11																		
13																		
15																		
17																		

When compared with the corresponding alkenes the opposite is apparently true. Overall it appears that formulations that contain the hydroxylamine (**Aminic-2**) are more effective inhibitor for these routes than their corresponding phosphite-based formulations.

**Table 3.5:** Assignments for volatile alkanes from stabilised PP formulations in air at 150°C for pathways II to V to IX to XI (outlined in Schemes 3.8 to 3.11)

n	Mw	C-atoms	Assignment
0	56	3	isobutylene
1	98	5	2,4-dimethyl-1-pentene
2	140	7	2,4,6-trimethyl-1-heptene
3	182	9	2,4,6,8-tetramethyl-1-nonene
4	224	11	2,4,6,8,10-pentamethyl-1-hendecene
5	266	13	2,4,6,8,10,12-hexamethyl-1-tridecene
6	308	15	2,4,6,8,10,12,14-heptamethyl-1-pentadecene
7	350	17	2,4,6,8,10,12,14,16-octamethyl-1-heptadecene
8	392	19	2,4,6,8,10,12,14,16,18-nonamethyl-1-nonadecene

**Table 3.6:** Assignments of volatile alkenes from stabilised PP formulations in air at 150°C

C-atoms	A	B	D	F		A	C	E	G		H	I	J	K		L	M	O
3																		
5																		
7																		
9																		
11																		
13																		
15																		
17																		
19																		

**Table 3.7:** Assignments for volatile alkenes from stabilised PP formulations in air at 150°C for pathways II to V to IX to XI (outlined in Schemes 3.8 to 3.11)

n	Mw	C-atoms	Assignment
0	84	5	2-methyl-1-pentene
1	128	7	2,4-dimethyl-1-heptene
2	168	9	2,4,6-trimethyl-1-nonene
3	210	11	2,4,6,8-tetramethyl-1-hendecene
4	252	13	2,4,6,8,10-pentamethyl-1-tridecene
5	338	15	2,4,6,8,10,12-hexamethyl-1-pentadecene
6	380	17	2,4,6,8,10,12,14-heptamethyl-1-heptadecene
7	420	19	2,4,6,8,10,12,14,16-octamethyl-1-nonadecene
8	462	21	2,4,6,8,10,12,14,16,18-nonamethyl-1-uncosene

**Table 3.8:** Assignments of volatile alkenes from stabilised PP formulations in air at 150°C

C-atoms	A	B	D	F		A	C	E	G		H	I	J	K		L	M	O
5																		
7																		
9																		
11																		
13																		
15																		
17																		
19																		
21																		

Gijsman<sup>86</sup> has suggested that at processing temperatures, the recognised mechanism (**Scheme 1.22**) for phosphite and phosphonite antioxidants is doubtful under processing conditions, because the rate of decomposition of peroxides is high. It may be that the ability of phosphorus-based antioxidant to scavenge radicals ( $\text{ROO}\bullet$ ,  $\text{RO}\bullet$ ) becomes more important under these conditions, but this will clearly be a competitive process when other antioxidants are present. A table of peroxide decomposition temperatures and half-lives are given in the table below.

**Table 3.9:** Table of half lifes of typical peroxides

Common Types	Typical Formula	10 Hour Half-life Range (°C)
dialkyl peroxides	$R_1-O-O-R_2$	117 – 133
hydroperoxides	$R_1-O-O-H$	133 – 172
diacyl peroxides	$R_1-\overset{\overset{O}{\parallel}}{C}-O-O-\overset{\overset{O}{\parallel}}{C}-R_2$	20 – 75
peroxydicarbonates	$R_1-O-\overset{\overset{O}{\parallel}}{C}-O-O-\overset{\overset{O}{\parallel}}{C}-O-R_2$	49 – 51
peroxyesters	$R_2-O-O-\overset{\overset{O}{\parallel}}{C}-R_1$	49 – 107
ketone peroxides	$H-O-O-\left(\begin{array}{c} R_1 \\   \\ -C- \\   \\ R_2 \end{array} O-O \right)_n-H$	N/A
peroxyketals	$R_1-O-O-\overset{\overset{R_2}{\mid}}{\underset{\underset{R_3}{\mid}}{C}}-O-O-R_1$	92 – 115
alkylperoxy carbonates	$R_1-O-O-\overset{\overset{O}{\parallel}}{C}-O-R_2$	90 – 100

$R_1$  and / or  $R_2$  are generally alkyl groups, often tertiary-alkyl groups. If attached directly to the peroxy group,  $n$  is 1 - 3. One of the groups can be hydrogen.

The amount of monomer produced is quite small in comparison to oxidised species, suggesting that in the presence of oxygen this route to degradation is supplanted by the production of oxidised fragments.

Sample PP-F shows barely detectable levels of oxidised species (**Figures 3.28 and 3.29**), but it does produce larger amounts of  $CO_2$ . This thioester (**Thioester-3**) is linked by a pentaerythritol group and is analogous to the phenol (**Phenol-5**). In this structural arrangement the thioester, despite having a larger molar quantity of active sulfur groups, is less effective in suppressing the acyl peroxy species. A better understanding of this may be gained in the section on chemiluminescence.

**Figure 3.30** and **Figure 3.31** summarise the low-molecular weight fragments produced during oxidation of PP containing formulations A, C, E and G. This group of samples all contain the same ‘base’ stabiliser (an aryl phosphite, **Phosphite-3**) as for the previous set of samples. They differ from the previous set in the use of a different phenolic structure. PP-C includes this phenol (**Phenol-6**) and samples PP-E and PP-G the two different thioesters (**Thioester-2** and **Thioester-3** respectively).

Compared with sample PP-B this alternative phenol (PP-C) produces significantly more hydrocarbons and slightly less CO<sub>2</sub> and oxidised species. In this case, the latter consist more aldehydes, lesser amounts of ketones, acetic acid and methacrolein.

Unlike sample PP-D, the formulation PP-E produces large quantities of CO<sub>2</sub>, though the overall amounts of oxidised species are very low.

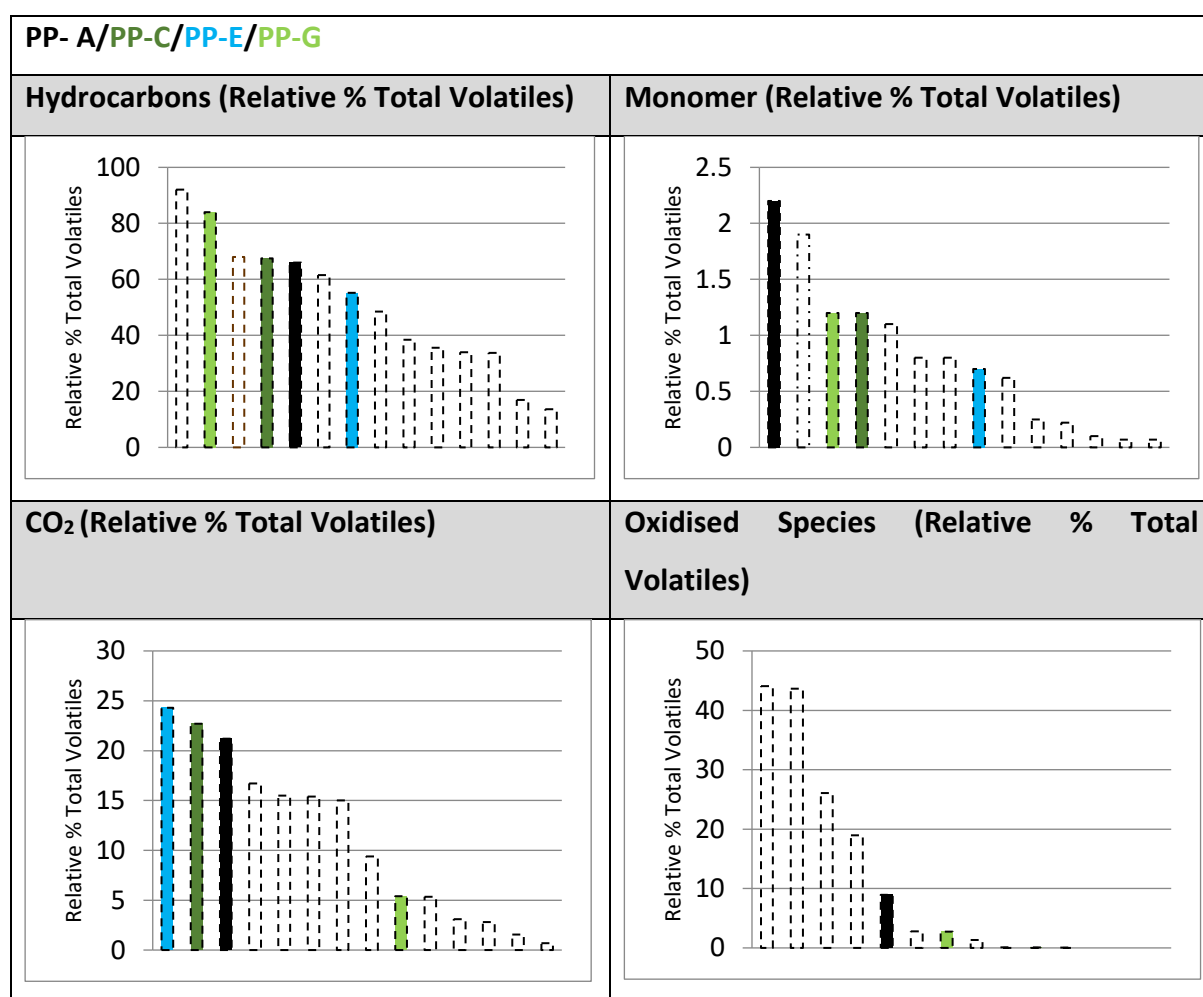


**Figure 3.30:** Volatiles as relative % total volatiles for polypropylene stabilised with formulations A, C, E and G, aged in air at 150°C for 2 hours and analysed by dynamic SPME-GC-MS

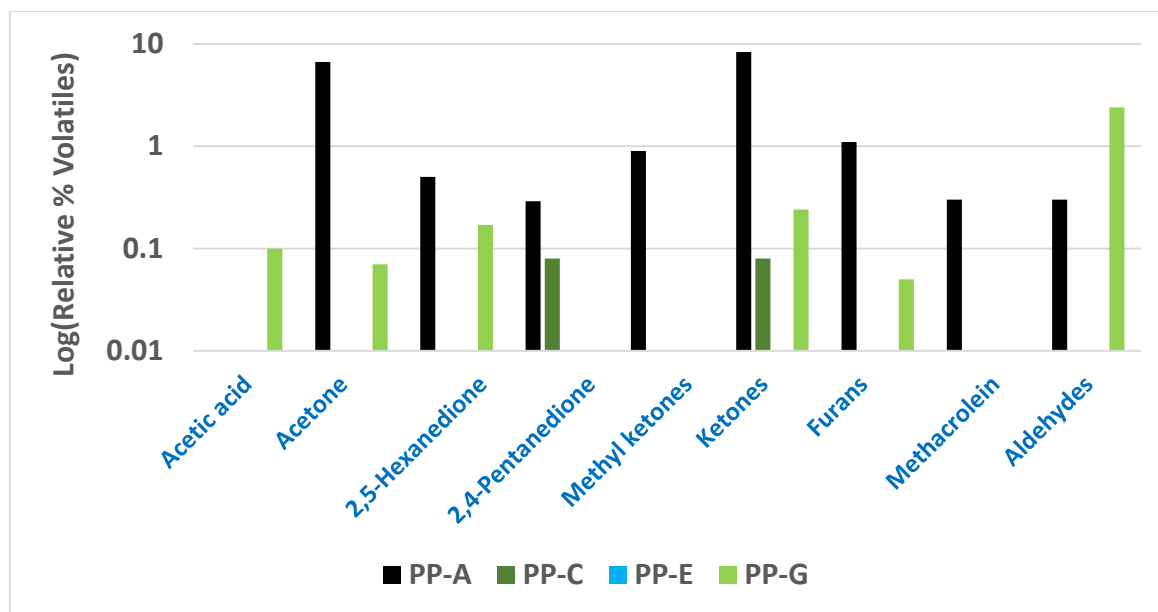


**Figure 3.31:** Oxidised species as Log of relative % total volatiles for polypropylene stabilised with formulations A, C, E and G, in air at 150°C for 2 hours by dynamic SPME-GC-MS

The next group of samples (**Figure 3.32** and **Figure 3.33**) replace the phosphite base stabiliser with hydroxylamine. PP-H contains the hydroxylamine alone (**Aminic-2**), PP-I includes the phenol (**Phenol-5**) and samples PP-J and PP-K the respective thioesters (**Thioester-2** and **Thioester-3**). The most notable feature of these formulations is the reduction in the relative % of hydrocarbons and monomer that are produced (**Figure 3.32**).

When the hydroxylamine is present alone it is unable to block the production of CO<sub>2</sub>: this sample producing the largest quantity of this volatile for all the formulations. When it is used in combination with the **Thioester-3** it can block routes to CO<sub>2</sub> production more effectively, but it produces the highest amount, relative to other formulations, of oxidised species.

For samples PP-H, PP-J and PP-K larger amounts of aldehydes comprise the oxidised species. Sample PP-I shows barely detectable oxidised species, this sample being the combination of the hydroxylamine and phenol with no thioester present.

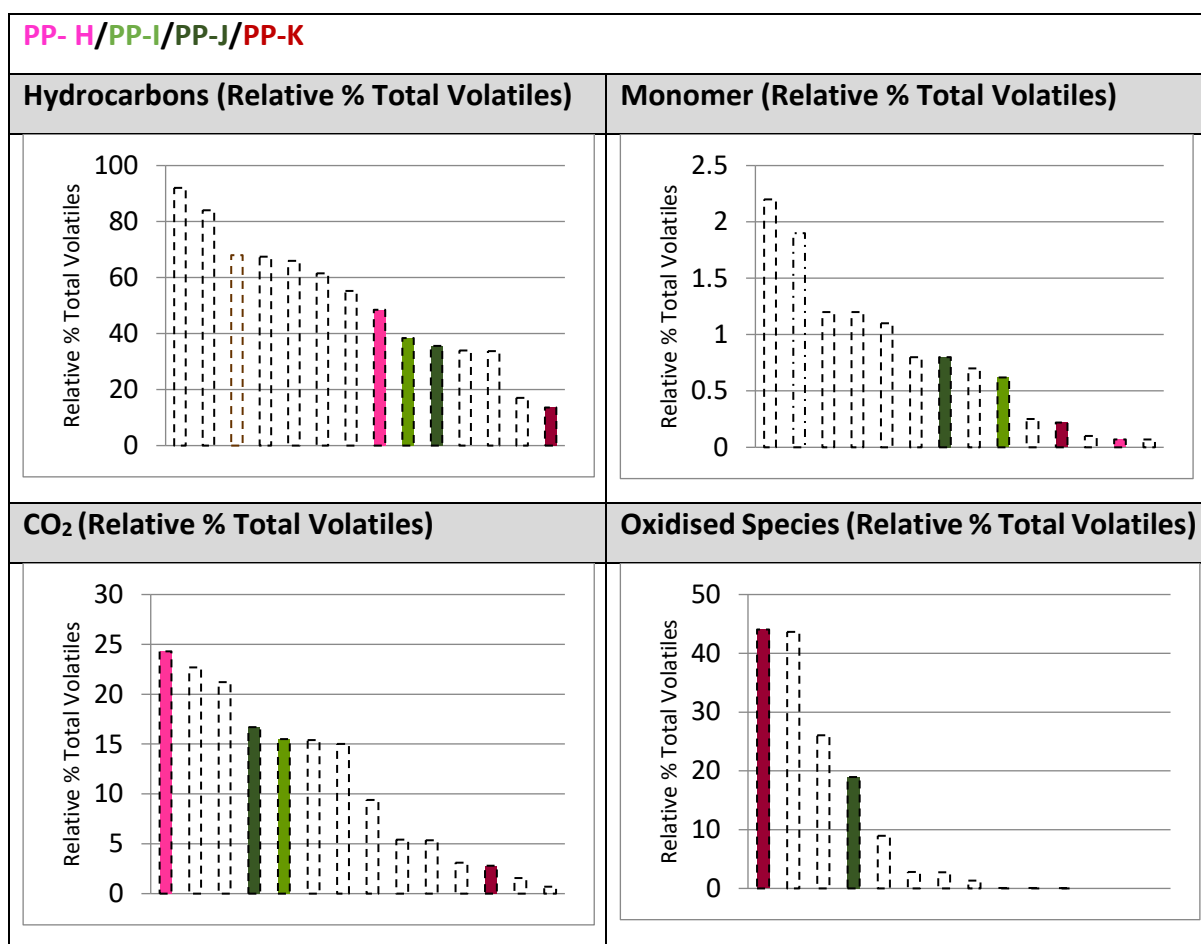


**Figure 3.32:** Volatiles as relative % total volatiles for polypropylene stabilised with formulations H, I, J and K, in air at 150°C for 2 hours by dynamic SPME-GC-MS

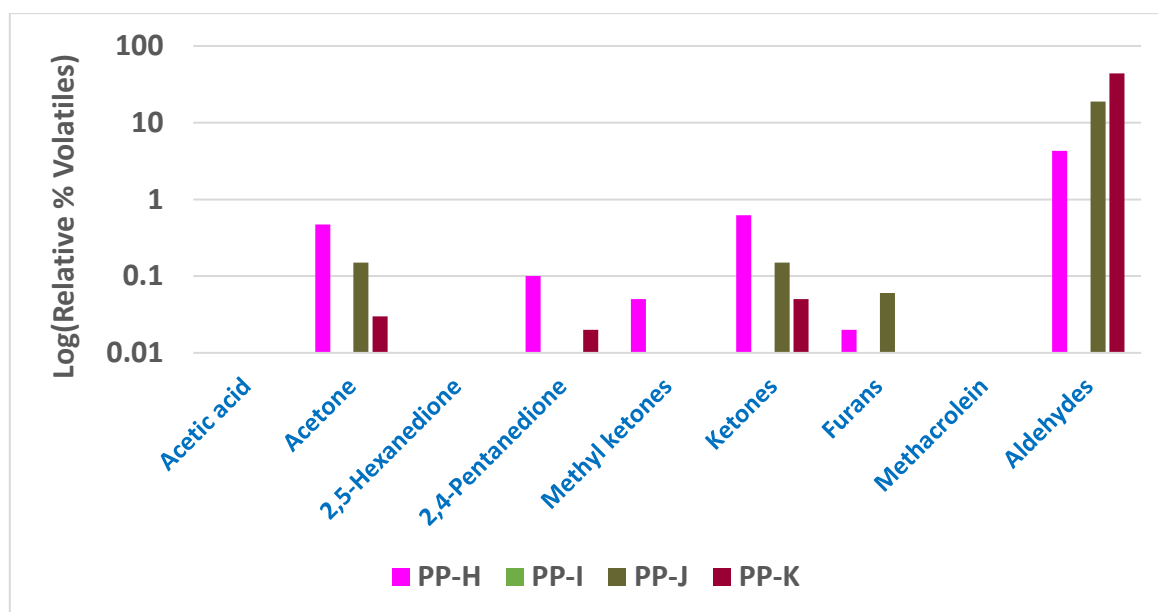


**Figure 3.33:** Oxidised species as Log of relative % total volatiles for polypropylene stabilised with formulations H, I, J and K, in air at 150°C for 2 hours by dynamic SPME-GC-MS

The final group of samples are PP-L, PP-M and PP-O. Sample PP-L follows the theme of samples PP-H to PP-K also containing a hydroxylamine as the base stabiliser, but here the phenol has been replaced with **Phenol-6**, giving the analogous formulation to PP-K. This has the effect of increasing the amounts of hydrocarbons observed in relation to other samples in the series.

Sample PP-M is analogous to samples PP-J and PP-D but replace base stabiliser with  $\alpha$ -tocopherol, although this compromises the route to CO<sub>2</sub> production. Sample PP-O contains a hindered amine (**Aminic-4**) along with the base stabiliser (**Phosphite-3**). This combination of AOs is better at preventing the production of oxidised species but has poorer performance for the suppression of hydrocarbons compared with the use of a hydroxylamine.

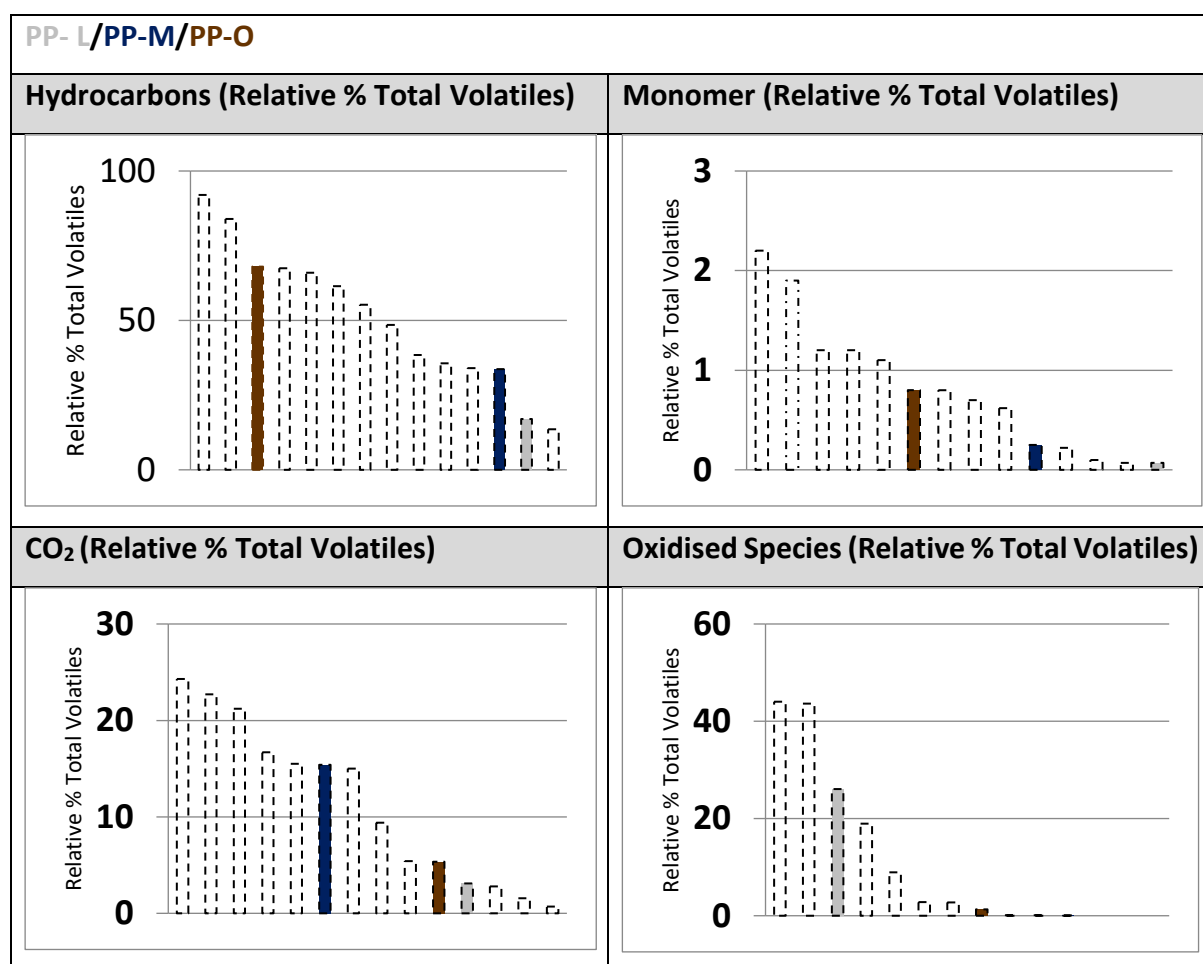


**Figure 3.34:** Volatiles as relative % total volatiles for polypropylene stabilised with formulations H, I, J and K, in air at 150°C for 2 hours by dynamic SPME-GC-M



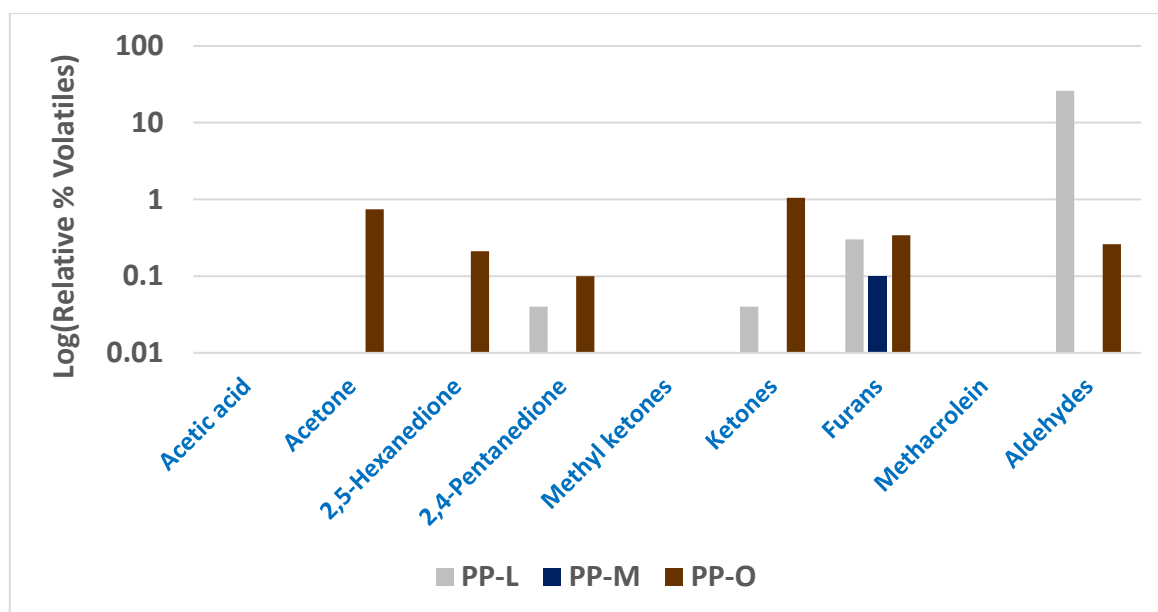


**Figure 3.35:** Oxidised species as Log of relative % total volatiles for polypropylene stabilised with formulations H, I, J and K, in air at 150°C for 2 hours by dynamic SPME-GC-MS

For extraction of fragments in hexane and ethanol for semi-volatiles the same trends in the distribution of the fragments is evidenced reinforcing earlier proposals regarding the degradation pathways. **Figure 3.36** and **Figure 3.37** shows the total relative percentage extractables from hexane and ethanol. It can be seen that similar overall trends apply for both volatiles and extractable for the relative trends in the amounts of hydrocarbons generated by the different formulations.

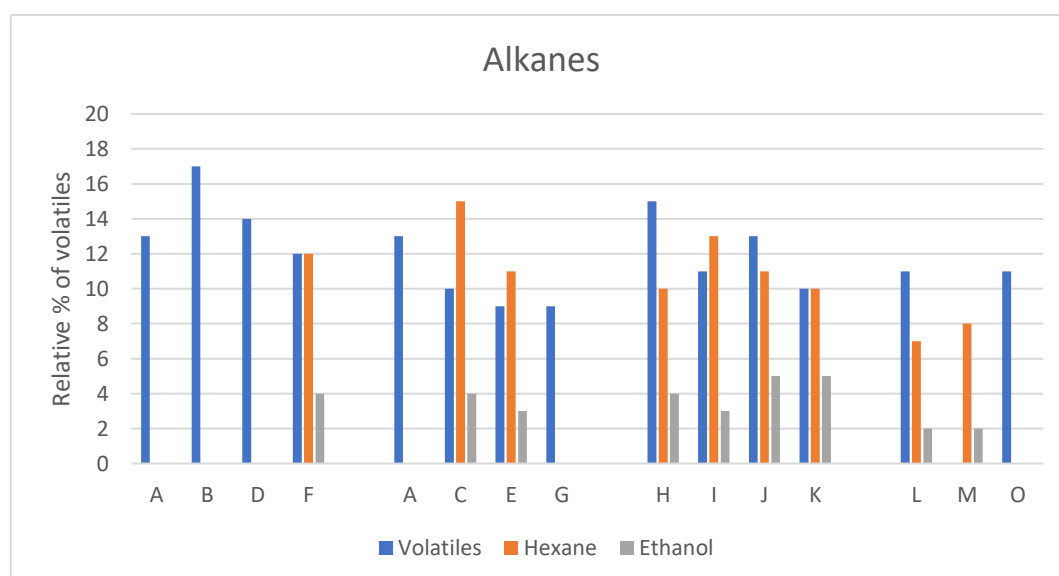


**Figure 3.36:** Alkanes as relative % total of volatiles and extractables in hexane and ethanol from stabilised PP (extrusion pass 5) formulations A to O during air oxidation at 150°C for 2-20 hours by SPME GC-MS

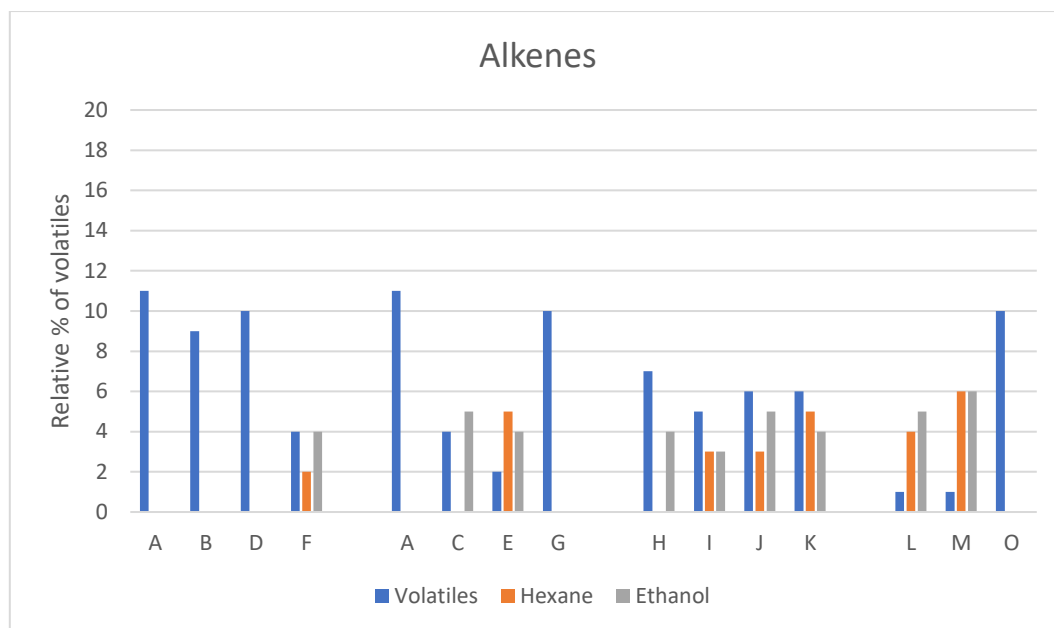


**Figure 3.37:** Alkenes as relative % total of volatiles and extractables in hexane and ethanol from stabilised PP (extrusion pass 5) formulations A to O during air oxidation at 150°C for 2-20 hours by SPME GC-MS

Specific volatiles highlighted in **Table 3.10** and **Table 3.11** show that extractables constitute the longer chain analogues of their volatile counterparts (note here rather than specify all isomers an indication of the presence of specific species is designated by the longest carbon chain length).

**Table 3.10:** Low molecular weight species (alkanes and alkenes) observed in GC-MS spectra following extractions to hexane (■) or ethanol (■) or both (■) from PP (stabilised with formulations C to M) after extrusion Pass 5

Alkanes	C	E	F	H	I	J	K	L	M
Cycloeicosane (C20)					■				
Cyclohexadecane			■			■			
Cyclopentadecane	■								
Cyclotetradecane	■					■		■	
Cyclododecane	■		■			■	■	■	■
Dodecane (C12)	■					■	■		
Eicosane (C20)	■	■	■	■	■	■	■		■
Heneicosane (C21)			■	■			■		■
Heptacosane (C27)	■					■			
Heptadecane	■					■	■	■	■
Hexacosane (C26)								■	
Hexadecane	■		■	■	■	■			
Nonadecane		■	■	■	■				
Octacosane (C28)		■	■	■	■				■
Octadecane	■	■	■	■	■	■	■	■	■
Hexadecane	■					■			
Pentadecane		■	■	■	■		■		
Tetradecane				■					
2-Methylhexacosane						■			
2-Methyltetracosane							■		
Eicosane, 3-methyl-								■	
Hentriacontane (C31)							■		
Cyclohexane, (1-hexyltetradecyl)-									■

Alkenes	C	E	F	H	I	J	K	L	M
1-Docosene		■	■					■	
1-Dodecene					■			■	■
1-Eicosene									■
1-Nonadecene	■					■			
1-Nonene								■	
1-Octadecene	■	■	■		■	■	■	■	■
1-Pentadecene							■		
1-Tetradecene									■
1-Tridecene									■
2-Tetradecene, (E)-							■		
2-Undecene, 6-methyl-, (Z)-		■							
3-Eicosene, (E)-	■						■		■
5-Eicosene, (E)-									■
Cetene		■				■			
Henicos-1-ene		■							
Z-5-Nonadecene					■				
1-Tetracosene	■	■							
3-Heptadecene, (Z)-	■								
1,19-Eicosadiene		■				■			
4-Tetradecene, (E)-		■							

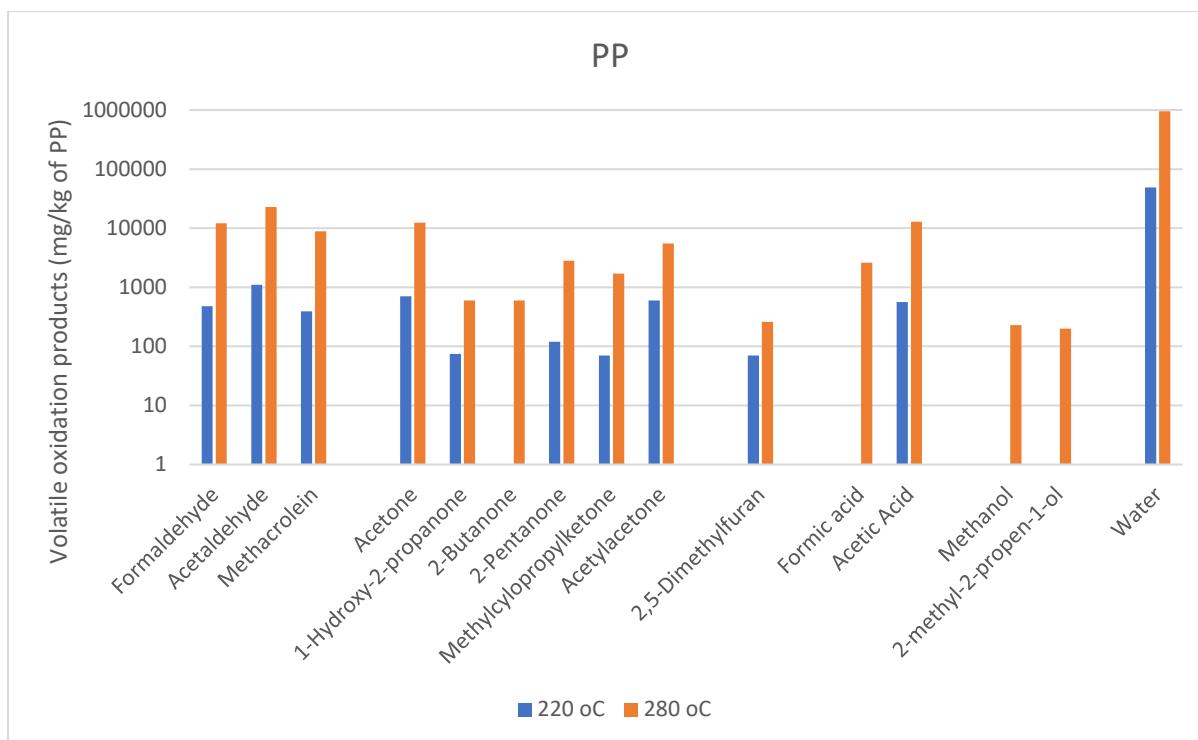
**Table 3.11:** Low molecular weight species (alcohols, aldehydes, ketones\*) extracted to hexane (■) or ethanol (■) or both (■) from PP (stabilised with formulations C to M) after extrusion Pass 5

Alcohols	C	E	F	H	I	J	K	L	M
1-Hexadecanol, 2-methyl-	■					■	■		
1-Octanol, 2-butyl-				■					■
1-Propanol, 2,2-dimethyl-		■	■						
2,4,7,9-Tetramethyl-5-decyn-4,7-diol						■			
2-Heptadecanol	■	■							
2-Hexyl-1-octanol						■			
3-Hexadecanol						■			
9-Hexadecen-1-ol, (Z)-								■	
n-Nonadecanol-1						■			
2-Hexadecanol	■								
2-Pentadecanol	■								
2-Tetradecanol	■								
E-2-Tetradecen-1-ol	■								
Ethanol, 2-(octadecyloxy)-	■			■	■				
1-Decanol, 2-hexyl-					■				
1-Heptacosanol					■				
2,3-Nonadecanediol					■				
Octacosanol								■	

Aldehydes	C	E	F	H	I	J	K	L	M
E-15-Heptadecenal		■							
Heptadecanal	■				■	■		■	
Hexadecanal					■	■	■		
Octadecanal				■		■	■	■	
Pentadecanal-	■				■	■		■	
Tetradecanal				■				■	■
Tridecanal	■						■		
Dodecanal								■	
Tetracosanal				■					

\*No ketones

Collectively, the findings in the study supports that from other researchers<sup>43-45</sup>. Hoff has shown that water is formed in the greatest quantity, but aldehydes, ketones and small chain carboxylic acids are also significant volatile oxidation products relative to lower quantities of alcohols and furans. The relatively higher quantities of acetone, formaldehyde/formic acid and acetaldehyde/acetic acid supports the premise that both direct  $\beta$ -scission (*tert*-P●) routes and incorporation of oxygen at tertiary sites followed by  $\beta$ -scission to produce methyl ketone (*tert*-PO●) routes are important, at least in the initial stages of degradation.



**Scheme 3.12:** Volatiles arising from thermal oxidation of iPP in air at 220°C and 280°C (adapted from data<sup>43</sup>)

Reich and Stivala<sup>42</sup> have also referred to the work on the evolution of volatiles during the oxidation of polyolefins showing that of the volatiles expressed in millimoles of volatile per mole polymer, water is the product that is generated in the largest amount<sup>42</sup>. Water is produced from the abstraction of hydrogen during chain-branching steps (and possibly initiation), so it may be that this process is more important than previously thought. The levels of carbon dioxide and carbon monoxide are also relatively high and of a similar level to the production of carboxylic acids. Relatively, the amounts of formaldehyde and acetaldehyde are lower. This suggests that cage recombination to form aldehydes from primary radicals is dominant in the early stages of degradation.

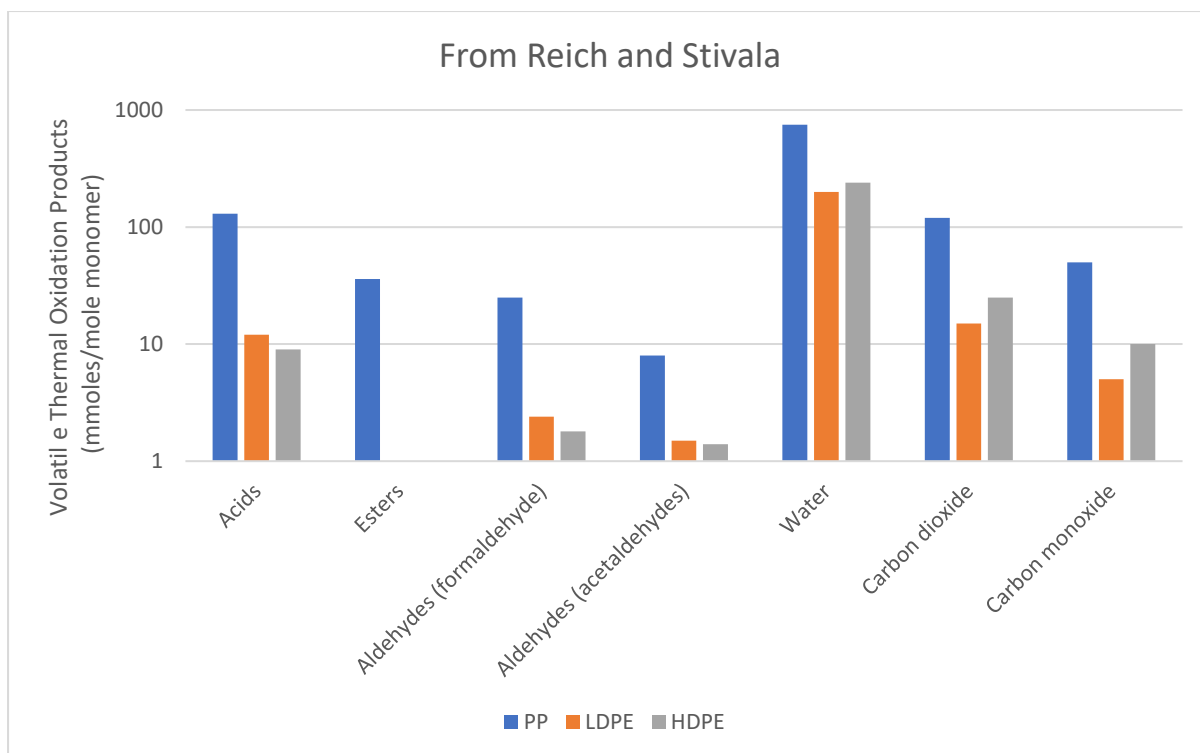
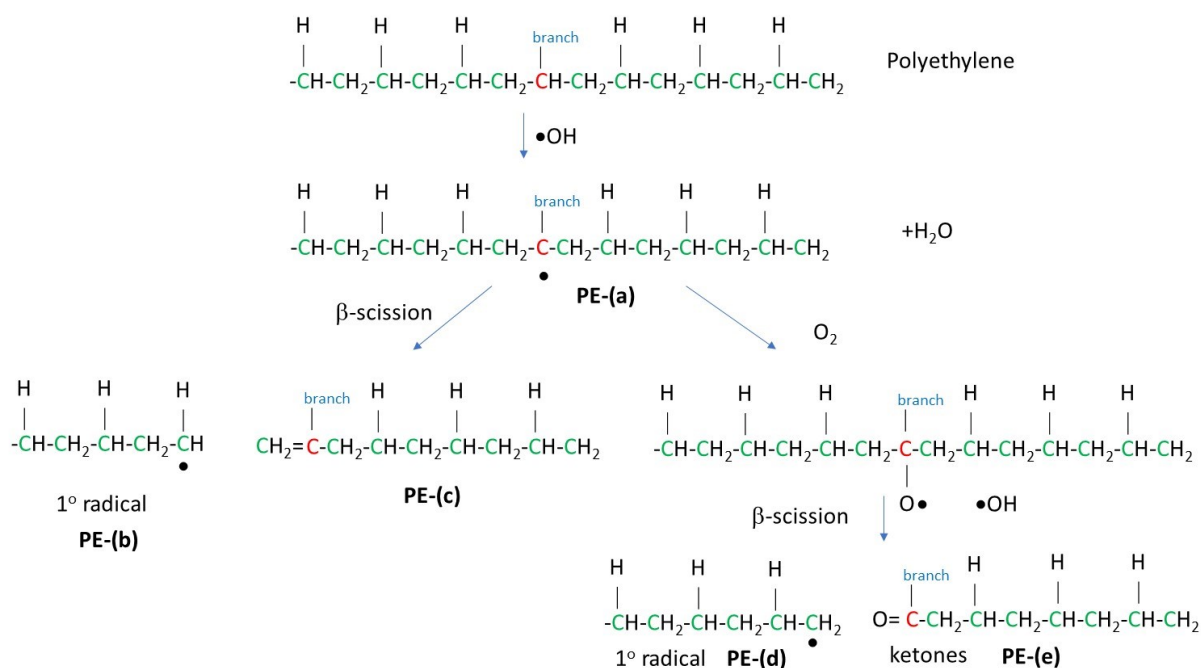


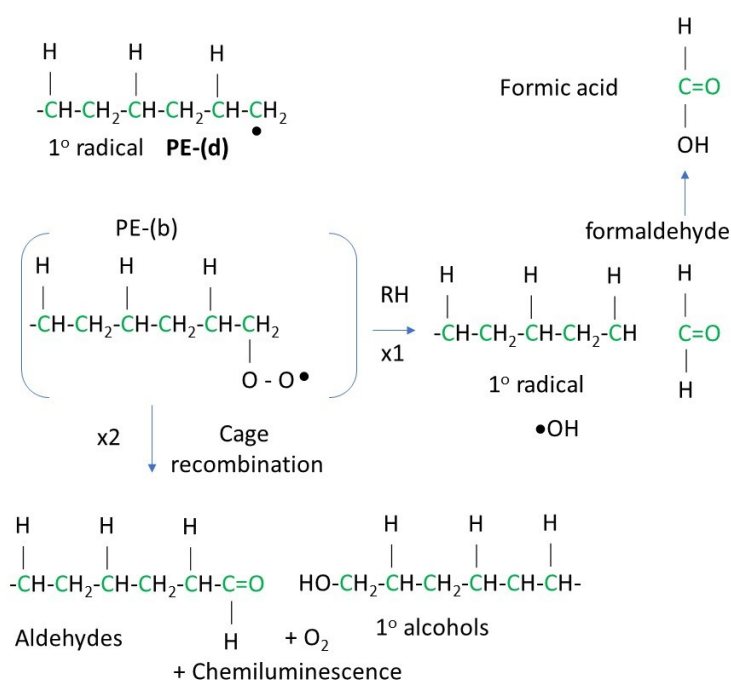
**Figure 3.38:** Volatiles arising from thermal oxidation of PP, PE-LD and PE-HD in air at 150°C (adapted from data<sup>42</sup>)

### 3.2.2 Volatiles from Polyethylene

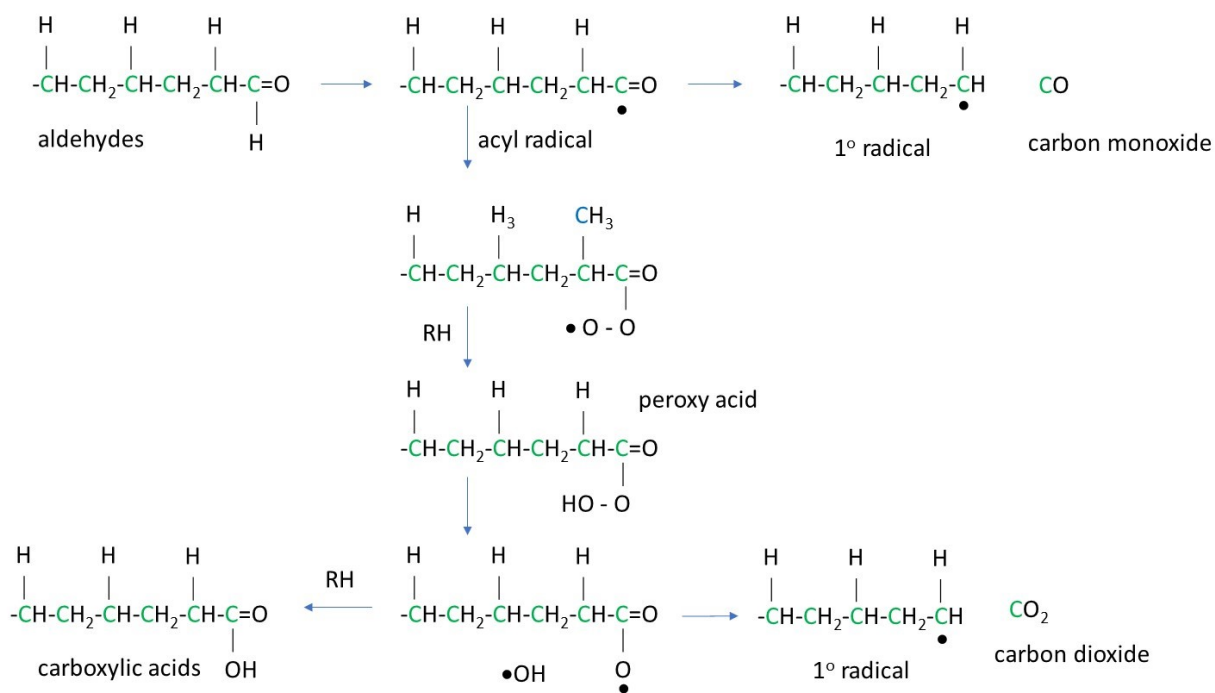
For polyethylene, unless oxidation occurs and unsaturated sites, then hydrogen abstraction is more likely at branch points in an analogous manner to at tertiary methyl sites in PP (**Scheme 3.13**). If this is the case, then ketones and primary radicals are the products of the initial stages of degradation. Aldehydes would then originate from the further oxidation, along with primary alcohols, if cage recombination takes place (**Scheme 3.14**). Again, as for PP, similar routes to the production of carboxylic acids and carbon oxides could take place. This would account for the similarity in the types of different oxidation products with differences only in their relative amounts. Subtle differences, for example the formation of acrolein rather than methacrolein would be accounted for by the predominance of methylene groups in PE compared with methine groups in PP (**Scheme 3.15**).



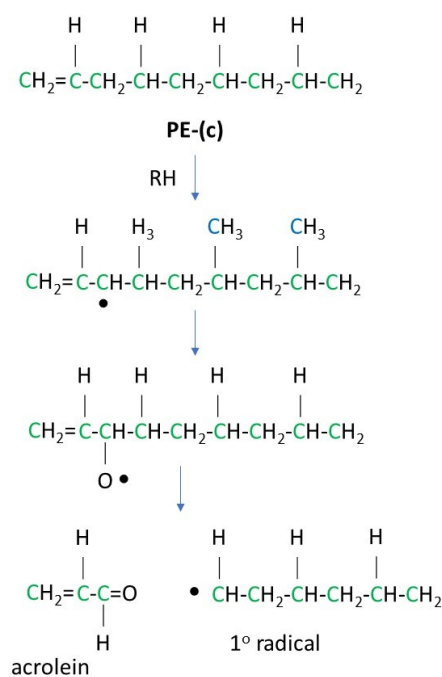
**Scheme 3.13:** Initial degradation pathways for generation of primary alkyl radicals in PE during polymer processing



**Scheme 3.14:** Initial degradation pathways for generation of primary alkyl radicals in PE during polymer processing



**Scheme 3.15:** Initial degradation pathways for generation of primary alkyl radicals in PE during polymer processing



**Scheme 3.16:** Initial degradation pathways for generation of primary alkyl radicals in PE during polymer processing



To test further commonality and differences in the modes of operation of stabilisers across the polyolefins, synthetic stabilisers have been added to PE-LLD as a contrast with PP, since PP has branch points (methyl) every monomer unit and PE-LLD has few branch points. In the case of PE-HD, natural antioxidants have been tested with and without a commercial phosphite. It should be borne in mind that although samples were selected from an available range provided by the sponsoring company, in support of the main thesis of this study, constraints are imposed by this.

#### **3.2.1.1 Volatiles from Polyethylene PE-LLD**

Stabilisation of the PE-LLD with three types of commercial antioxidant, namely phenol (**Phenol-1**), amine oxide (**Aminic-1**) and phosphite (**Phosphite-1**) attempts to mirror the more comprehensive studies undertaken for PP. An evaluation of the oxidised fragments produced shows that the phenol blocks production of aldehydes and ketones but still results in small quantities of alcohols and carboxylic acids. The phosphite when used alone produces a higher quantity of oxidised species, as does the amine oxide. It should be recognised that compared to volatiles that it is species with longer chain lengths that are detected in hexane extracts (**Figure 3.39** and **Tables 3.12 to 3.14**). In summary, this supports the premise that phenols are particularly effective at blocking the termination steps via cage recombination that lead to non-propagating (inert volatile) products.

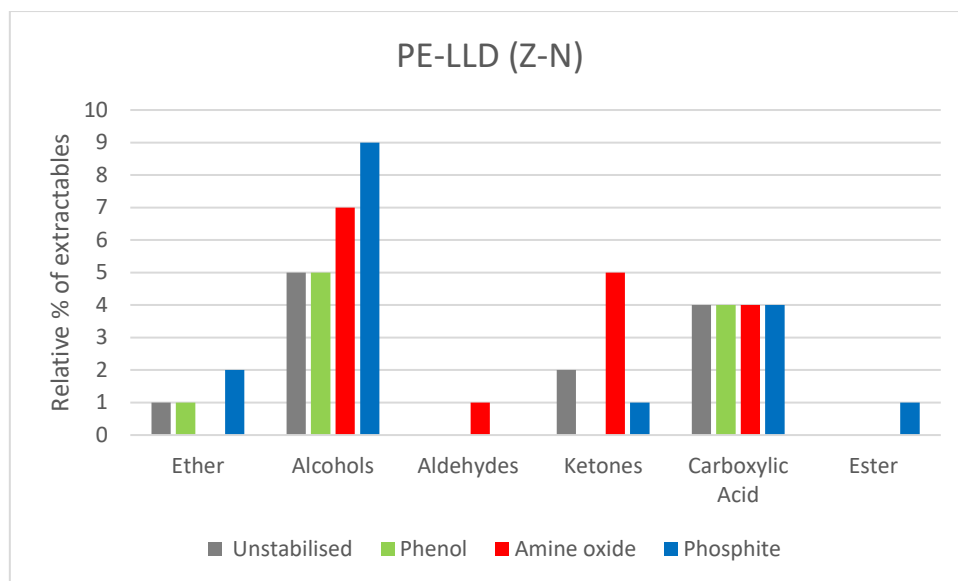


**Figure 3.39:** Oxidized fragments as relative % total of extractables in hexane from stabilised PE-HD for extrusion Pass 5

**Table 3.12:** Low molecular weight species (alkanes and alkenes) extracted to hexane from stabilised PE-LLD (Ti) after extrusion Pass 5

Linear Alkanes				
	A	B	C	D
Undecane				
Dodecane				
Docosane				
Tetradecane				
Hexadecane				
Pentadecane				
Hexatriacontane				
Tridecane				
Tetracosane				
Octadecane				
Heneicosane				
Nonacosane				
Pentatriacontane				
Tritetracontane				
Hexatriacontane				

Linear Alkenes				
	A	B	C	D
1-Heptadecene				
1-tetradecene				
Heneicos-9-ene				
1-pentene				
1-nonadecene				
2-nonadecene				

Branched alkanes				
	A	B	C	D
4-methyl-octane				
4-(1-methylethyl)-heptane				
5-methyl-undecane				
3-methyl-undecane				
4,4-dimethyl-undecane				
2,6,10,14-tetramethyl-hexadecane				
11-decyl-tetracosane				

Branched alkenes				
	A	B	C	D
5-methylene-nonane				
5-methyl-nonene				
3-methyl undecene				
5-methyl-4-nonene				
2,5,5-trimethyl-2-hexene				

Cyclic alkanes				
	A	B	C	D
1,2,4-trimethyl-cyclopentane				

**Table 3.13:** Low molecular weight species (alcohols, aldehydes, ketones) extracted to hexane from stabilised PE-LLD (Ti) after extrusion Pass 5

Linear Alcohols					
		A	B	C	D
	1-decanol				
	1-undecanol				
	1-dodecanol				
	1-docosanol				
	1-octadecanol				
	1-hexadecanol				
Aldehydes					
		A	B	C	D
	2-octadecenal				

Branched Alcohols					
		A	B	C	D
	2,3,4-trimethyl-1-pentanol				
	3-methylpent-3-en-2-ol				
	2-Propyldecan-1-ol				
	3,7,11-trimethyl-2,6,10-dodecatrien-1-ol				
Ketones					
		A	B	C	D
	1-octen-3-one				
	5-methylene-nonane				
	1-hydroxyundecan-3-one				
	4-norcaren-2-one				
	2-[(octyloxy)methyl]cyclobutanone				

**Table 3.14:** Low molecular weight species (ethers, epoxides, lactones, esters, carboxylic acids) extracted to hexane from stabilised PE-LLD (Ti) after extrusion Pass 5

Ethers					
		A	B	C	D
	Heptyl hexyl ether				
	Bis-(3,5,5-trimethylhexyl)ether				
	1-1'-oxybis-dodecane				
	Hexylisopropyl ether				
Esters					
		A	B	C	D
	acrylic acid tetradecanyl ester				

Carboxylic acids					
		A	B	C	D
	Hexanoic acid				
	Hexadecanoic acid				
	9-hexadecenoic acid				
	9-octadecenoic acid				
	Octadecanoic acid				
	4-methyl-methyl-ester hexanoic acid				
	6-octadecenoic acid				

### 3.2.1.2 Volatiles from Polyethylene PE-HD

The same trends are expected for PE-HD, though it is known that the HD grade of polyethylene contains small amounts of short chain (SCB) branches and very small amounts of long chain branches (LCB). The samples all show high levels of hydrocarbons, with the higher amounts of alkanes compared to alkenes that was previously observed for PP formulations (**Figure 3.40** and **Figure 3.41**). In comparison the levels of oxidised fragments produced (**Figure 3.42**) are relatively low suggesting that the natural AOs even when used alone are particularly effective in suppressing routes to the propagation of radical species resulting in oxidised products.

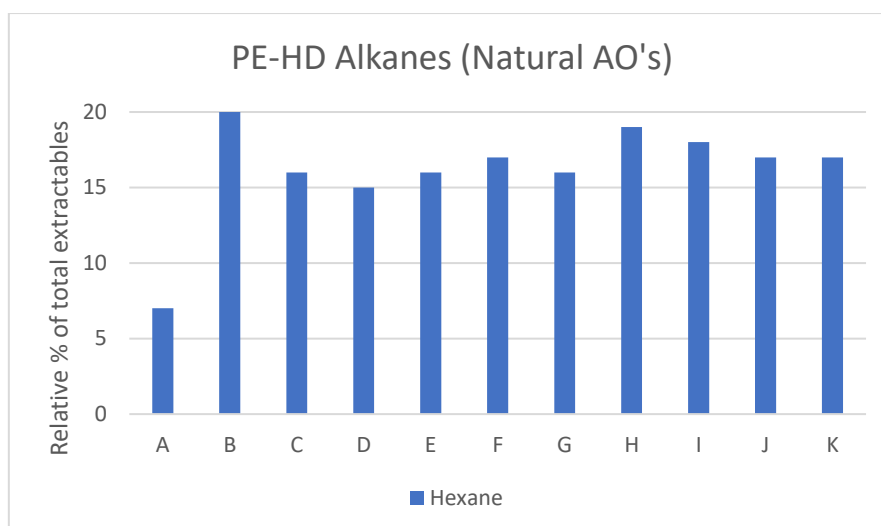


**Figure 3.40:** Alkanes as relative % of total extractables in hexane and ethanol from PE-HD stabilised with natural antioxidants (extrusion pass 5)

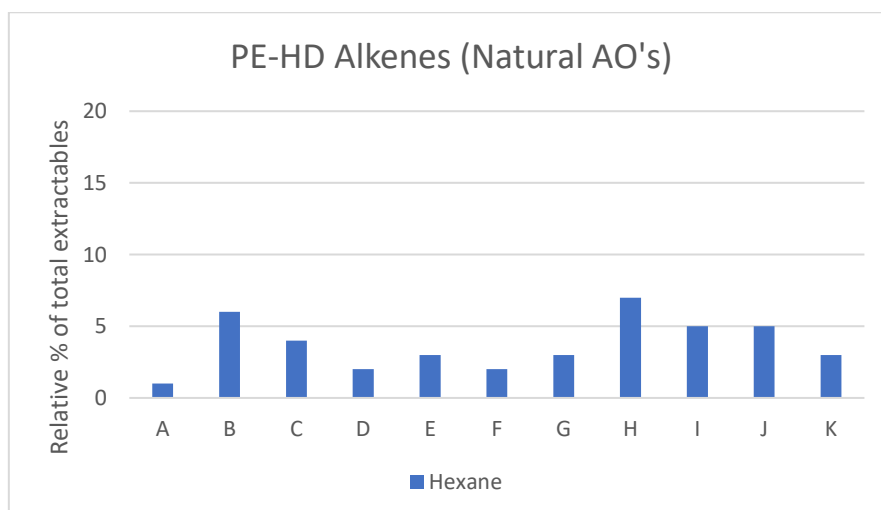


**Figure 3.41:** Alkenes as relative % of total extractables in hexane and ethanol from PE-HD stabilised with natural antioxidants (extrusion pass 5)

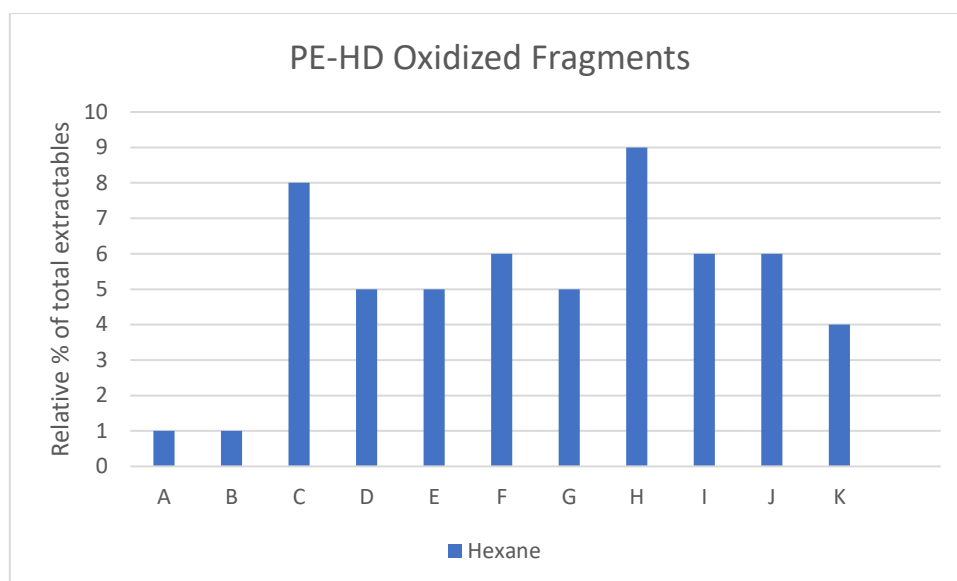


**Figure 3.42:** Oxidized fragments as relative % of total extractables in hexane and ethanol from PE-HD stabilised with natural antioxidants (extrusion pass 5)

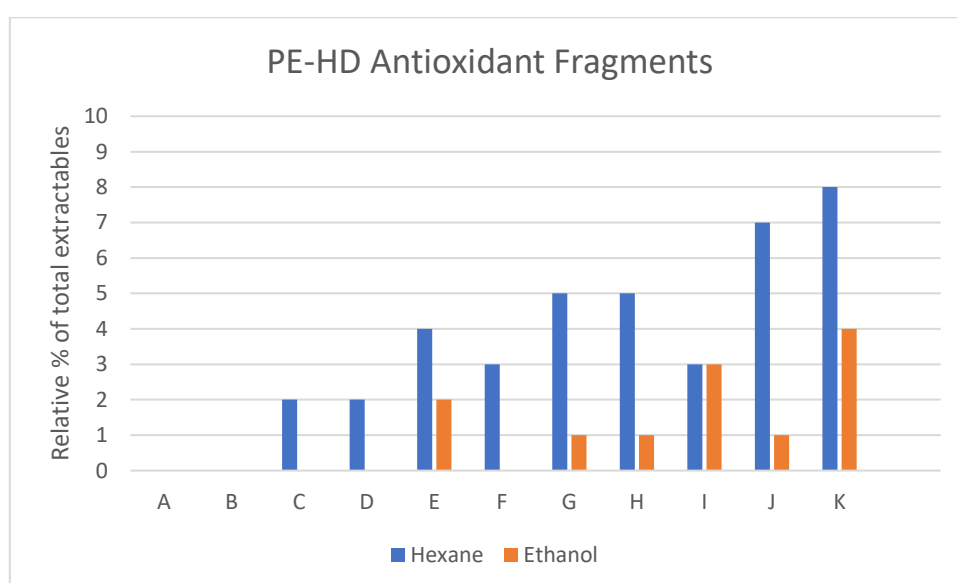


**Figure 3.43:** Antioxidant fragments as relative % total of extractables in hexane from unstabilised PE-HD as a function of extrusion pass

When combined with a phosphite stabiliser (**Phosphite-4**) larger quantity of oxidised fragments from the stabiliser samples G, H, I and J are observed and this is particularly notable when **Phosphite-4** is replaced by **Phosphite-3**. Consistent with the literature  $\alpha$ -tocopherol appears to be one of the better performing AOs with respect to reduction of oxidised species, although Gallic acid when combined with **Phosphite-3** is the most effective.

**Tables 3.15 to 3.16** characterise the specific volatiles from the PE-HD formulations. Here the smaller number of branches present in the HD grade of PE are consistent with the more linear structure.

**Table 3.15:** Low molecular weight species (alkanes and alkenes) extracted to hexane (■) or ethanol (■) or both (■) from PE-HD after extrusion Pass 5

C	Alkanes	A	B	C	D	E	F
10	Decane		■			■	
13	Tridecane		■				
14	Tetradecane	■	■	■	■	■	■
15	Pentadecane		■	■			
16	Hexadecane	■	■	■	■	■	■
17	Heptadecane	■	■	■	■	■	■
18	Octadecane	■	■	■	■	■	■
19	Nonadecane	■	■	■	■	■	■
20	Eicosane	■	■	■	■	■	■
21	Heneicosane	■	■	■	■	■	■
22	Docosane	■	■	■	■	■	■
24	Tetracosane	■	■	■	■	■	■
25	Pentacosane			■	■		
26	Hexacosane	■	■	■	■	■	■
27	Heptacosane			■			
28	Octacosane		■				■
30	triacontane		■	■	■	■	■
	count	10	15	14	11	12	11

	Alkanes	G	H	I	J	K
10	Decane		■	■	■	■
13	Tridecane					■
14	Tetradecane	■	■	■	■	■
15	Pentadecane					
16	Hexadecane	■	■	■	■	■
17	Heptadecane	■	■	■	■	■
18	Octadecane	■	■	■	■	■
19	Nonadecane	■	■	■	■	■
20	Eicosane	■	■	■	■	■
21	Heneicosane	■	■	■	■	■
22	Docosane	■	■	■	■	■
24	Tetracosane	■	■	■	■	■
25	Pentacosane					
26	Hexacosane			■	■	■
27	Heptacosane					
28	Octacosane		■			■
30	triacontane	■	■	■	■	■
	count	10	12	12	11	14

	Cyclic Alkanes	A	B	C	D	E	F
10	Cyclododecane			■	■		■
16	Cyclohexadecane		■			■	
14	Cyclotetradecane						
30	Cyclotriacontane					■	
6	Cyclohexane, 1,1'-(2-methyl-1,3-propanediyl)bis-					■	
18	Cyclooctadecane, ethyl-		■				

	Cyclic Alkanes	G	H	I	J	K
10	Cyclododecane	■	■	■	■	
16	Cyclohexadecane					
14	Cyclotetradecane			■		
30	Cyclotriacontane					
6	Cyclohexane, 1,1'-(2-methyl-1,3-propanediyl)bis-					
18	Cyclooctadecane, ethyl-					■

	Branched Alkanes	A	B	C	D	E	F
22	Docosane, 7-hexyl-						
12	Dodecane, 2,4-dimethyl-						
20	Eicosane, 2,4-dimethyl-						
20	Eicosane, 2-methyl-						
27	Heptacosane, 2-methyl						
17	Heptadecane, 2-methyl-						
17	Heptadecane, 3-methyl-						
17	Heptadecane, 8-methyl-						
26	Hexacosane, 2-methyl						
16	Hexadecane, 2-methyl-						
16	Hexadecane, 3-methyl-						
19	Nonadecane, 9-methyl-						
19	Nonadecane, 10-methyl-						
28	Octacosane, 2-methyl						
18	Octadecane, 3-methyl-						
18	Octadecane, 5-methyl-						
25	Pentacosane, 11-methyl						
15	Pentadecane, 5-methyl-						
15	Pentadecane, 8-hexyl-						
24	Tetracosane, 2-methyl						
14	Tetradecane, 4-ethyl-						
14	Triacontane, 2-methyl						
30	Tridecane, 3-methyl-						
33	Tritriacontane, 3-methyl- (C33)						
16	6,6-Diethylhexadecane						
16	Hexadecane, 2,6,10,14- tetramethyl-						
	count	2	6	4	5	3	6

	Alkanes	G	H	I	J	K
	Docosane, 7-hexyl-					
	Dodecane, 2,4-dimethyl-					
	Eicosane, 2,4-dimethyl-					
	Eicosane, 2-methyl-					
	Heptacosane, 2-methyl					
	Heptadecane, 2-methyl-					
	Heptadecane, 3-methyl-					
	Heptadecane, 8-methyl-					
	Hexacosane, 2-methyl					
	Hexadecane, 2-methyl-					
	Hexadecane, 3-methyl-					
	Nonadecane, 9-methyl-					
	Nonadecane, 10-methyl-					
	Octacosane, 2-methyl					
	Octadecane, 3-methyl-					
	Octadecane, 5-methyl-					
	Pentacosane, 11-methyl					
	Pentadecane, 5-methyl-					
	Pentadecane, 8-hexyl-					
	Tetracosane, 2-methyl					
	Tetradecane, 4-ethyl-					
	Triacontane, 2-methyl					
	Tridecane, 3-methyl-					
	Tritriacontane, 3- methyl-					
	6,6-Diethylhexadecane					
	Hexadecane, 2,6,10,14- tetramethyl-					
	count	7	7	4	4	5

	Alkenes	A	B	C	D	E	F
12	1-Docosene						
17	1-Heptadecene						
19	1-Nonadecene						
18	1-Octadecene						
24	1-Tetracosene						
23	1-Tricosene						
12	2-Dodecene, (Z)-						
12	3-Dodecene, (Z)-						
20	3-Eicosene, (E)-						
14	3-Tetradecene, (E)-						
14	5-Tetradecene, (E)-						
16	7-Hexadecene, (Z)-						
20	9-Eicosene, (E)-						
29	Nonacos-1-ene						
27	Heptacos-1-ene						

	Alkenes	G	H	I	J	K
	1-Docosene					
	1-Heptadecene					
	1-Nonadecene					
	1-Octadecene					
	1-Tetracosene					
	1-Tricosene					
	2-Dodecene, (Z)-					
	3-Dodecene, (Z)-					
	3-Eicosene, (E)-					
	3-Tetradecene, (E)-					
	5-Tetradecene, (E)-					
	7-Hexadecene, (Z)-					
	9-Eicosene, (E)-					
	Nonacos-1-ene					
	Heptacos-1-ene					

**Table 3.16:** Low molecular weight species (alcohols, aldehydes\*, ketones) extracted to hexane from PE-HD (Stabilised with formulations A to F and G to K) after extrusion Pass 5

Alcohols	A	B	C	D	E	F
2,4,7,9-Tetramethyl-5-decyn-4,7-diol						
Ethanol, 2-(octadecyloxy)-						
1-Hexanol, 2-ethyl-						
Ethanol, 2-(tetradecyloxy)-						

Ketones	A	B	C	D	E	F
2,5-cyclohexadien-1-one, 2,6-bis(1,1-dimethylethyl)-4-hydroxy-4-methyl-						
2-Pentadecanone, 6,10,14-trimethyl-						
2-Cyclopenten-1-one, 2-hydroxy-3-methyl-						

Alcohols	G	H	I	J	K
2,4,7,9-Tetramethyl-5-decyn-4,7-diol					
Ethanol, 2-(octadecyloxy)-					
1-Hexanol, 2-ethyl-					
Ethanol, 2-(tetradecyloxy)-					

Ketones	G	H	I	J	K
2,5-cyclohexadien-1-one, 2,6-bis(1,1-dimethylethyl)-4-hydroxy-4-methyl-					
2-Pentadecanone, 6,10,14-trimethyl-					
2-Cyclopenten-1-one, 2-hydroxy-3-methyl-					

**\*No aldehydes observed**

**Table 3.17:** Low molecular weight species (ethers, epoxides, lactones, esters, carboxylic acids) extracted to hexane from PE-HD (Stabilised with formulations A to F and G to K) after extrusion Pass 5

Ethers	A	B	C	D	E	F
Eicosyl isopropyl ether						
Isopropyl octacosyl ether						
Methoxyacetic acid, 2-tetradecyl ester						

Esters	A	B	C	D	E	F
Octacosyl acetate						
Triacetyl acetate						
1-Heneicosyl formate						

Carboxylic acids	A	B	C	D	E	F
Carbonic acid, tetradecyl vinyl ester						
Hexanedioic acid, bis(2-methylpropyl) ester						
n-Hexadecanoic acid						
Octadecanoic acid						
Carbonic acid, but-2-yn-1-yl octadecyl ester						
4,8,12,16-Tetramethylheptadecan-4-olide						

Ethers	G	H	I	J	K
Eicosyl isopropyl ether					
Isopropyl octacosyl ether					
Methoxyacetic acid, 2-tetradecyl ester					

Esters	G	H	I	J	K
Octacosyl acetate					
Triacetyl acetate					
1-Heneicosyl formate					

Carboxylic acids	G	H	I	J	K
Carbonic acid, tetradecyl vinyl ester					
Hexanedioic acid, bis(2-methylpropyl) ester					
n-Hexadecanoic acid					
Octadecanoic acid					
Carbonic acid, but-2-yn-1-yl octadecyl ester					
4,8,12,16-Tetramethylheptadecan-4-olide					



## 4 Conclusions

This study has used chemiluminescence (CL) and gas chromatography-mass spectroscopy (GC-MS) of volatiles from PP, PE-HD and PE-LD to question the accepted pathways for autoxidation of polyolefins.

Using information from the literature for initiation steps, it suggests that oxygen-containing species already present in polyolefin reactor powders ( $\text{ROO}\bullet$ ,  $\bullet\text{OH}$ ) abstract hydrogen and trigger  $\beta$ -scission reactions and oxidative propagation. An overview of the literature also supports the premise that, at least in the first instance, abstraction of hydrogen occurs preferentially from allylic sites, since this process is thermodynamically more favoured.

The CL studies undertaken in this work have demonstrated characteristic features of spectra in the range 350-680 nm that supports the work of others suggesting that luminescence arises from cage recombination of peroxy radicals. Here the lower wavelength band in the range 350-500 nm has been assigned to excited-state carbonyl species and the longer wavelength to singlet oxygen. At the point when the AO concentration is depleted the intensity of the longer wavelength band abruptly decreases. This suggests that in the absence of AOs this pathway to the formation of inert products (alcohols, ketones, aldehydes) is no longer promoted and that the conversion of tertiary peroxy radicals to alkoxy radicals (which can escape the cage in any event) then dominate propagation and chain-branching reactions. This supports work from the literature on molecular modelling of cage-recombination reactions that suggest, contrary to the accepted Russell mechanism, that there is asymmetric cleavage of peroxy radicals in the cage to excited-state carbonyls and singlet oxygen that can only take place for primary and secondary peroxy radicals.

Earlier work in the literature suggesting the correspondence of CL with the formation of  $\text{ROOH}$ , due to the identical sigmoidal curves that characterise the progress of autoxidation, are questioned. Rather than the build-up of peroxides being an artefact of all peroxy radical species (primary, secondary and tertiary) in the induction period of stabilisation, peroxides are more likely to originate from tertiary species. The correlation of  $\text{ROOH}$  curves with CL curves is therefore somewhat coincidental.

The analysis of volatiles supports this premise, more carbonyl and alcohol products are formed from AOs capable of promoting cage recombination (e.g. phenols) than those which are not (e.g. aminic AOs). This is reflected in the higher amounts of oxidised species in formulations with and without amines. The fact that this is not a simple picture is likely related to the fact that the degree to which an AO is hindered, along with its' conformation and HAT capability, can moderate its performance in this respect.

For stabilised formulations the results from both CL and analysis of volatiles suggests that contrary to expected practice (the industrial workhorse of a highly hindered phenol being used with an aryl phosphite) that the combination of a hydroxylamine with a less hindered phenol (with appropriate conformation and HAT transfer ability) may provide superior overall stabilisation (with respect to processing performance and reduction of volatiles) (see **appendix**). This may also explain the better performance of natural antioxidants (e.g. vitamin E and simple natural phenols) with respect to the reduction of oxidised volatile species (albeit that Vitamin E can also act as an alkyl radical scavenger).

In support of these observations a revised BAS is proposed below in **Table 4.1**.

**Table 4.1:** Revised BAS for the thermal oxidation of polyolefins

<b>Initiation</b>	$\text{RH} + \text{O}_2 \rightarrow \text{R}\bullet + \text{HOO}\bullet$ $\bullet\text{OH} + \text{RH} \rightarrow \text{R}\bullet + \text{H}_2\text{O}$ $\bullet\text{OOR} + \text{R}'\text{H} \rightarrow \text{R}\bullet + \text{R}'\text{OOH}$ $\text{R-R} \rightarrow \text{R}\bullet + \bullet\text{R}'$ $\beta\text{-scission (thermo-mechanical degradation)}$ $\text{R}'\bullet \rightarrow \beta\text{-scission} \rightarrow \text{R}''\bullet + \text{low molecular weight species}$
<b>Propagation</b>	$\text{R}\bullet + \text{O}_2 \rightarrow \text{ROO}\bullet$ $\text{ROO}\bullet + \text{R}'\text{H} \rightarrow \text{ROOH} + \text{R}'\bullet \text{ (reversible process)}$ $\text{RO}\bullet + \text{R}'\text{H} \rightarrow \text{ROH} + \text{R}'\bullet \text{ (reversible process)}$ $\text{R}\bullet + \text{R}'\text{H} \rightarrow \text{RH} + \text{R}'\bullet \text{ (reversible process)}$
<b>Chain-Branching</b>	$\text{ROOH} \rightarrow \text{RO}\bullet + \bullet\text{OH}$ $2\text{ROOH} \rightarrow \text{ROO}\bullet + \text{RO}\bullet + \text{H}_2\text{O}$ $\text{RO}\bullet + \text{RH} \rightarrow \text{ROH} + \text{R}\bullet$ $\text{HO}\bullet + \text{RH} \rightarrow \text{R}\bullet + \text{H}_2\text{O}$ $\text{ROO}\bullet + \text{ROO}\bullet (3^\circ) \rightarrow 2\text{RO}\bullet + \text{O}_2$
<b>Termination</b>	$\text{ROO}\bullet + \text{ROO}\bullet (1^\circ \text{ or } 2^\circ) \rightarrow \text{ROH} + \text{R(=O)H} + \text{O}_2$ $\text{RO}_2\bullet + \text{R}\bullet \rightarrow \text{ROOR}$ $2\text{R}\bullet \rightarrow \text{R-R}$ $\text{RO}_2\bullet + \text{HO}_2\bullet \rightarrow \text{ROOH} + \text{O}_2 \text{ (reversible process)}$

## 5 Further work

Although this study has gone part of the way to a better understanding of thermal autoxidation mechanisms several areas require further clarification.

### 5.1 Computational Analysis

#### 5.1.1 Kinetic Modelling of thermo-oxidative degradation in PP/PE

A further test of the validity of these routes would be to use the information in kinetic models to refine those that already exist and examine whether the data provides a better fit. The emissions data collated during the current work can be incorporated in kinetic modelling for the thermo-oxidative degradation of PP and PE. In order to achieve this the use of computational-based kinetic modelling will be required and entails:

- Establishing kinetic model from mechanistic considerations.
- Determination of the elementary rate constants for the selected mechanistic scheme, at various temperatures. Generally, this is the most difficult part of the methodology as it is highly dependent on previously published kinetic data in scientific literature. The work of Heude<sup>47</sup> provides the foundation for this approach.
- Once the elementary rate constants are determined, the next step will include the extrapolation of the elementary rate constants for various temperatures later to be used in kinetic modelling. The intention being that these models can then be used to predict the rate of change in the kinetic functions under a given set of experimental conditions.

Previously, the modelling has been done using ordinary differential equations solvers on MATLAB i.e. MATLAB ODE23 and ODE45<sup>87</sup>. The same can be used for statistical analysis of the data acquired in the current study.

### **5.1.2 Ab initio molecular orbital theory calculations**

To provide further evidence for the interaction of AOs with the cage for primary and secondary peroxy it is suggested that high-level ab initio calculations are used, employing model primary and secondary peroxy radicals in the presence of AOs with varying conformation and degree in hindrance of the HAT moiety. This should be undertaken for phenolic, aminic, phosphite and sulphur-based AOs, both synthetic and natural, to build on the work of Coote *et al*<sup>1</sup>.

## **5.2 Further experimental work**

### **5.2.1 GC-MS - Quantitative Analysis**

SPME-GC-MS analysis was conducted for the analysis of leachates and extractables from various solvent mediums (hexane and ethanol) in the current study using a semi-quantitative method. However, this is not an accurate method to calculate the concentration of the extractables of interest. Instead using a quantitative approach, using calibration standards along with Quadrupole GC-MS should provide the sensitivity required for such determinations.

### **5.2.2 CL Studies – Natural AO**

Because time was not available to undertake CL studies, in addition to volatiles analysis, on the natural AOs used in the formulations for PE-HD this would help to complete the work already undertaken. In addition, extending the formulations used for PP, PE-HD and PE-LLD (and including PE-LD) would help rationalise the pathways to degradation that have been proposed.

### 5.2.3 Metallocene Polymers

As mentioned in the introduction, metallocene based polymers were not considered in the current study. However, since Ziegler-Natta (ZN) and Phillips catalyst was used in this study, to gain an overall picture of the polymer stabilization routes, metallocene based polyolefins should be considered.

The use of metallocene catalyst polymerisation methods are relatively new and is used to produce polymers with less polydispersion. Each catalyst contains only one type of active site, all of them polymerizing the available monomers in an identical fashion. They are known as Single-site catalyst (SSC) and uniform-site catalyst<sup>88</sup>, in comparison to Phillips and ZN catalysts, where these catalysts are multisite catalysts. The advantage of using metallocene catalysts over Phillips and ZN is that the single-site catalysts produce PE with a narrow molecular mass distribution (polydispersity  $M_w/M_n$  of 2). Whereas, multisite catalysts generate PE with narrow to broad molecular mass distribution (polydispersity index  $M_w/M_n$  of 4 and 12).

Due to the variety of active centres at multisite catalysts (ZN and Phillips catalysts) the comonomer units varies with molecular mass, whereas PE produced with single-site metallocene catalyst systems show a uniform comonomer content, independent on the molecular mass<sup>89</sup>.

The conditions used to create metallocene polymers are mild (temperature and pressure), similarly to ZN production. In general a metallocene is formed with a metal atom from group IV of the periodic table (titanium, zirconium, or hafnium) attached to two substituted cyclopentadienyl ligands and two alkyl, halide, or other ligands with a methylalumoxane (-MeAlO)<sub>n</sub> cocatalyst known as MAO<sup>90</sup> (**Figure 5.1**). Metallocene catalyst enables true molecular design of polyolefins this facilitates modelling and predicting the structural properties of the polymer<sup>91</sup>.

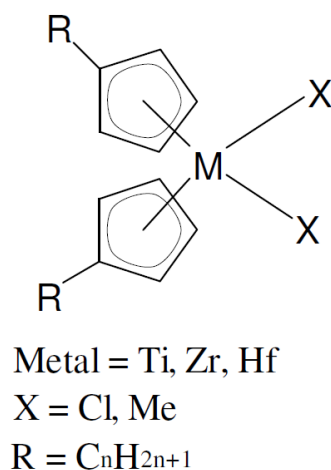


**Figure 5.1:** Structure of metallocene catalyst and examples of specific catalyst

Further work would look at the use of the stability of metallocene PE and PP on the low molar mass degradation products, this would then be validated by GC-MS and CL studies which would then be compared to the results obtained in the study. Observing these low molecular mass degradation products has various exciting applications such as food packaging applications, where extractables of such degradation products can affect the taste of the product.

#### 5.2.4 Various Stabilisers

This study looked at a relatively narrow group of AO's structures, but this can be extended to cover stabilisers that have varied and specific functionalities. One example is the use of DABCO (diazobicyclooctane) which is an aminic AO that can effectively quench singlet oxygen. Enko *et al*<sup>92</sup>, used DABCO to limit photo-degradation processes in optical sensing materials caused by photosensitized singlet oxygen. The study demonstrated that DABCO was effective at reducing the rate of the total photon emission (TPE) by singlet oxygen as well as reducing the oxygen consumption rates, this significantly improved the photostability of the optical sensing equipment used in the study. Applying DABCO as an aminic AO to this study can help limit the singlet oxygen bands found in the CL data for wavelength bands between 500-680 nm.

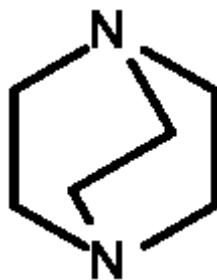


Figure 5.2: DABCO structure

#### 5.2.5 Other work

- Extending the work on isotopic labelling of the polyolefins, particularly PP, in the presence of AOs would further verify some of the proposed pathways to degradation.
- Since short term sample aging was conducted in this study, studying the long term effects of the thermal oxidative performance of the individual AOs and polyolefin samples should be investigated and related to the melt stability performance as measured by melt flow rate (MFR) and yellowness index (YI). This will also improve the reliability of the kinetic models proposed above.
- Adjusting various parameters on the extruder should also be investigated, i.e. monitoring different screw speeds since this can effect shear rate on the melt stability of the polymers, broadening the temperature range between 160-280°C to see if this affects the type of degradation products formed (crosslinking and chain-scission).



## References

1. R. Lee, G. Gryn'Ova, K. Ingold and M. L. Coote, *Physical Chemistry Chemical Physics*, 2016, **18**, 23673-23679.
2. N. S. Allen, *Degradation and stabilisation of polyolefins*, Sole distributor in the USA and Canada, Elsevier Science Pub. Co., 1983.
3. H. Zweifel, *Effect of stabilization of polypropylene during processing and its influence on long-term behavior under thermal stress*, ACS Publications, 1996.
4. T. Ojeda, A. Freitas, K. Birck, E. Dalmolin, R. Jacques, F. Bento and F. Camargo, *Polymer degradation and stability*, 2011, **96**, 703-707.
5. T. Aida, E. Meijer and S. I. Stupp, *Science*, 2012, **335**, 813-817.
6. K. del Teso Sánchez, N. S. Allen, C. M. Liauw, F. Catalina, T. Corrales and M. Edge, *Polymer degradation and stability*, 2015, **113**, 32-39.
7. J. Bolland, *Transactions of the Faraday Society*, 1948, **44**, 669-677.
8. G. Gryn'ova, J. L. Hodgson, M. L. J. O. Coote and b. chemistry, 2011, **9**, 480-490.
9. G. Gedraitite, A. Mar'in and Y. A. Shlyapnikov, *European polymer journal*, 1989, **25**, 39-41.
10. J. F. Rabek, *Photostabilization of Polymers: Principles and Application*, Springer Science & Business Media, 2012.
11. V. Y. Shlyapintokh and V. Ivanov, *Ed G Scott, London: Elsevier Applied Science*, 1982, **41**.
12. M. C. Celina, *Polymer Degradation and Stability*, 2013, **98**, 2419-2429.
13. T. Tobita, P. Chammingkwan, M. Terano and T. Taniike, *Polymer Degradation and Stability*, 2017, **137**, 131-137.
14. T. Kashiwagi, A. Inaba, J. E. Brown, K. Hatada, T. Kitayama and E. Masuda, *Macromolecules*, 1986, **19**, 2160-2168.
15. Y.-H. Hu and C.-Y. Chen, *Polymer Degradation and Stability*, 2003, **82**, 81-88.
16. G. Gryn'ova, J. L. Hodgson and M. L. Coote, *Organic & biomolecular chemistry*, 2011, **9**, 480-490.
17. L. M. Smith, H. M. Aitken and M. L. Coote, *Accounts of chemical research*, 2018, **51**, 2006-2013.
18. H. Nakatani, D. Kurniawan, T. Taniike and M. Terano, *Science and technology of advanced materials*, 2008, **9**, 024401.
19. L. Shibryaeva, *Polypropylene, InTech, Rijeka*, 2012, 63-86.
20. M. Edge, *Polymer Chain Dynamics & Polymer Stability: a review, Journal*, 2011.
21. Y. A. Shlyapnikov, S. Kiryushkin and A. M. i. Taylor, *Journal*, 1997.
22. A. Tobolsky, *J. Amer. Chem. Soc.*, 1950, **72**, 1942.
23. E. Niki, J. Tsuchiya, R. Tanimura and Y. Kamiya, *Chemistry Letters*, 1982, **11**, 789-792.
24. D. Knorre, Z. Maizus, L. Obukhova and N. Emanuel, *Usp. khim*, 1957, **26**, 416-458.
25. F. Gugumus, *Polymer Degradation and Stability*, 1995, **49**, 29-50.
26. N. Billingham and M. Grigg, *Polymer degradation and stability*, 2004, **83**, 441-451.
27. P. Gijsman, J. Hennekens and J. Vincent, *Polymer Degradation and Stability*, 1993, **42**, 95-105.
28. F. Gugumus, *Re-examination of the thermal oxidation reactions of polymers 2. Thermal oxidation of polyethylene*, 2002, **76**, 329-340.
29. F. Gugumus, *Polymer degradation and Stability*, 2002, **76**, 329-340.
30. F. Gugumus, *Polymer Degradation and Stability*, 2002, **77**, 147-155.
31. F. Gugumus, *Polymer degradation and stability*, 1996, **53**, 161-187.
32. F. Gugumus, *Journal*, 2000, 210-229.
33. E. M. Hoang, N. S. Allen, C. M. Liauw, E. Fontán and P. Lafuente, *Polymer degradation and stability*, 2006, **91**, 1356-1362.
34. K. del Teso Sánchez, N. S. Allen, C. M. Liauw and M. Edge, *Journal of Vinyl and Additive Technology*, 2016, **22**, 117-127.

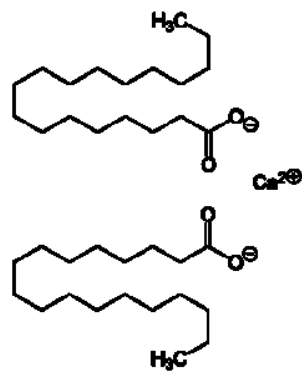
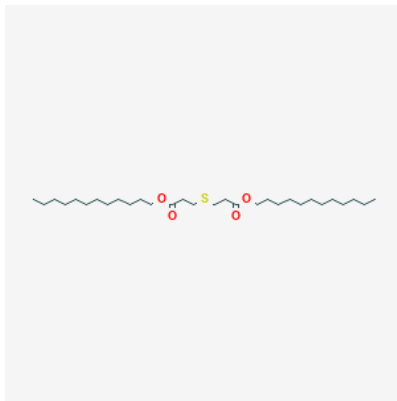
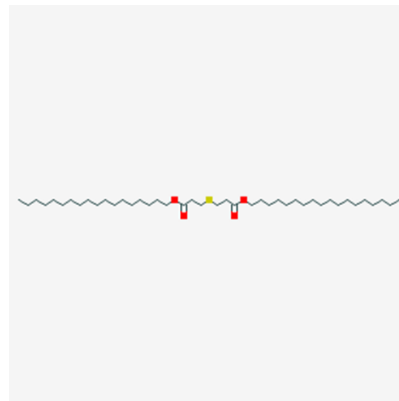
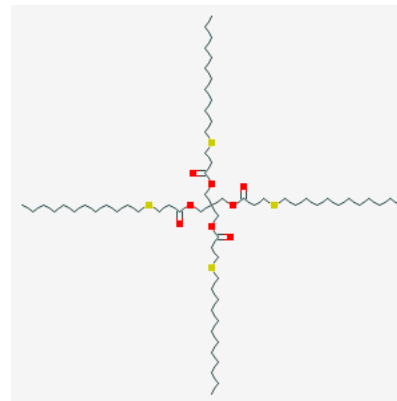
35. J. A. Howard, *Journal*, 1997, 283-334.
36. M. Schard and C. Russell, *Journal of Applied Polymer Science*, 1964, **8**, 985-995.
37. P. Citovický, D. Mikulášová, V. Chrastova and G. Benč, *European Polymer Journal*, 1977, **13**, 655-660.
38. P. Citovický, I. Šimek, D. Mikulášová and V. Chrastová, *Chemical Papers*, 1976, **30**, 342-350.
39. J. Adams and J. Goodrich, *Journal of Polymer Science Part A-1: Polymer Chemistry*, 1970, **8**, 1269-1277.
40. K. Barabas, M. Iring, T. Kelen and F. Tüdös, Study of the thermal oxidation of polyole-fins. V. Volatile products in the thermal oxidation of polyethylene, **57**, 65-71, 1976.
41. E. Bevilacqua, E. English and J. Gall, *Journal of Applied Polymer Science*, 1964, **8**, 1691-1698.
42. L. Reich and S. S. Stivala, 1969.
43. A. Hoff and S. Jacobsson, *Journal of applied polymer science*, 1984, **29**, 465-480.
44. A. Hoff and S. Jacobsson, *Journal of Applied Polymer Science*, 1982, **27**, 2539-2551.
45. A. Hoff, S. Jacobsson, P. Pfäffli, A. Zitting and H. Frostling, *Scandinavian journal of work, environment & health*, 1982, 1-60.
46. T. Andersson, B. Stålbom and B. Wesslén, *Journal of applied polymer science*, 2004, **91**, 1525-1537.
47. F. Djouani, E. Richaud, B. Fayolle and J. Verdu, *Polymer degradation and stability*, 2011, **96**, 1349-1360.
48. J. C. Chien and J. K. Kiang, *Die Makromolekulare Chemie: Macromolecular Chemistry and Physics*, 1980, **181**, 47-57.
49. R. Bernstein, S. M. Thornberg, A. N. Irwin, J. M. Hochrein, D. K. Derzon, S. B. Klammo and R. L. Clough, *Polymer Degradation and Stability*, 2008, **93**, 854-870.
50. Robert Bernstein, Steven M. Thornberg, Roger A. Assink, Adriane N. Irwin, James M. Hochrein, Jason R. Brown, Dora K. Derzon, Sara B. Klammo and Roger L. Clough, *Journal*, 2007, **92**, 2076-2094.
51. S.M. Thornberg, R. Bernstein, A.N. Irwin, D.K. Derzon, B. S. Klammo, and R. L. Clough, *Journal*, 2007, **92**, 94-102.
52. A. Arshad, *Analysis and Control of Emissions arising from Stabilised Polypropylene and the Incorporated Additives*, Manchester Metropolitan University, 42-43, 2015.53. J.-F. Poon and D. A. Pratt, *Accounts of chemical research*, 2018, **51**, 1996-2005.
54. M. Kutz, *Handbook of environmental degradation of materials*, William Andrew, 2018.
55. M. Galleano, S. V. Verstraeten, P. I. Oteiza and C. G. Fraga, *Archives of Biochemistry and Biophysics*, 2010, **501**, 23-30.
56. R. Guitard, J.-F. Paul, V. Nardello-Rataj and J.-M. Aubry, *Food chemistry*, 2016, **213**, 284-295.
57. S. F. Laermer and F. Nabholz, *Plastics and Rubber Processing and Applications*, 1990, **14**, 235-239.
58. C. Schneider, *Molecular nutrition & food research*, 2005, **49**, 7-30.
59. M. A. Peltzer, J. R. Wagner and A. J. Migallon, in *Polymer and biopolymer analysis and characterization*, Nova Publishers New York, 2007, pp. 13-27.
60. M. Wijnmans, D. A. Pratt, L. Valgimigli, G. A. DiLabio, G. F. Pedulli and N. A. Porter, *Angewandte Chemie-International Edition*, 2003, **42**, 4370-4373.
61. C. M. Houlihan, C. T. Ho and S. S. Chang, *Journal of the American Oil Chemists Society*, 1985, **62**, 96-98.
62. P. F. Zambetti, S. L. Baker and D. C. Kelley, *Alpha tocopherol as an antioxidant for extrusion coating polymers*, *Tappi journal (USA)*, 1995.
63. R. L. Clough, N. C. Billingham and K. T. Gillen, *Polymer durability: degradation, stabilization, and lifetime prediction*, American Chemical Society, 1996.
64. J. A. Howard and K. U. Ingold, *Canadian Journal of Chemistry*, 1963, **41**, 2800-2806.
65. K. D. Breese, J. F. Lamèthe and C. DeArmitt, *Polymer degradation and stability*, 2000, **70**, 89-96.

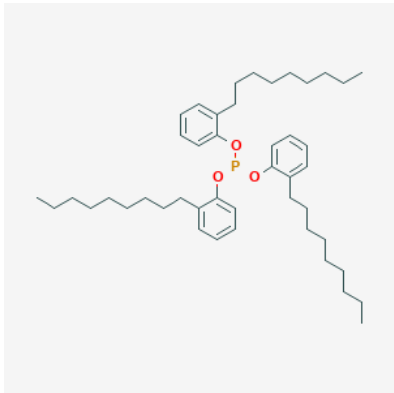
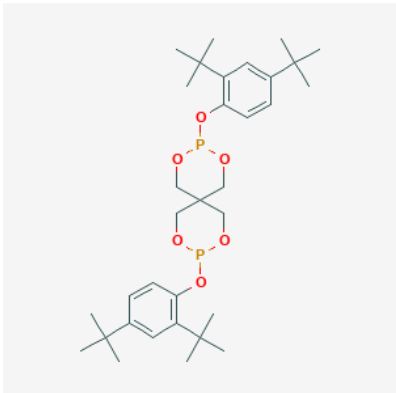
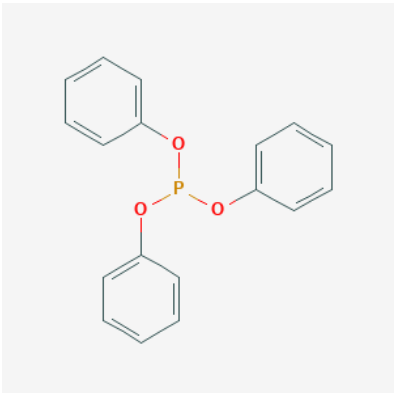
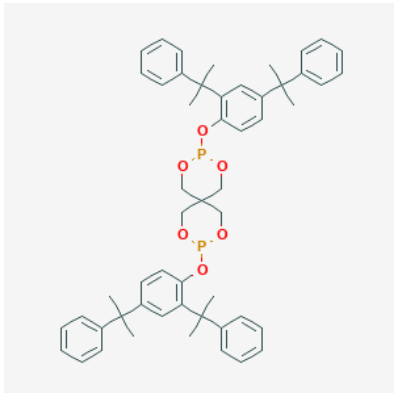
66. G. W. Burton and K. U. Ingold, *Journal of the American Chemical Society*, 1981, **103**, 6472-6477.
67. R. M. Pérez-Gregorio, M. S. García-Falcón, J. Simal-Gándara, A. S. Rodrigues and D. P. Almeida, *Journal of Food Composition and Analysis*, 2010, **23**, 592-598.
68. M. Dopico-García, M. Castro-López, J. López-Vilariño, M. González-Rodríguez, P. Valentao, P. Andrade, S. García-Garabal and M. Abad, *Journal of Applied Polymer Science*, 2011, **119**, 3553-3559.
69. P. Iacopini, M. Baldi, P. Storch and L. Sebastiani, *Journal of Food Composition and Analysis*, 2008, **21**, 589-598.
70. D. Tátraaljai, E. Földes and B. Pukánszky, *Polymer Degradation and Stability*, 2014, **102**, 41-48.
71. M. Samper, E. Fages, O. Fenollar, T. Boronat and R. Balart, *Journal of Applied Polymer Science*, 2013, **129**, 1707-1716.
72. S. Kreft, M. Knapp and I. Kreft, *Journal of agricultural and food chemistry*, 1999, **47**, 4649-4652.
73. A. Ganeshpurkar and A. K. Saluja, *Saudi pharmaceutical journal*, 2017, **25**, 149-164.
74. B. Kirschweg, D. M. Tilinger, B. Hégyel, G. Samu, D. Tátraaljai, E. Földes and B. Pukánszky, *European Polymer Journal*, 2018, **103**, 228-237.
75. A. M. Pisoschi and A. Pop, *European journal of medicinal chemistry*, 2015, **97**, 55-74.
76. A. H. Elhamirad and M. H. Zamanipoor, *European journal of lipid science and technology*, 2012, **114**, 602-606.
77. J. Pospíšil, W.-D. Habicher, J. Pilař, S. Nešpůrek, J. Kuthan, G.-O. Piringner and H. J. P. D. a. S. Zweifel, 2002, **77**, 531-538.
78. S. T. Ryssel, E. Arvin, H.-C. H. Lützhøft, M. E. Olsson, Z. Procházková and H.-J. Albrechtsen, *Degradation of specific aromatic compounds migrating from PEX pipes into drinking water, Water Research*, 4-5, 2015.
79. K. Schmidt and I. Podmore, *Journal of biomarkers*, 2015, **2015**.
80. F. a. D. Administration, *Guidance Compliance Regulatory Information*, 2007.
81. D. A. Skoog and D. M. West, *Principles of instrumental analysis*, Saunders College Philadelphia, 1980.
82. E. Hoffmann, *Mass spectrometry*, Wiley Online Library, 1996.
83. D. H. Williams and I. Fleming, *Spectroscopic methods in organic chemistry*, McGraw-Hill, 1980.
84. Y. Ohki and N. Hirai, *Chemiluminescence as a clear diagnostic tool of polymer oxidation*, 2012, 1-4.
85. R. H. YOUNG, R. Martin, D. Feriozi, D. Brewer and R. Kayser, *Photochemistry and Photobiology*, 1973, **17**, 233-244.
86. P. Gijsman, in *Handbook of Environmental Degradation of Materials (Third Edition)*, Elsevier, 2018, pp. 369-395.
87. D. N. Theodorou, *Chemical engineering science*, 2007, **62**, 5697-5714.
88. K. W. Swogger, in *Commercial Applications*, 1999, 283.
89. H. Enderle, *Science and Technology. Amsterdam, the Netherlands: Elsevier*, 2001.
90. M. Bochmann, G. J. Pindado and S. J. Lancaster, *Journal of Molecular Catalysis A: Chemical*, 1999, **146**, 179-190.
91. M.-C. Polymers, *Plastics Design Library, William Andrew Inc.: New York*, 1998.
92. B. Enko, S. M. Borisov, J. Regensburger, W. Bäuml, G. Gescheidt and I. Klimant, *The Journal of Physical Chemistry A*, 2013, **117**, 8873-8882.

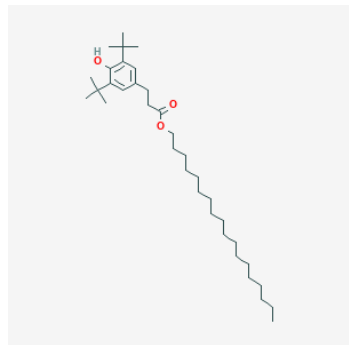
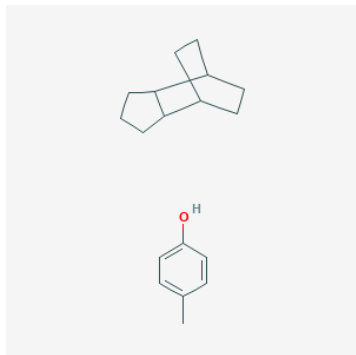
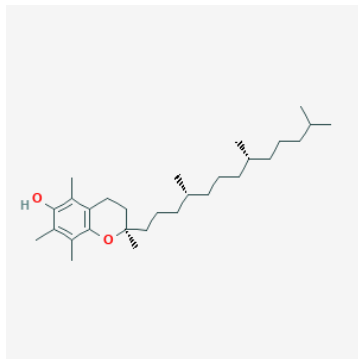


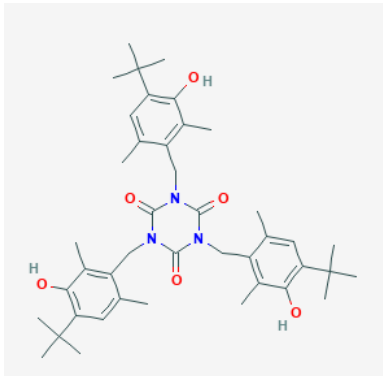
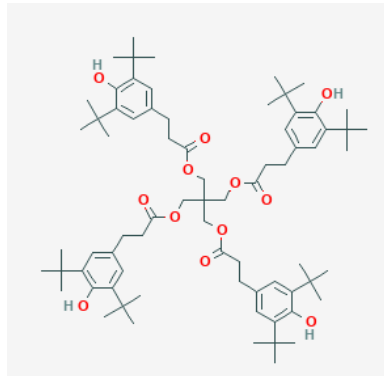
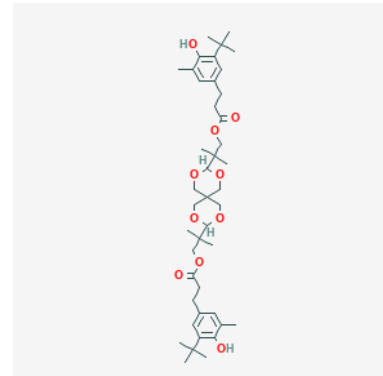
## 6 Appendix

### 6.1 Antioxidant description

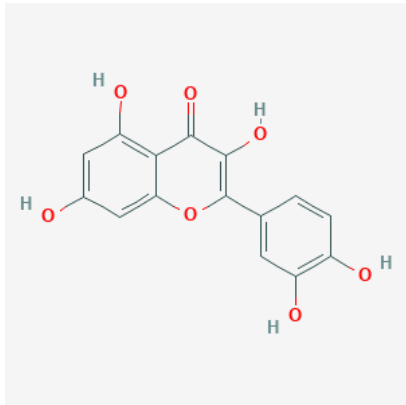
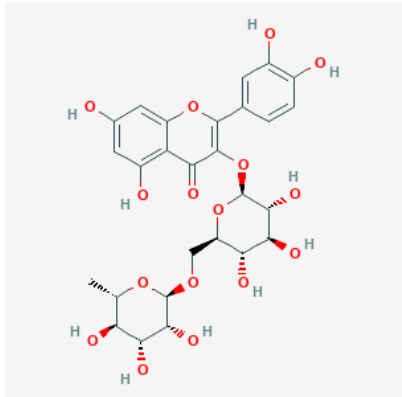
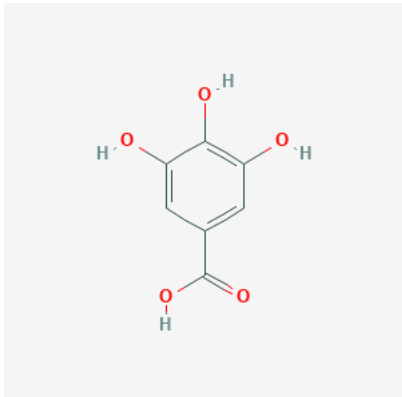
Acid Scavenger Calcium Stearate (AS)	Thioester-1	Thioester-2	Thioester-3																																																
																																																			
<table><tr><td>Molecular Weight (g/mol)</td><td>607.03</td></tr><tr><td>XLogP3-AA</td><td>-</td></tr><tr><td>Hydrogen Bond Donor Count</td><td>0</td></tr><tr><td>Hydrogen Bond Acceptor Count</td><td>4</td></tr><tr><td>Rotatable Bond Count</td><td>30</td></tr><tr><td>Melting Point (°C)</td><td>179</td></tr></table>	Molecular Weight (g/mol)	607.03	XLogP3-AA	-	Hydrogen Bond Donor Count	0	Hydrogen Bond Acceptor Count	4	Rotatable Bond Count	30	Melting Point (°C)	179	<table><tr><td>Molecular Weight (g/mol)</td><td>514.85</td></tr><tr><td>XLogP3-AA</td><td>11.7</td></tr><tr><td>Hydrogen Bond Donor Count</td><td>0</td></tr><tr><td>Hydrogen Bond Acceptor Count</td><td>5</td></tr><tr><td>Rotatable Bond Count</td><td>30</td></tr><tr><td>Melting Point (°C)</td><td>43-44</td></tr></table>	Molecular Weight (g/mol)	514.85	XLogP3-AA	11.7	Hydrogen Bond Donor Count	0	Hydrogen Bond Acceptor Count	5	Rotatable Bond Count	30	Melting Point (°C)	43-44	<table><tr><td>Molecular Weight (g/mol)</td><td>683.174</td></tr><tr><td>XLogP3-AA</td><td>18.2</td></tr><tr><td>Hydrogen Bond Donor Count</td><td>0</td></tr><tr><td>Hydrogen Bond Acceptor Count</td><td>5</td></tr><tr><td>Rotatable Bond Count</td><td>42</td></tr><tr><td>Melting Point (°C)</td><td>66</td></tr></table>	Molecular Weight (g/mol)	683.174	XLogP3-AA	18.2	Hydrogen Bond Donor Count	0	Hydrogen Bond Acceptor Count	5	Rotatable Bond Count	42	Melting Point (°C)	66	<table><tr><td>Molecular Weight (g/mol)</td><td>1161.939</td></tr><tr><td>XLogP3-AA</td><td>24.6</td></tr><tr><td>Hydrogen Bond Donor Count</td><td>0</td></tr><tr><td>Hydrogen Bond Acceptor Count</td><td>12</td></tr><tr><td>Rotatable Bond Count</td><td>68</td></tr><tr><td>Melting Point (°C)</td><td>63-68</td></tr></table>	Molecular Weight (g/mol)	1161.939	XLogP3-AA	24.6	Hydrogen Bond Donor Count	0	Hydrogen Bond Acceptor Count	12	Rotatable Bond Count	68	Melting Point (°C)	63-68
Molecular Weight (g/mol)	607.03																																																		
XLogP3-AA	-																																																		
Hydrogen Bond Donor Count	0																																																		
Hydrogen Bond Acceptor Count	4																																																		
Rotatable Bond Count	30																																																		
Melting Point (°C)	179																																																		
Molecular Weight (g/mol)	514.85																																																		
XLogP3-AA	11.7																																																		
Hydrogen Bond Donor Count	0																																																		
Hydrogen Bond Acceptor Count	5																																																		
Rotatable Bond Count	30																																																		
Melting Point (°C)	43-44																																																		
Molecular Weight (g/mol)	683.174																																																		
XLogP3-AA	18.2																																																		
Hydrogen Bond Donor Count	0																																																		
Hydrogen Bond Acceptor Count	5																																																		
Rotatable Bond Count	42																																																		
Melting Point (°C)	66																																																		
Molecular Weight (g/mol)	1161.939																																																		
XLogP3-AA	24.6																																																		
Hydrogen Bond Donor Count	0																																																		
Hydrogen Bond Acceptor Count	12																																																		
Rotatable Bond Count	68																																																		
Melting Point (°C)	63-68																																																		

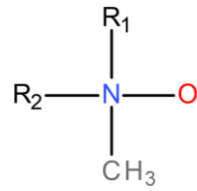
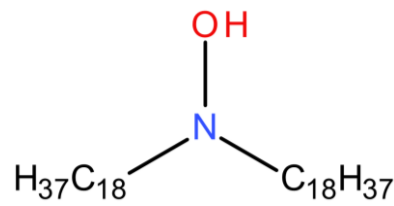
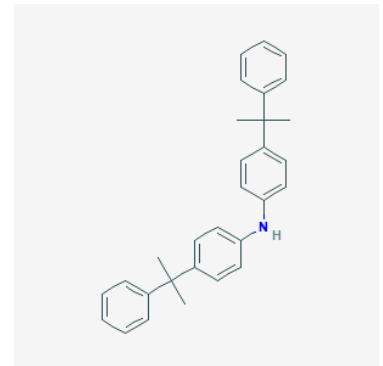
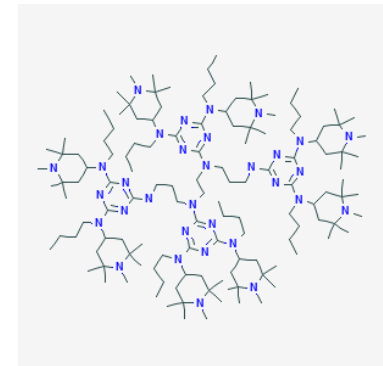
Phosphite-1	Phosphite-2	Phosphite-3	Phosphite-4																																																
																																																			
<table><tr><td>Molecular Weight (g/mol)</td><td>689.018</td></tr><tr><td>XLogP3-AA</td><td>19.3</td></tr><tr><td>Hydrogen Bond Donor Count</td><td>0</td></tr><tr><td>Hydrogen Bond Acceptor Count</td><td>3</td></tr><tr><td>Rotatable Bond Count</td><td>30</td></tr><tr><td>Melting Point (°C)</td><td>6</td></tr></table>	Molecular Weight (g/mol)	689.018	XLogP3-AA	19.3	Hydrogen Bond Donor Count	0	Hydrogen Bond Acceptor Count	3	Rotatable Bond Count	30	Melting Point (°C)	6	<table><tr><td>Molecular Weight (g/mol)</td><td>604.705</td></tr><tr><td>XLogP3-AA</td><td>9.9</td></tr><tr><td>Hydrogen Bond Donor Count</td><td>0</td></tr><tr><td>Hydrogen Bond Acceptor Count</td><td>6</td></tr><tr><td>Rotatable Bond Count</td><td>8</td></tr><tr><td>Melting Point (°C)</td><td>170-180</td></tr></table>	Molecular Weight (g/mol)	604.705	XLogP3-AA	9.9	Hydrogen Bond Donor Count	0	Hydrogen Bond Acceptor Count	6	Rotatable Bond Count	8	Melting Point (°C)	170-180	<table><tr><td>Molecular Weight (g/mol)</td><td>310.289</td></tr><tr><td>XLogP3-AA</td><td>5.5</td></tr><tr><td>Hydrogen Bond Donor Count</td><td>0</td></tr><tr><td>Hydrogen Bond Acceptor Count</td><td>3</td></tr><tr><td>Rotatable Bond Count</td><td>6</td></tr><tr><td>Melting Point (°C)</td><td>22-25</td></tr></table>	Molecular Weight (g/mol)	310.289	XLogP3-AA	5.5	Hydrogen Bond Donor Count	0	Hydrogen Bond Acceptor Count	3	Rotatable Bond Count	6	Melting Point (°C)	22-25	<table><tr><td>Molecular Weight (g/mol)</td><td>852.989</td></tr><tr><td>XLogP3-AA</td><td>14.4</td></tr><tr><td>Hydrogen Bond Donor Count</td><td>0</td></tr><tr><td>Hydrogen Bond Acceptor Count</td><td>6</td></tr><tr><td>Rotatable Bond Count</td><td>12</td></tr><tr><td>Melting Point (°C)</td><td>-</td></tr></table>	Molecular Weight (g/mol)	852.989	XLogP3-AA	14.4	Hydrogen Bond Donor Count	0	Hydrogen Bond Acceptor Count	6	Rotatable Bond Count	12	Melting Point (°C)	-
Molecular Weight (g/mol)	689.018																																																		
XLogP3-AA	19.3																																																		
Hydrogen Bond Donor Count	0																																																		
Hydrogen Bond Acceptor Count	3																																																		
Rotatable Bond Count	30																																																		
Melting Point (°C)	6																																																		
Molecular Weight (g/mol)	604.705																																																		
XLogP3-AA	9.9																																																		
Hydrogen Bond Donor Count	0																																																		
Hydrogen Bond Acceptor Count	6																																																		
Rotatable Bond Count	8																																																		
Melting Point (°C)	170-180																																																		
Molecular Weight (g/mol)	310.289																																																		
XLogP3-AA	5.5																																																		
Hydrogen Bond Donor Count	0																																																		
Hydrogen Bond Acceptor Count	3																																																		
Rotatable Bond Count	6																																																		
Melting Point (°C)	22-25																																																		
Molecular Weight (g/mol)	852.989																																																		
XLogP3-AA	14.4																																																		
Hydrogen Bond Donor Count	0																																																		
Hydrogen Bond Acceptor Count	6																																																		
Rotatable Bond Count	12																																																		
Melting Point (°C)	-																																																		

Phenol-1	Phenol-2	Phenol-3																																				
																																						
<table><tr><td>Molecular Weight (g/mol)</td><td>530.878</td></tr><tr><td>XLogP3-AA</td><td>13.8</td></tr><tr><td>Hydrogen Bond Donor Count</td><td>1</td></tr><tr><td>Hydrogen Bond Acceptor Count</td><td>3</td></tr><tr><td>Rotatable Bond Count</td><td>23</td></tr><tr><td>Melting Point (°C)</td><td>49-53</td></tr></table>	Molecular Weight (g/mol)	530.878	XLogP3-AA	13.8	Hydrogen Bond Donor Count	1	Hydrogen Bond Acceptor Count	3	Rotatable Bond Count	23	Melting Point (°C)	49-53	<table><tr><td>Molecular Weight (g/mol)</td><td>258.405</td></tr><tr><td>XLogP3-AA</td><td>-</td></tr><tr><td>Hydrogen Bond Donor Count</td><td>1</td></tr><tr><td>Hydrogen Bond Acceptor Count</td><td>1</td></tr><tr><td>Rotatable Bond Count</td><td>0</td></tr><tr><td>Melting Point (°C)</td><td>&gt;105</td></tr></table>	Molecular Weight (g/mol)	258.405	XLogP3-AA	-	Hydrogen Bond Donor Count	1	Hydrogen Bond Acceptor Count	1	Rotatable Bond Count	0	Melting Point (°C)	>105	<table><tr><td>Molecular Weight (g/mol)</td><td>430.717</td></tr><tr><td>XLogP3-AA</td><td>10.7</td></tr><tr><td>Hydrogen Bond Donor Count</td><td>1</td></tr><tr><td>Hydrogen Bond Acceptor Count</td><td>2</td></tr><tr><td>Rotatable Bond Count</td><td>12</td></tr><tr><td>Melting Point (°C)</td><td>3</td></tr></table>	Molecular Weight (g/mol)	430.717	XLogP3-AA	10.7	Hydrogen Bond Donor Count	1	Hydrogen Bond Acceptor Count	2	Rotatable Bond Count	12	Melting Point (°C)	3
Molecular Weight (g/mol)	530.878																																					
XLogP3-AA	13.8																																					
Hydrogen Bond Donor Count	1																																					
Hydrogen Bond Acceptor Count	3																																					
Rotatable Bond Count	23																																					
Melting Point (°C)	49-53																																					
Molecular Weight (g/mol)	258.405																																					
XLogP3-AA	-																																					
Hydrogen Bond Donor Count	1																																					
Hydrogen Bond Acceptor Count	1																																					
Rotatable Bond Count	0																																					
Melting Point (°C)	>105																																					
Molecular Weight (g/mol)	430.717																																					
XLogP3-AA	10.7																																					
Hydrogen Bond Donor Count	1																																					
Hydrogen Bond Acceptor Count	2																																					
Rotatable Bond Count	12																																					
Melting Point (°C)	3																																					

Phenol-4	Phenol-5	Phenol-6																																				
																																						
<table><tr><td>Molecular Weight (g/mol)</td><td>699.933</td></tr><tr><td>XLogP3-AA</td><td>10</td></tr><tr><td>Hydrogen Bond Donor Count</td><td>3</td></tr><tr><td>Hydrogen Bond Acceptor Count</td><td>6</td></tr><tr><td>Rotatable Bond Count</td><td>9</td></tr><tr><td>Melting Point (°C)</td><td></td></tr></table>	Molecular Weight (g/mol)	699.933	XLogP3-AA	10	Hydrogen Bond Donor Count	3	Hydrogen Bond Acceptor Count	6	Rotatable Bond Count	9	Melting Point (°C)		<table><tr><td>Molecular Weight (g/mol)</td><td>1177.6</td></tr><tr><td>XLogP3-AA</td><td>19.4</td></tr><tr><td>Hydrogen Bond Donor Count</td><td>4</td></tr><tr><td>Hydrogen Bond Acceptor Count</td><td>12</td></tr><tr><td>Rotatable Bond Count</td><td>32</td></tr><tr><td>Melting Point (°C)</td><td>110-125</td></tr></table>	Molecular Weight (g/mol)	1177.6	XLogP3-AA	19.4	Hydrogen Bond Donor Count	4	Hydrogen Bond Acceptor Count	12	Rotatable Bond Count	32	Melting Point (°C)	110-125	<table><tr><td>Molecular Weight (g/mol)</td><td>741</td></tr><tr><td>XLogP3-AA</td><td>8.9</td></tr><tr><td>Hydrogen Bond Donor Count</td><td>2</td></tr><tr><td>Hydrogen Bond Acceptor Count</td><td>10</td></tr><tr><td>Rotatable Bond Count</td><td>16</td></tr><tr><td>Melting Point (°C)</td><td>-</td></tr></table>	Molecular Weight (g/mol)	741	XLogP3-AA	8.9	Hydrogen Bond Donor Count	2	Hydrogen Bond Acceptor Count	10	Rotatable Bond Count	16	Melting Point (°C)	-
Molecular Weight (g/mol)	699.933																																					
XLogP3-AA	10																																					
Hydrogen Bond Donor Count	3																																					
Hydrogen Bond Acceptor Count	6																																					
Rotatable Bond Count	9																																					
Melting Point (°C)																																						
Molecular Weight (g/mol)	1177.6																																					
XLogP3-AA	19.4																																					
Hydrogen Bond Donor Count	4																																					
Hydrogen Bond Acceptor Count	12																																					
Rotatable Bond Count	32																																					
Melting Point (°C)	110-125																																					
Molecular Weight (g/mol)	741																																					
XLogP3-AA	8.9																																					
Hydrogen Bond Donor Count	2																																					
Hydrogen Bond Acceptor Count	10																																					
Rotatable Bond Count	16																																					
Melting Point (°C)	-																																					



Phenol-7	Phenol-8	Phenol-9																																				
																																						
<table><tr><td>Molecular Weight (g/mol)</td><td>302.238</td></tr><tr><td>XLogP3-AA</td><td>1.5</td></tr><tr><td>Hydrogen Bond Donor Count</td><td>5</td></tr><tr><td>Hydrogen Bond Acceptor Count</td><td>7</td></tr><tr><td>Rotatable Bond Count</td><td>1</td></tr><tr><td>Melting Point (°C)</td><td>316-318</td></tr></table>	Molecular Weight (g/mol)	302.238	XLogP3-AA	1.5	Hydrogen Bond Donor Count	5	Hydrogen Bond Acceptor Count	7	Rotatable Bond Count	1	Melting Point (°C)	316-318	<table><tr><td>Molecular Weight (g/mol)</td><td>610.521</td></tr><tr><td>XLogP3-AA</td><td>-1.3</td></tr><tr><td>Hydrogen Bond Donor Count</td><td>10</td></tr><tr><td>Hydrogen Bond Acceptor Count</td><td>16</td></tr><tr><td>Rotatable Bond Count</td><td>6</td></tr><tr><td>Melting Point (°C)</td><td>125</td></tr></table>	Molecular Weight (g/mol)	610.521	XLogP3-AA	-1.3	Hydrogen Bond Donor Count	10	Hydrogen Bond Acceptor Count	16	Rotatable Bond Count	6	Melting Point (°C)	125	<table><tr><td>Molecular Weight (g/mol)</td><td>170.12</td></tr><tr><td>XLogP3-AA</td><td>0.7</td></tr><tr><td>Hydrogen Bond Donor Count</td><td>4</td></tr><tr><td>Hydrogen Bond Acceptor Count</td><td>5</td></tr><tr><td>Rotatable Bond Count</td><td>1</td></tr><tr><td>Melting Point (°C)</td><td>258-265</td></tr></table>	Molecular Weight (g/mol)	170.12	XLogP3-AA	0.7	Hydrogen Bond Donor Count	4	Hydrogen Bond Acceptor Count	5	Rotatable Bond Count	1	Melting Point (°C)	258-265
Molecular Weight (g/mol)	302.238																																					
XLogP3-AA	1.5																																					
Hydrogen Bond Donor Count	5																																					
Hydrogen Bond Acceptor Count	7																																					
Rotatable Bond Count	1																																					
Melting Point (°C)	316-318																																					
Molecular Weight (g/mol)	610.521																																					
XLogP3-AA	-1.3																																					
Hydrogen Bond Donor Count	10																																					
Hydrogen Bond Acceptor Count	16																																					
Rotatable Bond Count	6																																					
Melting Point (°C)	125																																					
Molecular Weight (g/mol)	170.12																																					
XLogP3-AA	0.7																																					
Hydrogen Bond Donor Count	4																																					
Hydrogen Bond Acceptor Count	5																																					
Rotatable Bond Count	1																																					
Melting Point (°C)	258-265																																					

Aminic-1	Aminic-2	Aminic-3	Aminic-4																																																
<div></div> <div>R<sub>1</sub>, R<sub>2</sub> = C<sub>14</sub>-C<sub>24</sub> alkyl chains</div>	<div></div>	<div></div>	<div></div>																																																
<table><tr><td>Molecular Weight (g/mol)</td><td>-</td></tr><tr><td>XLogP3-AA</td><td>-</td></tr><tr><td>Hydrogen Bond Donor Count</td><td>-</td></tr><tr><td>Hydrogen Bond Acceptor Count</td><td>-</td></tr><tr><td>Rotatable Bond Count</td><td>-</td></tr><tr><td>Melting Point (°C)</td><td>-</td></tr></table>	Molecular Weight (g/mol)	-	XLogP3-AA	-	Hydrogen Bond Donor Count	-	Hydrogen Bond Acceptor Count	-	Rotatable Bond Count	-	Melting Point (°C)	-	<table><tr><td>Molecular Weight (g/mol)</td><td>538</td></tr><tr><td>XLogP3-AA</td><td>17.4</td></tr><tr><td>Hydrogen Bond Donor Count</td><td>1</td></tr><tr><td>Hydrogen Bond Acceptor Count</td><td>2</td></tr><tr><td>Rotatable Bond Count</td><td>34</td></tr><tr><td>Melting Point (°C)</td><td>96-99</td></tr></table>	Molecular Weight (g/mol)	538	XLogP3-AA	17.4	Hydrogen Bond Donor Count	1	Hydrogen Bond Acceptor Count	2	Rotatable Bond Count	34	Melting Point (°C)	96-99	<table><tr><td>Molecular Weight (g/mol)</td><td>-</td></tr><tr><td>XLogP3-AA</td><td>-</td></tr><tr><td>Hydrogen Bond Donor Count</td><td>-</td></tr><tr><td>Hydrogen Bond Acceptor Count</td><td>-</td></tr><tr><td>Rotatable Bond Count</td><td>-</td></tr><tr><td>Melting Point (°C)</td><td>-</td></tr></table>	Molecular Weight (g/mol)	-	XLogP3-AA	-	Hydrogen Bond Donor Count	-	Hydrogen Bond Acceptor Count	-	Rotatable Bond Count	-	Melting Point (°C)	-	<table><tr><td>Molecular Weight (g/mol)</td><td>-</td></tr><tr><td>XLogP3-AA</td><td>-</td></tr><tr><td>Hydrogen Bond Donor Count</td><td>-</td></tr><tr><td>Hydrogen Bond Acceptor Count</td><td>-</td></tr><tr><td>Rotatable Bond Count</td><td>-</td></tr><tr><td>Melting Point (°C)</td><td>-</td></tr></table>	Molecular Weight (g/mol)	-	XLogP3-AA	-	Hydrogen Bond Donor Count	-	Hydrogen Bond Acceptor Count	-	Rotatable Bond Count	-	Melting Point (°C)	-
Molecular Weight (g/mol)	-																																																		
XLogP3-AA	-																																																		
Hydrogen Bond Donor Count	-																																																		
Hydrogen Bond Acceptor Count	-																																																		
Rotatable Bond Count	-																																																		
Melting Point (°C)	-																																																		
Molecular Weight (g/mol)	538																																																		
XLogP3-AA	17.4																																																		
Hydrogen Bond Donor Count	1																																																		
Hydrogen Bond Acceptor Count	2																																																		
Rotatable Bond Count	34																																																		
Melting Point (°C)	96-99																																																		
Molecular Weight (g/mol)	-																																																		
XLogP3-AA	-																																																		
Hydrogen Bond Donor Count	-																																																		
Hydrogen Bond Acceptor Count	-																																																		
Rotatable Bond Count	-																																																		
Melting Point (°C)	-																																																		
Molecular Weight (g/mol)	-																																																		
XLogP3-AA	-																																																		
Hydrogen Bond Donor Count	-																																																		
Hydrogen Bond Acceptor Count	-																																																		
Rotatable Bond Count	-																																																		
Melting Point (°C)	-																																																		